Isolation, Evaluation and Optimization of Waste Derived *Citrus Aurantifolia* Peel Pectin as a Polymer in Furosemide Floating and Bioadhesive Matrix Tablet Formulation

By

Ebrahim Abdela (BPharm)

Addis Ababa University

Addis Ababa, Ethiopia

August, 2023

Isolation, Evaluation and Optimization of Waste Derived *Citrus Aurantifolia* Peel Pectin as a Polymer in Furosemide Floating and Bioadhesive Matrix Tablet Formulation

A thesis submitted to the Department of Pharmaceutics and Social Pharmacy in partial fulfillment of the requirements for the Degree of Master of Science in Pharmaceutics Under the Supervision of Dr. Anteneh Belete and Mr. Yohannes Mulualem

By

Ebrahim Abdela (BPharm)

Addis Ababa University

Addis Ababa, Ethiopia

August, 2023

Addis Ababa University

School of Graduate studies

This is to certify that the thesis prepared by Ebrahim Abdela, entitled: Isolation, Evaluation and Optimization of Waste Derived *Citrus Aurantifolia* Peel Pectin as a Polymer in Furosemide Floating and Bioadhesive Matrix Tablet Formulation. Submitted in partial fulfillment of the requirements for the Degree of Master of Science in Pharmaceutics complies with the regulations of the University and meets the accepted standards concerning originality and quality.

By: Ebrahim Abdela

Approved by:

Name	Signature	Date
Dr. Anteneh Belete (Advisor)	…….	……
Mr. Yohannes Mulualem (Advisor)	…….	…….
Mr. Yonas Birhane (Internal Examiner)	……	……..
Dr Yitayal Admasu (External Examiner)	……	……

Dean, School of Pharmacy, AAU

ABSTRACT

The *Citrus aurantifolia* (Christm) Swingle species can be found in many parts of the world including the subtropical and tropical areas. It is a small shrubby tree, about 5 m length and has fruit has globule to oval nearly 3-6 cm diameter with a color range from light yellow to purple. Some studies revealed that citrus waste derived pectin- becoming promising way for based gastro-retentive (floating and bioadhesive) drug delivery systems formulation due to pectin's economic, environmental and health related benefits. However, the floating and bioadhesive ability of the *citrus aurantifolia* peel pectin is not yet established. The bioavailability of furosemide is irregular through oral route and subjected to inter- or intra-subject variability. Hence, on the basis of its physico-chemical properties, it is a candidate drug for gastro-retentive formulations. Therefore, this study aimed to evaluate the potential of *citrus Aurantifolia* peel pectin as a polymer for preparing floating and bioadhesive matrix tablet using furosemide as a model drug.

The citrus peel pectin was extracted from local *citrus aurantifolia* tree fruit peel using hot water extraction technique and characterized for several physicochemical properties such as the presence of carbohydrate, loss on drying, total ash, pH, water solubility index, swelling power, relative solubility, moisture sorption-desorption pattern, viscosity, powder flow properties and its compatibility with the model drug were investigated. Wet granulation method was employed to prepare the furosemide granules and the prepared granules were evaluated for particle size and distribution, bulk and tapped densities, compressibility index and Hausner ratio, angle of repose, flow rate, and the friability of the formulated tablets were evaluated. Other tablet quality parameters including friability, hardness, thickness, diameter, weight variation and content uniformity were assessed and in acceptable pharmacopeial standard. Based on the preliminary investigation, the pectin (10-40%) and effervescent agent ($NaHCO_3$) (5-20%) concentrations were significantly affecting the response variables (p value < 0.05) such as floating duration (FD), bioadhesive strength (BS), swelling index (SI), drug release at 1 hr (DR_{1hr}) and drug release rate (DRR)). Hence, further optimization study was conducted using central composite design (CCD) approach of design-expert 13 software. Both numerical and graphical optimization techniques were used for optimization. The *Citrus aurantifolia* tree fruit peel yielded 34.4% (w/w) purified pectin with light yellow color. Its pH and ash values were 4.6 and 2.29%, respectively. It showed solubility in hot water. The equivalent weight, methoxy content, anhydronic acid, and the degree

of esterification were 81.5, 13.84, 91.68, and 85.49, respectively which showed high methoxy pectin. The purified pectin powder had a Carr's index of 36.6, Hausner ratio of 1.36 and angle of repose 32.78^{o} which necessitates to conduct wet granulation technique. The compatibility study using FTIR and DSC analysis revealed that furosemide and citrus peel pectin were compatible.

The drug release kinetic analysis of 13 formulations as per the CCD revealed best fits for Higuchi model with diffusion and erosion release mechanisms. The optimization results indicated that quadratic model was selected for swelling index and linear for the other responses. The adequacy of the model was evaluated using analysis of variance (ANOVA). Accordingly, the model provided an optimum formulation at 22.3% of pectin concentration and 5 % of effervescent agent. Under this condition, the software predicted floating duration (14.07 %), bioadhesive strength (28.57gm), swelling index (254.08%), drug release at 1hr (27.86%) and drug release rate (28.045 % / $h^{-1/2}$**)**. The optimization result predicted the optimized value of the independent variables to achieve desired responses was evaluated. The validity of this optimum formulation was confirmed experimentally. Based on the experimental studies, the validity of the model or software prediction was confirmed and the relative error are less than 5%. The flowability of the granule of optimized tablet was found excellent as the angle of repose was found to be <30^{0} while the Carr's and Hausner ratios were determined as < 10 and < 1.11 respectively.

In conclusion, the results of this study enable to suggest that waste-derived citrus pectin can be used as an abundant alternative pharmaceutical excipient in the formulation and manufacture of floating and bioadhesive matrix tablets, leading to the formulation of an optimal floating and bioadhesive formulation.

Keywords: *Citrus aurantifolia*, floating, bioadhesive, pectin, optimization, furosemide.

ACKNOWLEDGMENTS

I would like to offer my thanks to the Almighty God who gave me the strength, healthiness, and courage to finalize this study.

It is an honor to express my heartfelt gratitude to my advisors Dr. Anteneh Belete, Mr. Yohannes Mulualem, and Mr. Fantahun Molla whose meticulous guidance, valuable suggestions, and endless motivation made me complete this thesis work.

I extend my genuine acknowledgments to the Ethiopian Pharmaceuticals Manufacturing PLC (EPHARM) for generous gift of raw materials (Furosemide API, Lactose, talc, magnesium stearate), East Africa Pharmaceuticals Factory PLC for allowing me conduct tablet formulations in their facilities, Cadila Pharmaceuticals for providing me HPMC,$NaHCO_3$ and Ethiopian Food and Drug Control Authority (EFDA) headquarter and Bahir Dar branch, and Bahir Dar University, Department of Organic Chemistry for allowing me access to their laboratories.

I would like to acknowledge Bahir Dar University for sponsoring my postgraduate study and Addis Ababa University for sponsoring my thesis research.

I would also like to thank my family, friends and others who were directly or indirectly involved in motivating, encouraging, and supporting me throughout my entire career.

Contents **Page**

ACRONYMS AND ABBREVIATIONS

ANOVA	:	Analysis of Variance
API	:	Active Pharmaceutical Ingredient
CCD	:	Central Composite Design
CV	:	Coefficient of Variation
DE	:	Degree of Eterification
DSC	:	Differential Scanning Calorimetry
EC	:	Ethyl Cellulose
ESA	:	Ethiopian Statistics Authority
FT-IR	:	Fourier Transform Infrared Spectroscopy
GalA	:	D-galacturonic Acid
GI	:	Gastrointestinal
GRDDS	:	Gastro Retentive Drug Delivery System
HG	:	Homogalacturonan
HM	:	High Methoxy
HPMC	:	Hydroxyl Propyl Methyl Cellulose
LM	:	Low Methoxy
LOF	:	Lack of Fit
MeO	:	Methoxy Content
NACMC	:	Sodium Carboxy Methyl Cellulose
PRESS	:	Predicted Residual Sum of Square
RG	:	Rhamnogalacturonan
USD	:	United States Dollar
USP	:	United States of Pharmacopoeia
XRD	:	X-Ray Diffraction

LIST OF FIGURES Pages

LIST OF TABLES Pages

1. INTRODUCTION

1.1 Pharmaceutical Excipients

Pharmaceutical dosage forms contain both active pharmaceutical ingredient (API) and inactive (excipients) components in the dosage form. Excipients are inactive constituents employed for many reasons including aiding the formulation process, improve patient acceptability, and increases stability (Haywood and Coast, 2011). In oral dosage forms, excipients such as lubricant, binder, diluent, glidant, and disintegrant are used (Saluja and Sekhon, 2013; Kar *et al.*, 2018). The pharmaceutical industries expend a lot of resources in order to purchase or develop excipients. The global market forecasting studies indicate that the excipient market nowadays is continually growing, with 6.8$ billion in each year and will reach around 9.5$ in 2022. These may be due to the persistent necessity for the development of advanced drug delivery systems. The excipient market will continually grow as the need for new and modified excipients is rising for the development of the currently available and modified formulations parallel with the advancement of medical technologies (Gandhi, *et al* 2012; Kar *et al.*, 2018; Dhanal *et al.*, 2022).

Excipients can be obtained from plant, animal and mineral sources and could be utilized in intact (natural) or modified (synthetic) forms for their diversified functions (Ogaji, *et al*, 2012; Abrantes, *et al*, 2019).Though synthetic polymers are widely available, utilization of natural polymers for pharmaceutical applications becomes attractive research area as these types of polymers are renewable, sustainably, abundant, cost-effective, biodegradable, environmental friendly, and relatively safe. Nowadays, plant based excipients deliver different functions and the demand for these substances is increasing and new sources are being developed (Choudhary and Pawar, 2014).

1.2. Gastro-Retentive Drug Delivery Systems

1.2.1. Principle of Gastro-Retentive Drug Delivery Systems

Currently, gastro-retentive drug delivery system (GRDDS) becomes a popular way to deliver drugs. The most common types of gastro retentive drug delivery systems are swellable or expanding, floating, bioadhesive, and combination system (Mandal, Chatterjee and Senjoti, 2016). The swellable and expandable systems work by swelling and expanding the tablet to increase the size while in contact with the gastrointestinal (GI) fluid that delays the tablet to escape through sphincter, even though the formulation process is difficult and costly (Porwal, *et al*, 2017).

Mucoadhesive system functions by the attachment of the drug with the mucosal membrane, yet targeting and coping with mucin and its turnover rate is challenging (Sravya *et al.*, 2012; Khan, 2013).

High density system formulations act by interacting with denser material rather than the GI fluid for rendering the drug to sediment while the magnetic system is designed by incorporating a small magnetic substance and an extra-corporal magnet to controls the drug transit inside the GI mucosa (Nigusse *et al*, 2021). But it is reported that patients are not comfortable and complied with these delivery systems (Tripathi *et al.*, 2019; Başarır *et al*, 2021).The floating system can be designed by incorporating effervescent or non-effervescent agents that can form a gel by interacting with the aqueous environment to remain buoyant. However, these type of delivery system needs high level of gastric fluid (Yilma *et al*, 2015; Ibrahim *et al.*, 2019; Shinde *et al*, 2021). The combination system alleviates shortcomings of a single system and not influenced by irregular gastric emptying or physiological condition (Lopes *et al.*, 2016; Wilson and Stevenson, 2019).

GRDDSs with matrix systems are designed with a polymer that can form a gel layer once it is in contact with the GI fluid which controls the release by erosion and dissolution mechanisms. As a result, the release pattern will be altered to offer a controlled and extended drug action. Nonetheless, those properties can only be achieved if the matrix remains intact and the drug is optimally controlled (Nigusse *et al*, 2021).

In all the above delivery systems, physiological (patient related) and pharmaceutical factors should strictly be considered. The gastric motility, pH, nature of the meal (frequency and caloric content), age of the patient, gender, posture, disease status, co-administered drugs are the patient related factors. The pharmaceutical factors indicate the property of dosage form size, density, surface area, dissolution rate, & shape (Pasupathi, 2020; Prinderre *et al*., 2011). The pharmaceutical and patient related factors affect the gastric residence time in the stomach thereby delivering drugs for extended periods of time. Hence, it necessitates to control the drug release as it may result fluctuations in plasma drug levels, irregular bioavailability (Porwal, *et al*, 2017).

1.2.2. Drug Candidates for GRDDS

The candidate drugs for gastro retentive drug delivery system comprises drugs that have a short absorption window (riboflavin, levodopa, furosemide), those that are not stable in the small intestine environment (captopril, ranitidine hydrochloride), locally acting drugs in the stomach (antacids and misoprostol), and drugs that eradicate the colonic bacteria (ranitidine and metronidazole) (Nayak *et al*, 2010). Furosemide, a high-ceiling diuretic, is a good candidate to be formulated as a floating and bioadhesive drug delivery system. It is used for treating edematous conditions caused by congestive heart failure, renal disorders, and liver cirrhosis. It is absorbed from the stomach and upper part of the small intestine. The bioavailability of furosemide is irregular through oral route (37-51%) and subjected to inter or intra subject variability among the healthy (50-70%) and patients with renal disorders (30%) due to its short or narrow absorption window (Granero *et al.*, 2010; Nafei, 2014). The chemical structure of furosemide is presented in **Figure 1**.

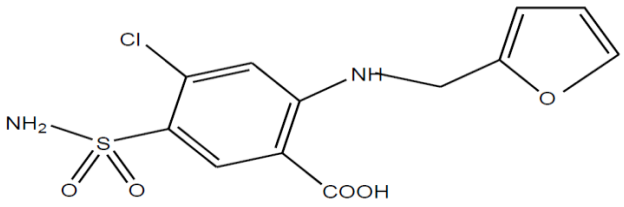

Figure 1: Chemical structure of furosemide.

1.2.3. Polymers Used for Floating and Bioadhesion

Selection of the suitable polymers is crucial to obtain a good floating and bioadhesive formulations. In the market, there are numerous types of polymers for this purpose. Natural polymers including pectin, starch, chitosan, sodium alginate, and the semisynthetic polymers such as chitosan derivatives, hydroxyl propyl methyl cellulose (HPMC), and ethyl cellulose (EC) can be used as a floating agent. In addition, the synthetic derivatives like lactic acid derivatives, acrylic acid derivatives, and modified cellulose derivatives are proper hydrocolloids that can be employed as hydrate-forming floating polymers in the acidic environment. Specifically, the polymers used for the floating tablet formulation should possess a tablet with a lower density than the GI fluid. Ideally, a bioadhesive polymer should be non-reactive, non-irritant, and free from toxicity. It should also be well-attached to the mucosal membrane with better specificity. Most importantly,

the bioadhesive polymers should rather form a strong, non-covalent bond with the mucin epithelial cell surface (Patil *et al*, 2016; Başarır *et al,* 2021). The most frequently used bioadhesive polymers include carbopol, chitosan, sodium alginate, HPMC, polyethylene glycol, sodium carboxyl methyl cellulose (NaCMC), and poly (acrylic acid). Nowadays, several studies are focusing on the combination of floating and bioadhesion to achieve the optimal outcome response from GRDDSs (Tripathi *et al.,* 2019). Study reports indicated that combined floating and bioadhesive formulations can be prepared by using HPMC, pectin, carbopol, NaCMC and sodium bicarbonate as effervescent agent (Yusif *et al.,* 2015).

1.3. Pectin as a Floating and Bioadhesive Agent

1.3.1. Pectin

Almost all plants contain pectin, a high-molecular-weight carbohydrate polymer that contributes to the construction of the cell. The name "pectin" refers to a range of polymers that varies in terms of their molecular weight, chemical make-up, and neutral sugar concentration. Additionally, different plant species produce pectin with various functional characteristics (Arias *et al.,* 2021). The word "pectin" is derived from the Greek word pektos, which means stiff and unyielding refering to pectin's capacity to form gels. Citrus plants are abundant sources of pectin. Pectin is part of plant cell walls made up of neutral sugar side chains attached to an acidic sugar backbone. Pectin crosslinking affects cell wall porosity and plant morphogenesis. It also aids in cell adhesion and wall hydration (Horowitz *et al.*, 2000). It is the commonest naturally abundant constituent of the cell wall which supports the growth of the plant (Willats *et al*, 2006).

Pectin is toxic-free aqueous soluble hetro-polysaccharide which contains methoxyl groups of esterified uronic acids that can be stated as a percent esterification (carboxyl groups). Pectin solubility and gel forming properties largely depend on the degree of esterification. Due to this pectin be classified according to their gelling properties and its methoxyl groups (Miao *et al.*, 2005). Those pectin powders contain more than 50% of degree of esterification are high methoxyl pectin (HM) whereas, low methoxyl (LM) types comprises less than 50% (Dhanal *et al.,* 2022). It has an average molecular mass ranges 50, 000 to about 180,000 (Ogaji *et al*, 2012). The aqueous solubility of HM pectin is comparably lesser than LM pectin which makes a preferred polymer. Nonetheless, it is stated that LM pectin coated with HM pectinate beads shows a good drug release profile than non-coated counterparts (Wong *et al*, 2021). The matrix made of pectin is prone to

swelling as well as erosion in aqueous medium leading to premature drug release at upper gastrointestinal tract and thereby defeating its ability as colon-specific drug delivery vehicle (Wong *et al*, 2021). The chemical structure of pectin is illustrated in **Figure 2**.

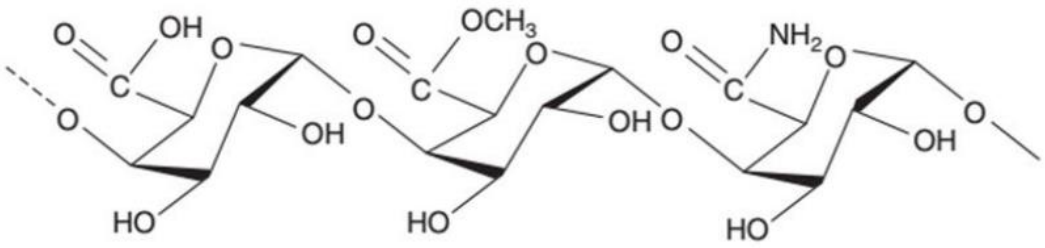

Figure 2: Chemical structure of pectin

1.3.2. Sources and Production of Pectin

Even though majority of plant species contain pectin, citrus peel (25-35%), apple pomace (10-15%), sugar beet (10-20%), and sunflower (15-25%) have exhibited significant yield in a dry form. The type and quality of fruits used, the harvesting time, and the enzymatic degradation are some of the factors influencing the pectin quality and concentration. The maximum yield occurs prior to ripening and varies from year to year due to different environmental conditions. High pectin content fruits include lime, lemon, orange and apple. Apricot and blackberry demonstrated average pectin content, whereas fruits like cherry, peach and pineapple have low pectin content. Pectin is obtained from fruit peels and waste products of juice producing plants. Different citrus fruits and their average yield are depicted in **Table 1** (Yin *et al.*, 2017).

Table 1: Different citrus fruits and their average pectin yield

(Yin *et al.*, 2017)

Citrus Fruit	**Pectin Yield (%)**
Orange peel	10.9-24.8
Grapefruit	21.6-28
Lemon peel	20.9-30.6
Lime peel	9-33.6

Globally, more than 40,000 metric tons of pectin is being consumed every year and costs around 319 million USD (Sundarraj and Ranganathan, 2017). Many of food industries dispose pectin as a

by-product which is estimated to be nearly 1600M ton per year which might be conserved to save huge economy and environmental problems (Mokhena *et al*., 2016; Omale *et al*, 2017). The overall geographical distribution of pectin is presented in **Figure 3**.

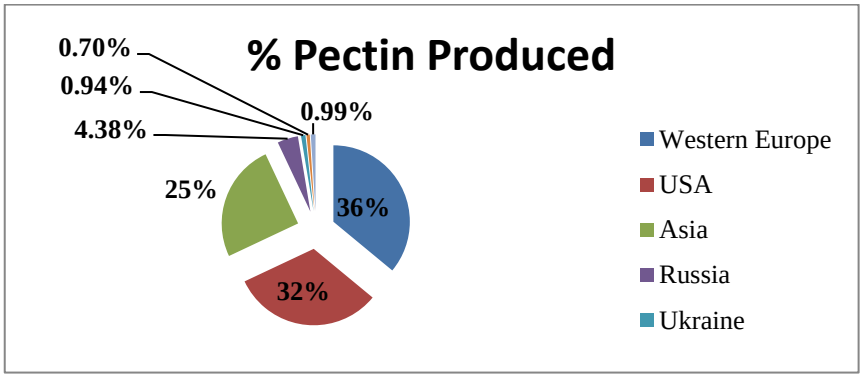

Figure 3: Global pectin production data (Sundarraj and Ranganathan, 2017)

1.3.3. Extraction and Characterization of Pectin

Pectin extraction from natural sources can be achieved with a variety of techniques. The direct boiling (hot water) extraction, thermo-mechanical press extraction, acid extraction, and microwave extraction are among the commonly applied techniques. Direct boiling method has the advantages of being relatively easy, inexpensive, and functioning at lower temperature (Sandarani, 2017). The extracted pectin color may range from light brown to dark brown for sun and microwave assisted drying techniques, respectively. After extraction, the pectin will undergo physicochemical characterization tests including equivalent weight, methoxyl content, anhydronic acid level, and degree of esterification. These tests are used to determine the identity, purity and amount of the pectin present in a specified natural source (Belkheiri *et al.*, 2021).

1.3.4. Physicochemical Properties & Toxicological Profile of Pectin

Pectin is a non-toxic anionic polymer of glycan domains (cell wall polysaccharides) that is biocompatible, biodegradable, and edible to humans which enables its wide nutraceutical and pharmaceutical applications. Studies showed that pectin is considerably safe and no safety issues have been raised with its utilization (Mortensen *et al.*, 2017). Pectin contributes approximately 70% of D-galacturonic acid remnants (GalA) associated at α-1,4 positions and several neutral sugars such as arabinose, rhamnose, and galactose. The GalA linked at α-1,4 positions can be methyl esterified or acetylated. There are different domains of pectin: homogalacturonan (HG),

rhamnogalacturonan I (RG-I), and rhamnogalacturonan II (RG-II). HG is the linear homopolymer and constitutes about 65% pectin in plant cell structures. HG contributes α-(1–4) linked GalA residues and is considered a smooth region of pectin due to the absence of side chains. After HG, RG-I constitutes maximum pectin of about 20–35%. Compared to HG, RG-I has a more complex structure and a high number of neutral sugars. It has about a hundred repetitive units of (1,2)- α-L-Rha-(1,4)- α-D-GalA. RG-II has roughly 10% pectin and has a more complex structure than RG-I. Despite its less contribution to pectin, it plays a crucial role in the architecture of plant cells. Both RG-I and RG-II are considered the hairy region of pectin due to non-ionic side chains (Singhal & Hulle, 2022).

At higher temperature, pectin loses its mucilaginous consistency and becomes unstable. Pectin is soluble in hot water and insoluble in cold water. It is soluble in a mixture of water with an organic solvent, such as alcohol, while di- and tri-salts are still either insoluble or only faintly soluble. However, alcohol and chemical solvents render it insoluble. When properly dissolved in water and maintained in a cool, dry environment, pectin demonstrates gel-forming, thickening, and stabilizing capabilities. When dry powdered pectin is mixed with water, it tends to hydrate very quickly and clump up. The formation of clumps can be avoided by dry mixing pectin powder with a hydrophilic carrier substance or by using pectin that has better dispersibility due to unique manufacturing processing. To obtain effective use and prevent the production of heterogeneous gels, pectin must be thoroughly dissolved. Pectin must be kept in a cold, dry area for storage (Shaha *et al*, 2013; Da Gama *et al.*, 2015). Pectin will degrade at higher temperatures than ambient because of a decrease in molecular weight. Pectin functions best at a pH of 2.8 to 4.7. In comparison to other thickening agents, pectin solutions have lesser viscosity. The viscosity of LM pectin solutions is raised by polyvalent salts like Ca^{++} and Mg^{++}. The acidity is increased in calcium-free solutions, the viscosity decreases. The dried pectin powder is mixed with water, it tends to hydrate quickly and create gels. While moderate concentrations of a solution show non-Newtonian, pseudo plastic behavior characteristics, diluted solutions are Newtonian. Gelation, solubility, and viscosity are typically connected. Those factors that rises the gel strength improves the viscosity, reduces the solubility and vice versa (Shaha *et al*, 2013).

1.3.5. Floating and Bioadhesive Applications of Pectin

Pectin can be used intact or in modified form as a carrier for controlling release and delivering a drug to the GI environment as a matrix tablet (Kedir *et al*, 2022). The gelation of pectin reduces water penetration and controls the drug release from the dosage forms (Chomto and Nunthanid, 2017). The dual responsiveness (pH and enzyme) of pectin also makes it the polymer of choice for colon targeted drugs (Wong *et al*, 2021). The hydration volume and floating ability of gel matrix tablets can be improved with the addition of effervescent agents (Chen *et al*., 2015). Pectin-based floating drug delivery systems present promising approaches for increasing the bioavailability of drugs with absorption windows in the upper small intestine. Pectin also exhibits excellent mucoadhesive properties for different pectin based pharmaceutical formulations (Sriamornsak, 2011). The mucoadhesive process involved in the formation of bioadhesive bonds has been described in three steps: i) wetting and swelling of the polymer to permit intimate contact with biological tissue, ii) interpenetration of bioadhesive polymer chains and entanglement of polymer and mucin chains, and iii) formation of weak chemical bonds between entangles chains (Srivastava and Malviya, 2011b).

1.3.6. Other Applications of Pectin

Readily availability and excellent physicochemical properties of pectin such as simplicity, environmental friendliness, biocompatibility, biodegradability, hot water solubility, and non-toxicity makes it and its structurally modified derivatives an auspicious excipient for nutraceutical and pharmaceutical industries for impending applications. The properties of pectin such as degree of methylation, degree of esterification, and degree of amidation might affect the application of pectin. Nowadays, pectin can be utilized for wide applications such as pharmaceutical, cosmetic, food, and biological products. Pectin is extensively useful as a gelling agent and as a viscosity modifier with in numerous food and cosmetics manufacturing. It is exploited to formulate jams, jellies, marmalades, and other products to improve product consistency. Pectin is furthermore used as a worthy dietary fiber; it can prevent diseases such as diabetes mellitus, hypercholesterolemia, and colonic cancer (Beyech & Abdissa, 2021). Generally, pectin is largely employed in the manufacturing of confectionaries, diary based products, food additives, food packaging, beverages, and in the fabrication of 3D printed nutraceuticals (Singhal & Hulle, 2022). Moreover, pectin has shown beneficial health effects in studies investigated for drug formulation, gene

delivery, wound healing, cholesterol lowering, tissue engineering, and drug delivery through the mucosa and gastrointestinal tract. In addition, pectin is being used as a biomaterial for the production of artificial corneas (Maria *et al.,* 2021).

1.4. Citrus as a Source of Pectin: Botanical and Geographical Distribution

The genus *citrus* (*Rutaceae* family) is from angiosperm sub family which is broadly spread in many parts of the world. It is indigenous in India, Northern Australia, New Caledonia and Southern China (Wu *et al.,* 2018). Among the genus *citrus,* historically the orange fruit, was cultivated 2400 B.C in China (Manner *et al.,* 2006). According to a report from Food and Agriculture Organization indicated that $1.17x10^8$ tons of citrus fruit is produced annually and nearly half of its weight would be the residue including the peel and other fruit wastes (FAO, 2020). It is stated that more than $5.5x10^4$ tons of waste would be release from different food and juice producing plants. Substantial amount of citrus is available as a byproduct. Even though the peel accounts a large proportion among the waste, still there is a gap of not utilizing for different applications. It becomes a huge asset by extracting pectin from the widely available citrus fruit wastes (Beyech & Abdissa, 2021; Jain *et al*., 2020). A significant amount of pectin is produced from the citrus genera peels compared to the other sources of pectin. In dry basis, the citrus peel contains 25-30% of pectin (Rehman *et al.,* 2019).

1.5. *Citrus aurantifolia* Peel Pectin

The *Citrus aurantifolia* (Christm) Swingle species can be found in many parts of the world including the subtropical and tropical areas. A typical *Citrus aurantifolia* plant is presented in **Figure 4**. It is a small shrubby tree, about 5 m length and has alternate flower which is elliptical to ovoid in shape ranging from 4-8cm×2-5cm with a round margin. Its flower reaches around 1 inch and has yellowish white colour with light purple margin. Its fruit has globule to oval nearly 3-6 cm diameter and usually contains papillae in its apical surface. The fruit color changes from green to yellow when it rips though it is marketed early on. Mostly the fruit becomes more abundant from May to September and has acidic nature with pleasant fragrance with sour taste like lemon (Narang & Jiraungkoorskul, 2016; Sunday *et al*., 2015). The *citrus aurantifolia* specious yields higher percentage of pectin with a good quality and purity (≥85% of galactouronic acid level) compared to the other types of citrus sources (Haggag *et al.,* 1998).

Figure 4: *Citrus auranitfolia* tree and its fruit (taken by Ebrahim Abdela Siraj, year)

1.6. Optimization

The optimization study was conducted by using response surface methodology (RSM) method as it is the most commonly employed technique for determining the independent and response variable values. It enables to identify the precise values for optimization, and to clearly realize the association of dependent and independent variables. Central composite designs (CCD), factorial designs, simple lattice design, box-behnken design are the most commonly used statistical designs in RSM for optimization of several gastro retentive drug deliveries. Among many of the methods, CCD becomes very influential statistical design to optimize a number of independent variables. It is an effective method for trials with limited number of variables ($2 \leq k \leq 6$). The experimental runs to be conducted in this design would be 2k factorial, 2k axial, and kc central run ($2^k + 2k + kn$). k stands for the number of independent variables. The factorial design part employed for approximating key impacts (linear terms) and two-factor interactions; 2k axial points for estimating the second-order terms, and kn repeated center points for the curvature and experimental error of the model (Khuri and Mukhopadhyay, 2010; Chelladurai *et al.*, 2020).

1.7. Granulation & Tablet Formulation

Granulation is a method of desirable particle aggregation that aims to improve the flow properties and compressibility of the powder by avoiding segregation by achieving uniform distribution of the particles (Solanki *et al.*, 2010). Ideally, granules should have a spherical shape and nearly similar particle size distribution in order to improve the flow ability, content uniformity and compressibility. This can be affected by particle size of the components, the volume of granulating fluid and its concentration, granulating time, and temperature. Particle size ranging from 0.2 to 4 mm is commonly applied in the pharmaceutical manufacturing. Generally, granulation can be broadly classified in to two categories as wet and dry granulation. In a dry granulation, the

agglomerates are prepared by using mechanical compressors or compactors of the particles whereas in wet granulation, the granulation fluid (either a binder solution or a wetting solvent) is employed to aid the agglomeration by creation of damp mass (Mashinchian *et al.*, 2014). Selecting the appropriate method needs well understanding of the flow, the physicochemical characteristics of the components, and the desirable release properties (Solanki *et al.*, 2010).

The pharmaceutical tablet compression needs to put necessary granules in the die cavity, then the granules compressed between the upper and lower punches and becomes single solid. Then, the tablet ejected from the die as intact tablet. A transitional repacking, distortion at contact sites, fragmentation and/or deformation, bonding, deformation of the solid body, decompression, and finally ejection of the tablet are the subsequent events that take place during the compression process (Mashinchian *et al.*, 2014).

2. THE PRESENT STUDY

The advances in drug delivery urged the discovery of novel excipients which are safe and capable of fulfilling specific functions (Vipul *et al*., 2018). Nowadays, the use of natural polymers in the pharmaceutical sector is greatly expanding as it offers better advantages in terms of cost, safety, availability, and bio-degradability. Natural sources have wide range of varieties and characteristics. So, they can be used numerously in pharmaceutical productions as excipients to serve for their desired properties (Saha *et al.*, 2018). Natural polymers like pectin are easy to isolate and purify; they are typically non-toxic and biocompatible, and they are extracted from waste byproducts of various natural sources (Khule *et al.*, 2012).

Pectin has been previously proved to be effective as a suspending agent for drugs such as paracetamol and ibuprofen (Jyotirmoy, 2010). Currently, pectin gets much attention due to its practical applications and implications in modified drug delivery because of its swelling and hydration capabilities in aqueous media. Nonetheless, one shall highlight that there is no clear picture on the exact complex structure of pectin and its physicochemical attributes that could vary with its varying sources and manufacturing processes (Wong *et al*, 2021). The present study would also give some insight regarding to the physicochemical properties and potential biopharmaceutical application of isolated pectin.

Citrus aurantifolia (Christm.) of the genus *rutaceae* is an edible plant in Ethiopia which assures its safety. It can be obtained from wild and cultivated sources (Teklehaymanot *et al.*, 2007). It is not well studied and characterized for their possible pharmaceutical applications. Due to the high demand in the global market, researchers are searching for new sources of this polysaccharide and have been investigating on its alternative non-commercial sources (Pasandide *et al.*, 2017) Therefore, the proper recycling of citrus fruits and the pectin wastes derived from them can be of multiple economic importance in addition to preventing environmental pollution. In this regard, the above gaps are expected to be filled by proper utilization of this crop as a source of pectin, which will have good impact on the country's economy by saving foreign exchange, creating jobs and keeping the environment safe and healthy. Hence, the current study aimed to bring benefits to society by opening a door in this regard and bringing an alternative excipient with several advantages.

2.1. Research Questions

This study attempts to answer the following research questions:

- Is *citrus aurantifolia* pectin amenable to floating, bio adhesive and swellable matrix tablets?
- What would be the effect of various polymers and other additives on release and other properties of furosemide matrix tablet?
- What are the critical factors in the optimization of furosemide matrix tablets as per RSM using CCD?

3. OBJECTIVES

3.1. General Objective

- To isolate, evaluate and optimize the *Citrus aurantifolia* waste derived peel pectin as a polymer in furosemide floating and bioadhesive matrix tablet formulation.

3.2. Specific Objectives

- To extract and characterize the peel pectin of *Citrus aurantifolia;*
- To prepare floating and bioadhesive matrix tablets of furosemide using peel pectin of *citrus aurantifolia* and characterize it
- To optimize the effect of citrus aurantifolia peel pectin and effervescent concentration on the prepared furosemide matrix tablet formulation
- To evaluate the floating duration, bioadhesive strength, swelling index, drug release at hr and drug release rate
- To validate the optimized formulation.

4. MATERIALS AND METHODS

4.1. Materials

Furosemide (Aurangabad, India) and other relevant excipients for the formulation, including lactose (Narula Exports Pvt. Ltd., New Delhi, India), Sodium Bicarbonate ($NaHCO_3$) (Newport Industries Ltd, UK), talc (Narula Exports Pvt. Ltd., New Delhi, India), and magnesium stearate (Narula Exports Pvt. Ltd., New Delhi, India) were sponsored by and collected from the Ethiopian Pharmaceuticals Manufacturing company (EPHARM). The chemicals used for extraction of pectin and characterizing the formulated tablet include, Hydrochloric acid 37% w/w (BDH Ltd., England), NaOH (Guangdong Guanghua Sci-Tech Co., Ltd, China), ethanol (96%), NaCl, Phenol red and muslin cloth were purchased from local market. Instruments magnetic stirrer, water bath, FTIR (FTIR-8400S, SHIMADZU, and Japan), XRD (XRD-7000 X-ray diffractometer MAXima, SHIMADZU Corporation, Japan), DSC (PerkinElmer DSC 4000).

4.2. Methods

4.2.1. Collection and Authentication of *Citrus aurantifolia (christm.) swingle*

Citrus aurantifolia (christm) *swingle* was collected from wild source from March - April 2022 around Zege village of Bahir Dar City, North-West Ethiopia. The collected plant material was authenticated at the botanical herbarium of the University of Gondar.

4.2.2. Extraction of the Peel Pectin from the Fruit

The peel was isolated from ripe and unripe fruit to compare the pectin yield. The wet peel was carefully isolated from the fruit & washed with tap water to remove remaining unwanted dirt soil; then dried with sun under shaded condition for 72 hr., and then further dried at 30 to 40 ℃ in the oven for 5 hrs. to obtain well dried and consistent peel. The dried peel was cut into smaller pieces; crushed with a grinder, and passed through #20 sieve to make it ready for further extraction and characterization processes (Srivastava and Malviya, 2011a). The dried peel powder of 5 g was put into 250 ml conical flask containing 150 ml of distilled water. The pH was adjusted to 2 using 0.1N of HCl while stirring using magnetic stirrer on a hot plate at 90°C. Then after, the solution was placed onto a hot water bath (Water bath CANTT1330, INDIA) at 90°C for 1.5 hr. The heated extract was filtered with muslin cloth and cooled at 4 ℃ in the refrigerator for 1 hr (Roy *et al.*, 2018). After that, equal volume of 96% alcohol was added to the concentrated extract for the

precipitate to form a gel due to the interaction of pectin with acid and alcohol which was followed by continuous stirring for 15 min. Then, the mixture was allowed to stand in 4 ℃ for about 2 hr to obtain the pectic substance float within the acidic water -alcohol mixture surface separately and to get better pectin precipitate. The floating pectic substance was then filtered using muslin cloth and successively washed three times by alcohol to remove the impurities. Finally, it was kept to dry at 40 ºC in hot air oven (Kottermann® 2711, Germany) for 2 hr until well dried and crushed using electronic grinder. The powder was finally sieved using #20 sieve size and stored for further use (Srivastava *et al*, 2010).

4.2.3. Pectin Powder Identification Tests

4.2.3.1. Determination of Equivalent Weight

Half gram of pectin powder was weighed and poured into a 250 ml conical flask. After moistening with 5 ml of ethanol, 1 g of NaCl and 100 ml of distilled water were added into the flask. A little drop of phenol red indicator was added. The procedure continued until all the pectin was well dissolved and no clump formed including on the flask sides. Finally, the mixture was back titrated using 0.1 M NaOH until a faint pink color formed. Then, the equivalent weight was determined using Equation 4.1 (Omale and Omale, 2017).

$$\text{Equivalent weight} = \frac{\text{Weight of pectin powder}}{\text{Volume of alkali} \times \text{Molarity of alkali}} \times 1000 \ldots\ldots\ldots\ldots \text{Equation 4.1}$$

4.2.3.2. Determination of Methoxyl Content

The determination of methoxyl content (MeO) was done using the neutral solution which was collected from equivalent weight determination, by adding 25 ml of 0.25 N NaOH. The mixed solution was stirred thoroughly and kept at room temperature for 30 min. After 30 min, 25 ml of 0.25 N HCl was added and titrated against 0.1 N NaOH. The methoxyl content was then calculated using Equation 4.2 (Azad, 2014).

$$\text{Methoxyl content}(\%) = \frac{\text{ml of Alkali} \times \text{Normality of Alkali} \times 3.1}{\text{Weight of the sample}} \ldots\ldots\ldots\ldots \text{Equation 4.2}$$

4.2.3.3. Anhydrouronic Acid (AUA) or Galactouronic Acid Level (%)

The %AUA was calculated from the volume of NaOH obtained from the equivalent weight and methoxyl content determination. It was determined using equation 4.3 (Ismail *et al.*, 2012).

$$\%\text{AUA} = \frac{176 \times 100}{\text{Z}} \ldots\ldots\ldots\ldots\ldots\ldots\ldots\ldots\ldots\ldots\ldots\ldots \text{Equation 4.3}$$

where 176 is the molecular weight of AUA and Z Value (the volume of NaOH in equivalent weight) was calculated applying Equation 4.4.

$$\text{Z} = \frac{\text{weight of the sample in mg}}{\text{meq of Titration A} + \text{meq Titration B}} \ldots\ldots\ldots\ldots\ldots\ldots\ldots\ldots \text{Equation 4.4}$$

Where Titration A (equivalent weight determination) and B (methoxy content determination).

4.2.3.4. Degree of Esterification

50 milligrams of the extracted pectin powder were dissolved in 100 ml of deionized water. After adding five drops of phenolphthalein, the solution was titrated with 0.05 M NaOH until it turned faint pink by which the endpoint was recorded as the initial titer. Then, 10 mL of 0.5 M NaOH was added to the previously treated solution, and allowed to stand for 15 min after shaking, followed by addition of 10 mL of 0.5 M HCl, and shook well until it became colorless. After that, five drops of phenolphthalein were added, and the sample was back titrated with 0.5 M NaOH until it exhibited a persistent faint pink color. This endpoint was recorded as the final titer. Degree of Esterification was determined from Equation 4.5 (Chaiwarit *et al.*, 2020a).

$$\text{DE (\%)} = [\text{Final titer}/(\text{Initial titer} + \text{Final titer})]\ 168 \times 100 \ldots\ldots\ldots\ldots\ldots \text{Equation 4.5}$$

Based on degree of esterification (DE) pectin can be classified as low methoxyl pectin with ≤ 50% DE and high methoxyl pectin with >50% DE (Twinomuhwezi *et al*, 2020).

4.2.4. Pectin Powder Physicochemical Characterization

4.2.4.1. Percentage Yield

The percentage yield of the C*itrus aurantifolia* peel pectin was calculated as per Equation 4.6:

$$\%\ \text{Yield} = \text{M/Mo x } 100\% \ldots\ldots\ldots\ldots\ldots\ldots\ldots\ldots\ldots \text{Equation 4.6}$$

Where, Mo is the initial weight of total dried peel matter and M is the weight of extracted pectin powder (Chaiwarit *et al.*, 2020b)**.**

4.2.4.2. Loss on Drying

The weight loss during drying process was evaluated by the method described elsewhere (Haile *et al* , 2020). Five grams of powder was dried by tray oven dryer (Kottermann® 2711, Germany) at 100 ± 5 °C until a constant weight was obtained. Then, the percentage loss on drying (% LOD) was determined by equation 4.7:

$$\text{LOD} = \frac{\text{weight of the water in the sample}}{\text{Weight of the sample}} \times 100\% \quad \text{Equation 4.7}$$

4.2.4.3. Phytochemical Studies

Phytochemical identification test was done for the presence of carbohydrate, proteins, and tannins. As described elsewhere, aqueous solution (1%) of the extracted pectin was used for the chemical characterization (Tyagi, 2016). The test for carbohydrate was done using a few drops of Molisch reagent added to 3 ml of extract, then drops H_2SO_4 on the sides of the test tubes. The ring formation at the liquid junction shows the presence of carbohydrate. Two drops of 3% copper sulphate and few drops of 10% sodium hydroxide were added to 1 mL of extract, violet or red color formation shows the presence of proteins (Murthy *et al.*, 2016; Kancherla *et al.*, 2019).

4.2.4.4. Solubility Studies

The solubility properties of pectin were determined at 25 ℃ in hot water (50 ℃), cold water (0-8 ℃), chloroform, acetone, and ethanol. One gram of pectin powder was added to 50 ml of each solvent and allowed to stand overnight. The percentage solubility was then calculated using equation 4.8 (Frederick *et al.*, 2021).

$$\%\ \text{Solubility} = \frac{\text{Soluble mass}}{\text{Initial weight}} x100\% \quad \text{..... Equation 4.8}$$

4.2.4.5. Moisture Sorption Study

Two grams of pre-dried pectin was transferred to five Petri dishes, further dried, weighed, and transferred into a pyrex desiccators filled with distilled water (100%RH), a saturated NaCl solution (75.6%RH) and the appropriate amounts of NaOH (24.66%, 31.58% and 40%) to achieve different relative humidity (RH) chambers of 60%, 40% and 20% RH, respectively. The samples were kept in equilibrium for four weeks at room temperature. After four weeks, each sample was withdrawn and weighed. Finally, the moisture uptake of each sample was determined by comparing the

weights of the pectin before and after adjusting the equilibrium to a specific RH chamber (Chomto and Nunthanid, 2017).

4.2.4.6. pH and Viscosity measurements

The pectin was weighed and dissolved in water to obtain a 1% (w/v) solution. Then, the pH of the prepared solution was determined using a digital pH meter (HANNA Instruments Ltd, Romania, Europe) in triplicate measurements (Srivastava and Malviya, 2011b).

Brookfield Viscometer (BROOKFIELD CAP 2000+ viscometer) was used to determine the viscosity of the sample. First, pectin solutions were prepared at 2%, 4%, 6%, 8%, 10%, and 12% (w/v) concentration level. Then, the viscosity measurements were taken using spindle number 2 at rotation speeds of 25 rpm and temperature of 25 ℃ (Pasandide *et al.*, 2017).

4.2.4.7. Swelling Index of Pectin Powder

One gram of dried pectin powder was placed in each 100 mL graduated measuring cylinder containing 25 ml of distilled water, HCl buffer of pH 1.2, phosphate buffer of pH 6.8 and 7.4. The solutions were stirred gently until all the powder was hydrated thoroughly. The hydrated pectin was allowed to settle to the bottom and the volume was recorded as V_1. After the addition of equal volume of respective solvents, all measuring cylinders with their contents were left for 24 h and the volume after 24 h was recorded as V_2. Finally, the swelling index was calculated using Equation 4.10 (Weh *et al.*, 2014).

$$\text{Swelling Index (\%)} = \frac{\text{V2} - \text{V1}}{\text{V1}} \times 100\% \ldots\ldots\ldots\ldots\ldots\ldots\ldots \text{Equation 4.10}$$

4.2.4.8. Ash Value

The ash value was determined by the method indicated elsewhere (Wathoni *et al.*, 2019). 0.5 g of pectin was weighed and put in a silicate crucible. Then, it was placed in a furnace (CARBOLITE, OAF 11/1, England) at a temperature of 600 ℃ for 4 h until constant weight is obtained. The ash content was determined from Equation 4.11

$$\text{Ash Content (\%)} = \frac{\text{Weight of } ash(\text{gm})}{\text{Weight of Pectin (gm)}} \times 100\% \ldots\ldots \text{Equation 4.11}$$

4.2.5. Drug-Excipient Compatibility Studies

4.2.5.1. FTIR Spectroscopy

Fourier transform infrared (FT-IR) spectroscopy (FTIR-8400S, SHIMADZU, and Japan) was used to determine the main functional groups of pectin and its compatibility with the drug. Initially, 1 g of furosemide, 1 g of pectin, and using mortar and pistle 1:1 combination of the pectin with furosemide were prepared. Then, 1 gm of the samples were placed on the KBr disk pellet face and the other plate placed above. The spectra was obtained from the spectrometer by scanning the sandwiched sample at the wavelength 4000-450 cm^{-1} (Pasandide *et al.*, 2017).

4.2.5.2. Differential Scanning Calorimetry (DSC)

DSC (PerkinElmer DSC 4000) was used to determine the nature, compatibility, purity, and the physical properties of the pectin. One gram of the pure drug, the pectin, and their 1:1 mixture were prepared and placed onto the aluminum pan under the nitrogen gas. Heating of sample was done from 40 to 450 ℃ with a rate of 10 ℃/min for evaluation of the compatibility between the drug and pectin (Barbosa *et al*., 2021).

4.2.6. X-ray Diffraction (XRD) Analysis

The diffraction pattern of the pectin powder was investigated using X-ray diffractometer (XRD-7000 X-ray diffractometer MAXima, SHIMADZU Corporation, Japan) at 40 KV to determine the crystalline or amorphous nature of pectin. The crystallinity index was then determined as a percentage by using Eq. 2.4 (Park *et al*., 2009). The area was calculated using Origin 7 software (Origin Lab Corporation, MA, and USA) (Wang *et al.*, 2016).

$$\%\ Crystalinity = \frac{Total\ area\ of\ crystalline\ form}{Total\ area\ of\ crstalline\ and\ amorphous\ form} \times 100 \ldots Equation\ 4.12$$

4.2.7. Micromeritic Properties of *Citrus Aurantifolia* Peel Pectin Powder

4.2.7.1. Flow Rate

A 30 g sample was weighed and allowed to flow through a funnel that was positioned 10 cm above the base. The duration it took for the powder to travel through the funnel was then recorded (Rosland Abel *et al.*, 2020). The experiment was done in triplicate for each of the formulations and the flow rate was determined by Equation 4.13.

$$Flow\ rate = WG/FT \ldots\ldots\ldots\ldots\ldots\ldots\ldots\ldots\ldots\ldots\ldots\ldots \text{Equation 4.13}$$

Where, WG is the weight of the powder and FT is the flow time for the powder.

After the flow rate measurement, the height (h) and radius of the powder heap (r) was measured and the angle of repose (θ) was then calculated using Equation 4.12 (Fatohy and Abdul-rasool, 2013).

$$\theta = \tan^{-1}(h/r) \ldots\ldots\ldots\ldots\ldots\ldots \text{Equation 4.12}$$

4.2.7.2. Bulk Density and Tapped Density

The bulk density (BD) and tapped density (TD) were determined by introducing 30 g of the pectin powder into a 100 ml measuring cylinder and the volume occupied by the powder was recorded. The tapped density was determined with continued tapping (500 times within 4 minutes) using tapped densitometer (ERWEKA, SVM 20, Germany). BD and TD were determined in triplicate measurement and the values were calculated by using Equations 4.14 & 1.45, respectively (Srivastava *et al*, 2010).

$$\text{BD} = \frac{\text{Weight of the powder}}{\text{Volume Before Tapping}} \ldots\ldots\ldots\ldots\ldots\ldots\ldots\ldots \text{Equation 4.14}$$

$$\text{TD} = \frac{\text{Weight of the powder}}{\text{Tapped Volume of Packing}} \ldots\ldots\ldots\ldots\ldots\ldots\ldots\ldots \text{Equation 4.15}$$

4.2.7.3. Carr's Index and Hausner Ratio

The Carr's compressibility index and the Hausner ratio were calculated from the previously determined densities of the pectin powder using Equations 4.16 & 4.17, respectively (Value *et al*, 2015).

$$\text{Carr's Index} = \frac{\text{Tapped density} - \text{Bulk density}}{\text{Tapped density}} \times 100\% \ldots\ldots\ldots\ldots \text{Equation 4.16}$$

$$\text{Hausner Ratio} = \frac{\text{Tapped density}}{\text{Bulk density}} \ldots\ldots\ldots\ldots\ldots\ldots\ldots\ldots \text{Equation 4.17}$$

4.2.8. Granule Preparation

Wet granulation method was used to prepare granules. The granules were prepared by initially mixing all necessary ingredients (**Table 2**) (furosemide, *Citrus aurantifolia* peel pectin, $NaHCO_3$,

HPMC) except magnesium stearate and talc using turbula mixer (Willy A. Bachofen AG, Turbula 2TF, Basel, Switzerland). Subsequently, using hydroalcoholic solvent (96% alcohol and distilled water mixture at 3:7 ratio) as a granulating fluid, the powder mixture was triturated in mortar and pestle to obtain a wet mass. Then, the wet blend was allowed to pass through a 1.6 mm sieve (ERWEKA, Type AR 401, Germany) and moved to the Petri dish. Afterwards, the samples were dried in an oven (Kottermann® 2711, Germany) at 105 ℃ for 1 hr and passed through 1mm sieve (ERWEKA, Type AR 401, Germany) to break the aggregates and achieve more uniform granule size. Finally, the dried granules were mixed in Turbula mixer (Willy A. Bachofen AG, Turbula 2TF, and Basel, Switzerland) with the rest of the ingredients (magnesium stearate & talc) (Salbu, 2011).

Table 2: Composition of granules for preparing furosemide matrix tablets.

Ingredients	Amount (%)
Pectin	10, 20, 30, 40
HPMC	10, 20, 30, 40
$NaHCO_3$	5,10, 20
Mg stearate	1
Talc	1
Lactose	q.s to 100
Net weight of each tablet	250 mg

q.s stands for the quantity sufficient

4.2.9. Characterization of the Granules

4.2.9.1. Density, Flowability and Compressibility Properties of the Granules

Granules were evaluated for all pre-compression parameters including angle of repose, bulk density, tapped density, bulkiness, Hausner's ratio and compressibility index, which were determined using the procedures and equations applied for the pectin powder characterization (Arun *et al.*, 2020).

4.2.9.2. Granule Size Distribution and Mean Granule Size

It was determined using a standard sieving method as described by Shekunov *et al*. (2007). Accordingly, 30 g of the granule was added to a set of sieves (ERWEKA, Type AR 401, Germany) arranged with the highest mesh wire size at the top and the least size at the bottom. After shaking the sieves for 2 min, the granule retained in each sieve was weighed and expressed as a percentage. The procedure was repeated three times for all batches and the average value was calculated with the standard deviation.

4.3. Formulation and Evaluation of Tablets

4.3.1. Formulation of Matrix Tablets

The prepared granules were compressed into round, flat matrix tablets using a tablet compressor (Manesty machines, England). The tablets were formulated using pectin and HPMC as polymer, $NaHCO_3$ as gas forming agent, lactose as a diluent, talc and magnesium stearate as lubricant and glidant, respectively. The concentration proportion of each ingredient for the different formulations is presented in **Table 3**.

Table 3: Composition of floating and bioadhesive matrix tablets for preliminary studies

	Ingredients (%)						
Formulation code	**Furosemide API**	**Pectin**	**HPMC K4M**	**$NaHCO_3$**	**Lactose**	**Talc**	**Mg Stearate**
PF1	16%	10%		10%	62%	1%	1%
PF2	16%	20%		10%	52%	1%	1%
PF3	16%	30%		10%	42%	1%	1%
PF4	16%	40%		10%	32%	1%	1%
PF5	16%		10%	10%	62%	1%	1%
PF6	16%		40%	10%	32%	1%	1%
PF7	16%	5%	5%	10%	62%	1%	1%
PF8	16%	2.5%	7.5%	10%	62%	1%	1%
PF9	16%	7.5%	2.5%	10%	62%	1%	1%
PF10	16%	20%	20%	10%	32%	1%	1%
PF11	16%	30%	10%	10%	32%	1%	1%
PF12	16%	10%	30%	10%	32%	1%	1%
PF13	16%	40%		5%	37%	1%	1%
PF14	16%	40%		20%	22%	1%	1%
PF15	16%		40%	5%	37%	1%	1%
PF16	16%		40%	20%	22%	1%	1%

4.3.2. Evaluation of Furosemide Floating and Bioadhesive Matrix Tablets

4.3.2.1. Friability

Friability testing was conducted using a tablet friability tester (ERWEKA, GERMANY). As per the pharmacopeial recommendation, pre weighed 20 tablets were rotated at 25 revolutions/min for 4 min and dedusted. The percentage weight loss was calculated as percentage friability using Equation 4.18 (USP43-NF38, 2020).

$$\% \text{ Friability} = \frac{\text{Wo} - \text{Wt}}{\text{Wo}} \times 100 \ldots\ldots\ldots\ldots\ldots\ldots\ldots\ldots \text{ Equation 4.18}$$

where, % F= percent friability, W_o = initial weight of 20 tablets, W_t = final weight of 20 tablets.

4.3.2.2. Weight Variation

The weight variation was evaluated by selecting 20 tablets from each batch and weighing separately using an electronic balance (ADAM, AAA 160L analytical balance). The average weights along with standard deviation were taken to determine the weight variation (Tamizharasi *et al*, 2011).

4.3.2.3. Diameter, Thickness and Hardness Determination

The diameter, thickness and hardness of the prepared tablets were determined by selecting 10 tablets from each batch using the same apparatus (Sotax HT, Model: HT 1,500 N, Switzerland) and the results were expressed as mean values with standard deviation (USP<1217>, 2021).

4.3.2.4. *In vitro* Buoyancy Study /Floating Lag Time & Total Floating Time/

Randomly selected 10 tablets from each formulation were kept in a 100 ml beaker containing simulated gastric fluid pH of 1.2 as per USP (USP43-NF38, 2020) at 37 ℃. The time taken for the tablets to rise to the surface and float was taken as Floating Lag Time (FLT). The duration of time the dosage form constantly remained on the surface of medium was determined as the Total Floating Time (TFT). The floating time of the tablets was observed for 12 h (Daisy *et al*., 2012).

4.3.2.5. Swelling Index and diameter

To study the swelling index, the method described elsewhere was used with some minor modifications (Tanwar *et al* , 2021). Initially three tablets from each formulation batch were taken

and weighed (W_0). Then, the tablets were added to a glass beaker (200 ml) that contains 0.1N of HCl at temperature of 37 ± 1 ℃. The tablets were taken out from the beaker carefully by removing the apparent liquid with tissue paper at fixed time interval up to 12 hr and the swelling behavior of the formulated tablets were studied three times for taking the average and standard deviation values. The weight of the swollen tablets was measured (Wt) and the swelling index percent was calculated by Equation 4.19:

$$\mathrm{SI}(\%) = \frac{\mathrm{Wt} - \mathrm{Wo}}{\mathrm{Wo}} \times 100 \ldots\ldots\ldots\ldots\ldots\ldots\ldots \text{ Equation 4.19}$$

Where, SI is swelling index, Wt is weight of swollen tablet at time t, W_0 is initial weight of tablet

The swollen tablet diameters were measured at 1 hr and 12 hr three times using a sliding caliper scale (Nippon Sokutei,Japan).

4.3.2.6. Matrix Integrity

Matrix integrity was determined by observing the intactness of the tablets during the *in vitro* dissolution studies and whether or not the swollen mass of the tablets remain intact was checked (Shinde *et al*., 2010).

4.3.2.7. Bioadhesive Strength

The bioadhesive strength determination was done using adjusted two-arm balance as shown in **Figure 5**. One side of the balance was used to hold the water and the other side was used to hold the glass vial. A small amount (3×3 cm) of fresh sheep stomach was purchased from the slaughter house and stored at 4℃ to be utilized as a simulated mucosal membrane within 3 hours after removing unnecessary fat and tissues from the mucosa using knife. The sheep stomach was tied to reversed 100-mL beaker and positioned to a larger beaker which has 250 ml holding capacity. Then after, 0.1N HCl simulated gastric fluid was poured into the larger beaker up to the edge of reversed beaker and kept the sheep stomach mucosa vulnerable to the simulated fluid. The matrix tablet was then attached to a glass vial using adhesive plaster. The glass vial with attached tablet was set aside to inverted beaker containing stomach mucosa for 5 min by using 50 g load weight to ensure a good bonding between the tablet and the mucosa. Then, the preload weight was detached from the vial and water was poured to the other side of the empty beaker. The addition of water was stopped when the tablet was detached from the simulated sheep mucosa. The amount

of water required to detach the tablet from the mucosa was considered as a bioadhesive strength. The investigation was done three times and the values reported as mean with standard deviation (Yusif *et al.*, 2015).

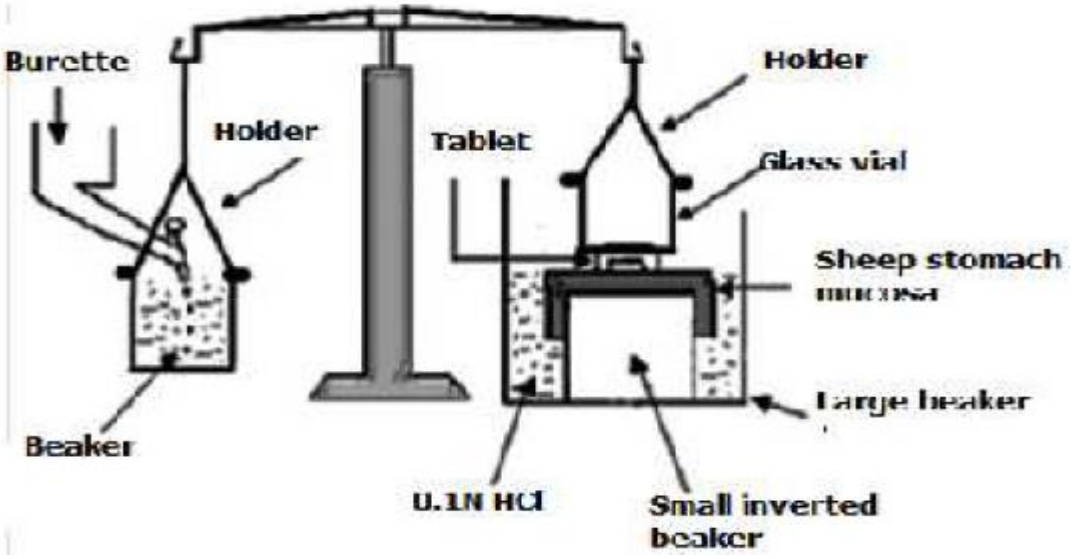

Figure 5: Schematic representation of bioadhesive strength measurement (Nigusse, Gebre-Mariam and Belete, 2021).

4.3.2.8. Mucoadhesion Time

The mucoadhesion time was measured by using the modified USP disintegration test apparatus (2T 504, Erweka, Germany). The experiment was conducted by adding 800 ml of 0.1N HCl to the beaker kept at 37 ℃. The small portion of sheep stomach 2.5 × 2.5 cm was attached to the glass slide using cyanoacrylate adhesive. One side of the tablet was moistened using 50 µL of 0.1 N HCl and the tablet was attached to the center of the sheep stomach by applying a slight force with a point finger for about 20 seconds and dipped into the solution containing 0.1 N HCl. After 5 min, the glass slide containing the tablet was taped vertically to the disintegration apparatus and adjusted to move up and down with 25 revolutions per min. The time by which a tablet separated from its attachment on the spindle was noted as the mucoadhesion time for the tablet from the mucosa. The investigation was performed three times to get the average values (Nigusse *et al*, 2021).

4.3.2.9. Calibration Curve Construction

Initially, before constructing the calibration curve, the maximum absorption of furosemide was investigated by UV/Visible spectroscopy (T92+ Spectrophotometer, PG Instruments limited, UK) from the prepared stock solution using 0.1M HCl and of 0.1N NaoH as medium.

The absorbance maxima of pure furosemide were also determined by dissolving 25 mg of the powder in a flask that were capable of containing 250 ml of fluid using 0.1N HCl as a medium in order to get a stock solution of 10 mg/100 ml. The 10 ml of the prepared stock solution was diluted to 100 ml to get 1 mg/100 ml and the sample maximum absorbance was investigated from 200-400 nm wavelength range by the UV/Visible spectrophotometer and it was found to be 235.5 nm. Then, the samples were prepared from the stock solution of 10 mg/100 ml such as 4 µg/ml, 6 µg/ml, 8 µg/ml, 10 µg/ml, 12 µg/ml, 14 µg/ml, 16 µg/ml 18 µg/ml, and 20 µg/ml and scanned at the predetermined wavelength (USP<1217>, 2021).

The maximum absorbance of furosemide was determined by dissolving 100 mg of the powder in 100 ml of volumetric flask using 0.1M of NaOH. The volume of the dissolving fluid was added until 100 ml to obtain 1mg/ml of the solution. Then, the sample was checked by the UV/Vis spectrometer from 200-400 nm for its maximum wavelength (λ_{max}) and found to be 239 nm. After that, calibration curve was constructed from 0.1M of 100 mg/100 ml NaOH of the stock solution with various concentrations (8 µg/ml, 10 µg/ml, 12 µg/ml, 14 µg/ml, 16 µg/ml, 18 µg/ml, and 20 µg/ml) at predetermined maximum absorption (USP<1217>, 2021). The calibration curve was then plotted from the absorbance readings as concentration versus absorbance. Finally, the calibration curve was plotted as shown in **Figure 6**.

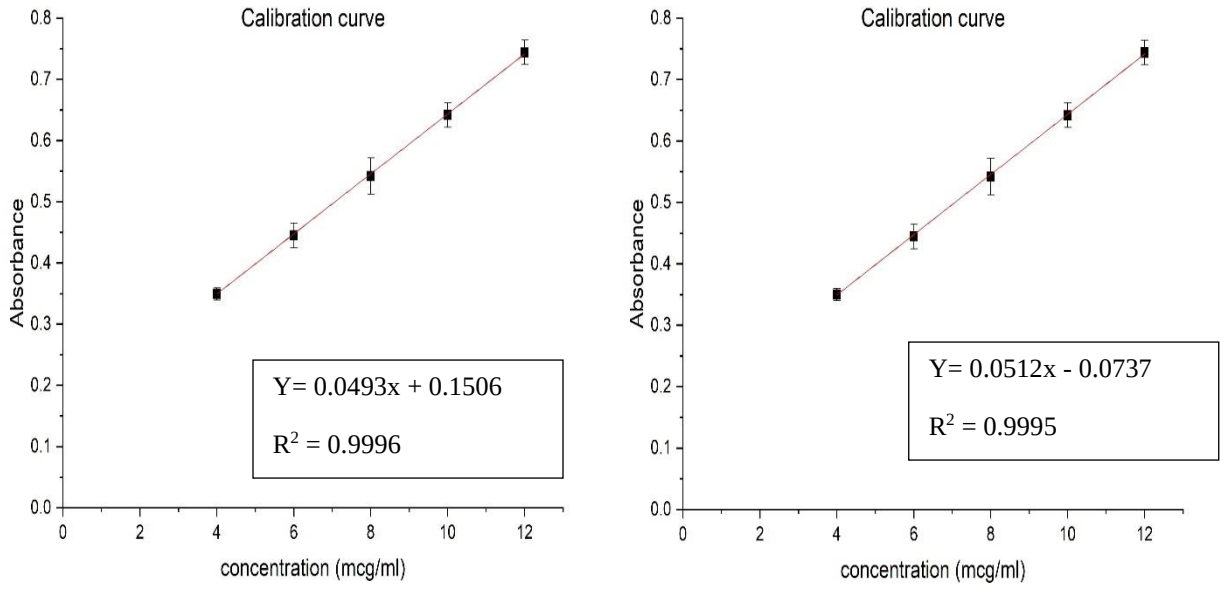

(a) (b)

Figure 6: Calibration curve of furosemide reference standard in different dissolution media (a) 0.1N HCl solution, (b) 0.1N NaOH solution.

4.3.2.10. Drug Content Assay

Twenty tablets from each batch were randomly selected and powdered with mortar and pestle. Then, an equivalent of 0.2 g of powdered furosemide was taken and added into 500 ml volumetric flask containing 300 ml of 0.1N NaOH. After 10 min of shaking, the solution was made to volume by adding 0.1M NaOH and filtered. From the filtered solution, 5 ml sample was taken and diluted to 250 ml with 0.1M NaOH and the absorbance of the resulting solution was measured at wavelength of maximum absorption (λ_{max} = 239 nm) using UV/Vis spectrophotometer and converted into concentration using the previously determined equation (USP43-NF38, 2020).

4.3.2.11. *In-vitro* Drug Release

The *in vitro* drug release studies were conducted using USP type II dissolution apparatus (Pharma test type PTDTT, Germany) at 50 rpm. The dissolution media was 900 ml of 0.1 N HCl at temperature of 37±0.5 ℃. An aliquot sample of 5 ml was withdrawn from each dissolution vessel at 0.25, 0.5, 1, 2, 3, 4, 6, 8, 10, and 12 h and each withdrawn sample was replaced with an equal volume of fresh dissolution medium which was kept at 37±0.5 ℃ to maintain the sink condition.

The withdrawn samples were filtered through a filter paper of 0.45 μm size and were then analyzed spectrophotometrically at maximum wavelength of 235.5nm (USP43-NF38, 2020).

4.4. Analysis of Kinetics and Mechanism of Drug Release

The dissolution data were fitted into zero order, first order, Higuchi, Hixson-Crowell and Korsmeyer-Peppas kinetic models in order to evaluate the rate and mechanism of drug release from prepared matrix tablets (Arun *et al.*, 2020). The order and mechanism of drug release from the matrix system were determined based on the regression (R^2) values of the fitted data in the respective kinetic models (Singh *et al*., 2020).

4.4.1. Zero Order Release Model

The drug release from zero order kinetics remains constant or predetermined amount of drug is released from the dosage form independent of the drug plasma concentration (Equation 4.20).

$$Q = Q_o - K_o.t \quad \text{Equation 4.20}$$

where, Q_o is the initial amount of drug, Q is amount of drug remaining at time t, K_0 is zero-order rate constant expressed in units of concentration/time and t is the time (Singh *et al*., 2020).

4.4.2. First Order Release Kinetic Model

The first order kinetics follows concentration dependent release by which the release of the drug from the dosage form depends on the amunt of drugs remaining in the dosage form (Weh *et al.*, 2014).

$$\log Q = \log Q_0 - K_1 t / 2.303 \quad \text{Equation 4.21}$$

Where, Q_o is the initial amount of drug, Q is amount of drug released at time t and K_1 is first order release constant (Arun *et al.*, 2020).

4.4.3. Higuchi Square Root Model

This model makes several key assumptions, including that the initial drug concentration in the matrix is much higher than the drug's solubility, that drug diffusion only occurs in one dimension (the edge effect must be negligible), that the drug particles are much smaller than the system thickness, that matrix swelling and dissolution are negligible, that drug diffusivity is constant, and that perfect sink conditions always exist in the release environment (Singh *et al*., 2020).

$$Q_H = K_H.t^{-1/2} \ldots\ldots\ldots\ldots\ldots\ldots\ldots\ldots\ldots\ldots\ldots\ldots \text{Equation 4.22}$$

Where, Q is amount of drug released at time t and K_H is the Higuchi constant

4.4.4. Hixson-Crowell Cube Root Model

The equation describes the amount of drug released from systems where the surface area and diameter of the particles or tablets fluctuate. Data from *in vitro* drug release tests were shown as the cube root of drug % remaining in matrix against time to analyze the release kinetics (Singh *et al*., 2020).

$$Q_0^{1/3} - Q_t^{1/3} = K_{HC}.t \ldots\ldots\ldots\ldots\ldots\ldots\ldots \text{Equation 4.23}$$

Where, Q_t is the amount of drug released in time t, Q_0 is the initial amount of the drug in the tablets and K_{HC} is the rate constant for Hixson-Crowell rate equation.

4.4.5. Korsmeyer–Peppas Model

In order to find out the mechanism of drug release from the polymeric tablets, the first 60% drug release data were fitted to the Korsmeyer–Peppas model:

$$M_t / M_\infty = Kt^n \ldots\ldots\ldots\ldots\ldots\ldots\ldots\ldots\ldots\ldots\ldots\ldots\ldots\ldots\ldots\ldots \text{Equation 4.24}$$

Where, M_t is the amount of drug released at time t, M_o is the amount of total drug in tablets, M_t/M_o is the fractional drug release at time t, K is a constant incorporating the structural and geometric characteristics of the matrix tablets and n is a diffusional exponent, indicative of the drug release mechanism (Weh *et al.,* 2014).

4.5. Formulation Optimization by Response Surface Methodology

4.5.1. Experimental Design

The optimization study was conducted using central composite design (CCD) as it is the most reliable method for analyzing the impact of different independent variables on the response variables and to obtain the optimized values of different responses. The total number of experiments was determined using $2^K + 2k + n$ formula, where k is the number of independent variables and n is the number of repetitions at the center point. The amount of pectin concentration

(X_1) and $NaHCO_3$ concentration (X_2) were found to be the independent variables (k=2) as per the preliminary study. Hence, with k value of 2, the total run was calculated as (2^2 x (2×2) +5) = 13. The 13 formulations as per the CCD are shown in **Table 4**. The five coded values were used in this study (**Table 5**) with constant levels of API, talc and magnesium stearate and a constant tablet weight of 250 mg was adjusted (**Table 6**).

Table 4: Factor combination for formulation of Furosemide (40 mg) matrix tablets as per Central Composite Design

Formulation Code	Space Type	Pectin conc. (%)	$NaHCO_3$ conc. (%)	Coded factors level	
				X_1	X_2
F1	Factorial	10	5	-1	-1
F2	Factorial	40	5	+1	-1
F3	Factorial	10	20	-1	+1
F4	Factorial	40	20	+1	+1
F5	Axial	3.7868	12.5	- α	0
F6	Axial	46.2132	12.5	+α	0
F7	Axial	25	1.8934	0	-α
F8	Axial	25	23.1066	0	+α
F9	Central	25	12.5	0	0
F10	Central	25	12.5	0	0
F11	Central	25	12.5	0	0
F12	Central	25	12.5	0	0
F13	Central	25	12.5	0	0

Table 5: Translational code for levels in actual units

Coded levels	-α	-1	0	+1	+α
X_1, amount of Pectin concentration (%)	3.7868	10	20	40	46.2132
X_2, amount of $NaHCO_3$ concentration (%)	1.8934	5	12.5	20	23.1066

α = 1.414

Table 6: Formula for the preparation of furosemide 40 mg matrix tablets as per Central Composite Design

Ingredient	Formulation code and composition (mg/tab)												
	F1	F2	F3	F4	F5	F6	F7	F8	F9	F10	F11	F12	F13
Furosemide	40	40	40	40	40	40	40	40	40	40	40	40	40
Pectin	25	100	25	100	9	115	62	62	62	62	62	62	62
$NaHCO_3$	12	12	50	50	31	31	4	57	31	31	31	31	31
Lactose	167	92	130	55	164	58	137	165	111	111	111	111	111

Mg. Stearate	2.5	2.5	2.5	2.5	2.5	2.5	2.5	2.5	2.5	2.5	2.5	2.5	2.5
Talc	2.5	2.5	2.5	2.5	2.5	2.5	2.5	2.5	2.5	2.5	2.5	2.5	2.5
Total Weight	250	250	250	250	250	250	250	250	250	250	250	250	250

4.5.2. Validation of the Experimental Design

The software prediction result was compared with the actual investigation results obtained to confirm whether the predicted values are best suited with the actual investigation. The deviation or relative percent error was calculated using Equation 4.22 (Sathish *et al.*, 2016).

$$\%\ \text{Relative error} = \frac{\{\text{Predicted Value} - \text{Experimetal Value}\}}{\text{Predicted Value}} \times 100 \ldots \text{Equation 4.25}$$

The response variable results such as floating duration, bioadhesive strength, swelling index, drug release at 1 hr and the release rate results were employed to validate the design.

4.5.3. Statistical Analysis

The experimental results were statistically analyzed using Origin pro 2021 Software (OriginLab Corporation, MA, and USA) and One way ANOVA was employed to associate the results. The optimization study was done using Design-Expert 10.0.7.0 software (Stat-Ease Inc., Minneapolis, MN, USA) for evaluating the impact of independent variables on the response variables and to get the optimized level of the variables at 95% confidence interval with a P value < 0.05. The experimental result data was analyzed by using the design of expert software using the 3D response surface methodology to determine the effect of a particular formulation factors on the response variables (Lee and Choo, 2020).

5. RESULTS AND DISCUSSION

5.1. Properties of the Extracted Pectin

The peel was obtained by peeling the *Citrus aurantifolia* fruit from the tree. The peel was taken from the ripe and unripe fruit in order to compare their yield. It was then washed, dried, extracted using acidic water (HCl) and ethanol, dried and crushed to obtain uniform pectin powder for use as a tablet polymer (see **Figure 7**).

(a) (b) (c)

Figure 7: Extraction process of *Citrus aurantifolia* peel pectin: (a) Picture of collected peel; ripe (yellow) and uripe (green); (b) Picture of the pectin extraction process; (c) Picture of dried and purified pectin powder (taken by Ebrahim Abdela Siraj).

5.1.1. Yield and Some Other Physicochemical Properties of Pectin

The percentage yield of pectin from the ripe vs unripe *Citrus aurantifolia* peel was found 24.02% and 34.4%, respectively. The color of isolated pectin was light-yellow color (Figure 7) and the pH was determined to be 4.6 ± 0.03. The yield is comparable with *Citrus sinensis* (29.4%), and *Citrus limetta* (32.42%) and (36.71%) for *Citrus limon* (Kanmani *et al.*, 2014). It showed higher pectin yield when compared to another citrus lemon (20.8%) and mango peel waste (13.04%) studies (Chaiwarit *et al*., 2020b; Beyech and Abdissa, 2021). The *Citrus aurantifolia* fruit has thick peel that might have contributed to the higher yield of pectin compared to some other sources. Beyond the species difference, the pectin yield is also largely affected by the extraction time, solvent, the pH and temperature employed for the extraction process. When pectin exposed for higher temperature and extended extraction time would result decomposition. In acidic medium (low

pH), the solvent contains higher concentration of hydrogen ion sufficient to promotes the hydrolysis of protopectin (pectin and cellulose). Hence, extraction at low pH improves the release of pectin molecules from the peel during acid-washing stage. In addition, the acid type strongly affects the macromolecular behavior as well as the gelling characteristics of extracted pectin (Shaha *et al*, 2013). Moreover, pectin yield reduces when the fruit maturity rises (Twinomuhwezi *et al*, 2020) which is similar to findings obtained from *Citrus aurantifolia* peel. The dragon fruit peel (15.12%), passion fruit (13.18%), apple pomace (10-15%), sun flower (11.6%), and peach pomace (9.68%) demonstrated lower pectin yield than citrus fruits (Dao *et al*, 2021). Therefore, *Citrus aurantifolia* waste peel can be the worthy alternative source of pectin. The result from other studies revealed that the color of pectin is different from species to species which may range from reddish purple (elderberry and black currant) to yellow (citrus and apple) (Cserjési *et al.*, 2011). The color of pectin might be differing due to the presence of impurities, environmental condition, the fruit type and individual errors (Mohamed, 2016). The pH of peel pectin extracted in this study is in line with other study reports from mango peel pectin (pH=4.15), citrus lemon (*Citrus limon*) (pH=4.1), grape fruit (*Citrus paradisi*) (pH=3.6) and sweet orange (*Citrus sinensis*) (pH=4.0) (Farooq *et al*, 2014; Boakye-Gyasi *et al.*, 2021). The pH value of pectin ranges from slightly acidic to neutral values which renders it to be non-irritant to the GI mucosa (Frederick *et al*., 2021).

The ash value of *Citrus aurantifolia* peel pectin (2.29 ± 0.48) was lower than the standard (3.77% ± 0.29) and higher than *Citrullus lanatus* (1.24%) (Pérez *et al*, 2022). A result reported by Sato *et al*. (2011) on apple pomace shows almost similar ash value (2.03% ± 0.13) with the results obtained with the study on apple pomace pectin. The lower level of the total ash content shows the lower extent of impurities in the pectin. The phytochemical content of the extracted pectin indicated the presence of carbohydrate, and the absence of hexose, gums, proteins, mucilages, fats, amino acids and oils. This result is in line with banana and mango peel pectin except the presence of hexose sugar in banana peel pectin (Bansal *et al*., 2014; Farooq *et al*., 2014). The physicochemical properties of the purified citrus peel pectin are summarized in **Table 7**.

Table 7: Physicochemical properties of pectin powder extracted from *citrus aurantifolia* peel.

Parameters	**Values**
Yield (%)	
Ripe	24.02 ± 0.33
Unripe	34.4 ± 0.10
Color	Light Yellow
pH	4.6 ± 0.11
Total ash determination (%)	2.29 ± 0.48
Phytochemical studies	
Carbohydrates	+
Hexose Sugar	_
Proteins	_
Fats and oils	_
Amino acids	_
Mucilage	_
Gums	_

+ Present, - Absent

The solubility study of isolated pectin revealed that it is practically insoluble in methanol, acetone, chloroform, and cold water while it is soluble in hot water, in 2% concentration of pectin (**Table 8**). These results are similar with the study conducted on mango peel pectin (Farooq *et al*, 2014). Solubility is very important physical parameter to characterize the polymer properties which determine its utilization as a pharmaceutical excipient. The extreme solubility of the polymers in hydrophilic environment is not a desirable characteristic for the polymers to be used in modified release dosage forms or suspending agents. Several reports showed that many of the pectin isolated from various genotype are less soluble in hydrophilic vehicles which renders it as a good alternative polymer for modified release formulation (Boakye-Gyasi *et al.*, 2021).

Table 8: Solubility of the pectin powder extracted from *Citrus aurantifolia* peel.

Types of Solvent	**Solubility Characteristics**	**% Soluble mass**
Ethanol	Insoluble	0
Acetone	Insoluble	0
Chloroform	Insoluble	0
Cold Water	Swells and forms a gel	0
Hot Water	Soluble	100

5.1.2. Chemical Characterization of Pectin

The methoxyl content (MeO) of pectin is important to control the gel strength, the setting time, the sensitivity to metal ions and to determine the functional properties of pectin solutions and pectin gel texture. The methoxyl content (MeO) values are recommended to be (0-8%) for low methoxyl (LM) content or (8-15%) for high methoxy (HM) pectin. The degree of esterification (DE) indicates the percentage of carbonyl groups that are esterified with methanol. DE compares the amount of methyl-esterified D-galacturonic acid (GalA) units with the total number of GalA. DE value greater than 50% shows the presence high methoxy group pectin. LM pectin forms a gel with multivalent cations such as calcium and aluminum while HM pectin forms a gel with sugar and acid (Raj, 2012; Sundarraj & Ranganathan, 2017; Belkheiri *et al*., 2021). In acidic medium, the carboxyl groups are changed to nonionized carboxylic acid groups, consequentially shows in a reduction in the number of negative charges. This effect decreases the attraction of pectin with water molecules and also reduces the repulsion forces between pectin molecules each other. The presence of sugar reduces the pectin hydration due to the competition for the aqueous molecules. Pectin isolated from sugar beet possess feruloyl ester substituents on the side chains, up on oxidization using peroxidase the gel formed showed excellent water absorbing capacity (50 to 160 times) than dry gel (Tibbits *et al*, 1998; Sriamornsak, 2011). The titration techniques were used to chemically characterize the extracted pectin and the results are shown in **Table 9**. The results from methoxyl content (13.84%) and degree of esterification (85.49%) indicated that the extracted pectin is high methoxy pectin. The % AUA result shows that the extracted pectin has higher purity as % AUA level is suggested to be not less than 65% for the application in pharmaceutical or food industries. This result is also comparable with papaya (*Carica papaya*) Linn citrus peel pectin (Altaf *et al.*, 2018), banana peel (Twinomuhwezi *et al*, 2020) and Moroccan citrus peel (El Fihry *et al.*, 2022). High methoxy nature of the pectin enables to form a gel with sugar or acidic environment.

Table 9: Chemical property of pectin extracted from *citrus aurantifolia* peel.

Physicochemical properties of pectin	**Value (***mean ± SD: (n=3)***)**
Equivalent Weight (%)	81.50 ± 0.50
Methoxyl Content (%)	13.84 ± 0.35
Anhydrouronic Acid Content (%)	91.68 ± 0.17
Degree of Esterification (%)	85.49 ± 1.10

5.1.3. Loss on Drying and Moisture Sorption Determination

The presence of moisture in any component affects the product stability that could largely affect the shelf life. Moisture content affects manufacturing process of the solid formulation (Khamsucharit *et al.*, 2018). Higher moisture content can result in poor powder flow, which could further result in irregular tablet quality parameters. It may also result in sticking problems on the surface of the tableting machine. The acceptance limit of moisture content for pectin powder is 12 % (USP43-NF38, 2020). The moisture content of pectin in the present study was 8.85% ± 0.73, which is within the acceptable range. Other studies also demonstrated that the moisture content of pectin from various citrus peels ranges from 6.4% to 10% (Khan and Bibi, 2015; Mada *et al.*, 2022).

On the other hand, a pharmaceutical excipient's ability to absorb moisture is a crucial characteristic because it affects the chemical and physical stability of dosage forms. It also determines the packing, storage, and choice of packaging materials for both excipients and finished products. The moisture sorption test demonstrates how sensitive a material is to availed moisture from the surrounding. The moisture sorption result of the present study is shown in **Figure 8**. The average moisture sorbed by the pectin powder varied from 2.61% at 20% RH to 10.8% at 100% RH. The increment in moisture absorption by the powder at high RH is probably due to the hydrophilic character of the pectin powder. Though the moisture content shows less hygroscopic nature of the pectin powder, it is advisable to consider mechanisms for preventing moisture absorption during storage as it greatly affects product stability. As water is the best media for microbial growth, higher moisture sorption may lead to dangerous microbiological and physicochemical quality problems for the formulation (Arollado *et al*, 2018). Therefore, it will be wise to store the products in an airtight container at the proper temperature & RH to prevent quality defects.

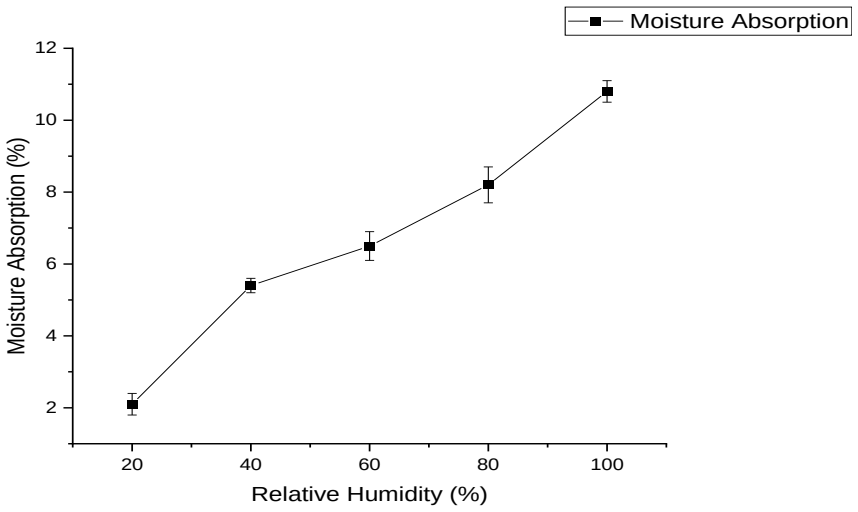

Figure 8*:* Moisture content of pectin extracted from *Citrus aurantifolia* peel at different relative humidity levels.

5.1.4. Viscosity Study

Viscosity is the measure of resistance of a certain fluid to flow. The rate of solvent flow resistance and the rate of drug release from a matrix tablet are both significantly influenced by viscosity. There are some factors responsible for increasing the pectin viscosity such as degree of esterification, temperature, pH, composition, and molecular weight (Hashim, 2018). As depicted in **Figure 9**, the viscosity of extracted pectin increased with increasing pectin concentration that may be due to the increase in composition and esterification. This is may also be due to the reduction of pectin molecule intermolecular distance that shows hydrogen bonding (intermolecular force of attraction and polymer chains entanglement). This demonstrates that when the concentration of pectin in matrix tablets rises, a more viscous gel layer will be formed with the entry of aqueous medium into the matrix. This renders a greater resistance to the erosion of the polymer, and a retarded release rate of the medication can be anticipated. The results are comparable with the other studies done on citrus peel using citric acid. The factors that increase gel strength will increase the tendency to gel, decrease solubility, and increase viscosity and vice versa (Kurita *et al*., 2008; Singh *et al*., 2011). On the other hand, increasing in shear rate, decreases viscosity of the isolated pectin. The hydrophilic solution of pectin showed non-Newtonian flow property, specifically pseudoplastic flow. This may be due to a reduced degree of entanglement or liberation of polymer chains.

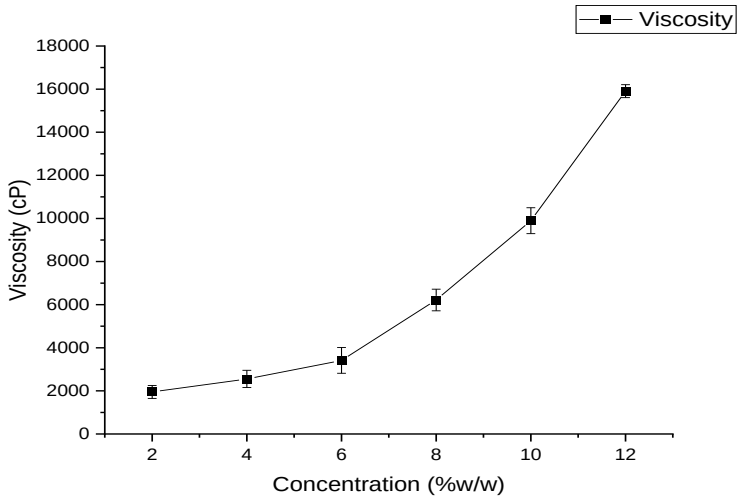

Figure 9: Viscosity of pectin extracted from *Citrus aurantifolia* peel at different concentrations.

5.1.5. Swelling Index

The swelling index of *Citrus aurantifolia* peel pectin was 9.68 ± 0.29%. The result is almost similar with the standard commercial pectin (9.39 ± 0.70%) (Arollado *et al*, 2018). Hydrophilic polymers used as release controlling agents act by hydration and swelling to produce a gel, which gradually becomes eroded to produce a release controlling-property. Polymers with good swelling property exhibit a good release controlling profile. This implies that a hydrophilic matrix with a faster polymer hydration capability will swell up quickly and exhibit better release controlling characteristics (Boakye-Gyasi *et al.*, 2021).

5.1.6. X-ray Diffraction Determination

Powder morphology significantly affects its flow properties, compressibility, drug stability, and dissolution rate. As can be seen in **Figure 10**, the characteristics peak of *Citrus aurantiflia* peel pectin at 20 theta indicates the polysaccharide units and numerous, wide, weak peaks with short-range ordering followed by numerous continuous halo peaks. Hence, this pectin is mostly amorphous in nature with partially crystalline fragments. This is in line with the particle nature of pectin from banana (*Musa sapientum* L) (Hosseini *et al.*, 2019). The crystalline index of the *Citrus aurantifolia* pectin was 30.18% which is below 50%, indicating its amorphous nature. Other reports also showed similar results for extracted pectin from different sources (Yang *et al.*, 2010).

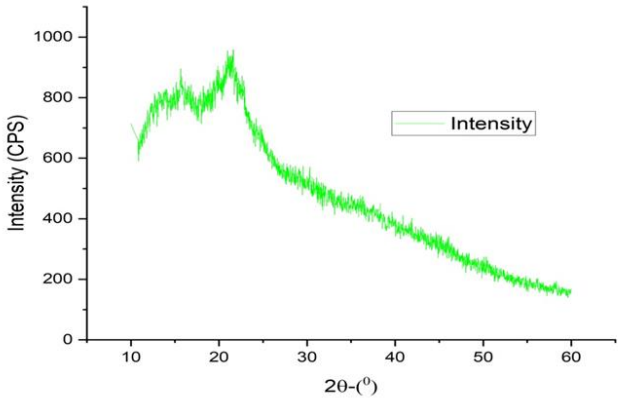

Figure 10: XRD pattern of pectin extracted from *citrus aurantifolia* peel.

5.1.7. Micromeritics Studies of the *Citrus Aurantifolia* Peel Pectin

Excipients with good flowability and low cohesive nature are desirable for pharmaceutical formulations. Density based evaluations including porosity, Hausner ratio and Carr's index are often used to indicate the flow property of powders (USP, 2011; USP43-NF38, 2020). A Carr's index ≤ 10% indicates excellent flow property while ≥ 26% represents poor flow. Likewise, Hausner ratio of less than 1.25 represents excellent flow while greater than 1.5 indicates poor flow (Srivastava and Malviya, 2011a; Boakye-Gyasi *et al.*, 2021) Other parameters such as flow rate and angle of repose are also used to predict the flow property of powders. Angle of repose measures the maximum angle between the surface of the pile powder and horizontal plane. The angle of repose is recommended to be less than 30^0 for good flow (USP43-NF38, 2020). The results of the present study indicated that the extracted pectin powders are poorly flowing and poorly compressible (**Table 10**). Hence, granulation process was employed to improve the flow property and compressibility of the granule.

Table 10: Density related properties of pectin extracted from *Citrus aurantifolia* peel.

Density Related Property	**Value (***mean ± SD: (n=3))*
Bulk Density (g/ml)	0.67 ± 0.004
Tapped Density (g/ml)	0.92 ± 0.009
Carr's Index (%)	36.3 ± 0.702
Hausner's ratio	1.36 ± 0.014
Flow rate (g/sec)	16.42 ±1.215
Angle of repose (φ)	32.78 ± 0.812

5.1.8. Drug-Excipient Compatibility Studies

5.1.8.1. FTIR Determination

The FT-IR spectra of pure furosemide, pectin, and mixture of furosemide and pectin are shown in **Figure 11 (a-c)**. The main peaks of furosemide are observed at 3395 cm^{-1}, peaks at 3347 cm^{-1} and 3254 cm^{-1} indicate stretching vibration of primary amines, 2953 cm^{-1} (acidic OH groups), 1687 cm^{-1} (amino group) and 1540 cm^{-1} (carbonyl group vibrations) (**Figure 11 a**) (Kurita *et al,* 2008). The peaks around 1120 - 990 cm^{-1} represent galacturonic acid of pectin substance. The other bands around 1646 and 1734 cm^{-1} show the ester group C-O stretching (Hosseini *et al.*, 2019). The fingerprint regions of pectin are from 1200-950 cm^{-1} which shows the presence of pyranose cycle vibration and the bands ranging from 1800-1200 cm^{-1} indicate the presence of carboxylic groups in pectin. All these bands are important characteristic bands found in pectin from different plants. Furthermore, the band for non-carboxylic groups of pectin which are located at 1650-1600 cm^{-1} (Lee and Choo, 2020). The peaks 3500–3000 cm^{-1} were due to OH stretching which extensively involved in H-bonding. The characteristic absorption band that was observed at 1736 cm^{-1} is assigned to C=O stretching of methyl ester (COOR) group and a peak around 1600 cm^{-1} is assigned to C=O stretching of COO^- group. It is known that pectin from different sources exhibit high intensity peaks around 1100 cm^{-1} and 1018 cm^{-1} which represents uronic content (**Figure 11 b**) (Owusu *et al*., 2021). The presence of all the characteristic peaks of furosemide and pectin in the mixture suggest that there is no incompatibility between the furosemide and pectin (**Figure 11 c**).

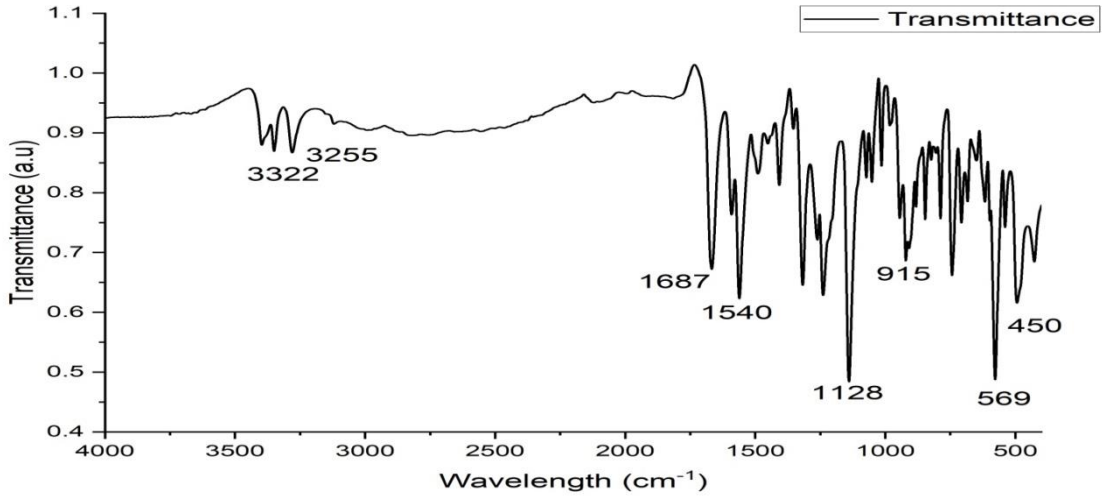

(a)

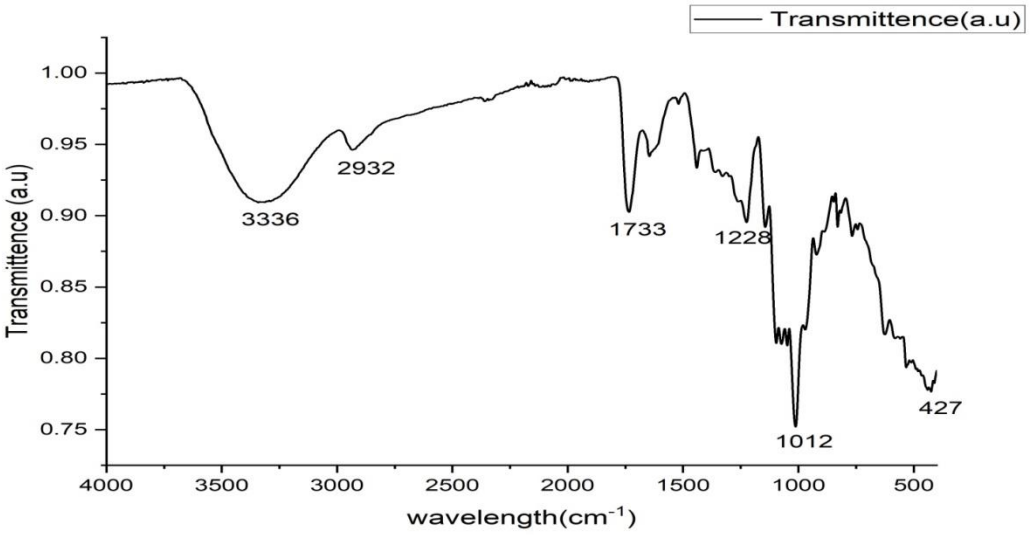

(b)

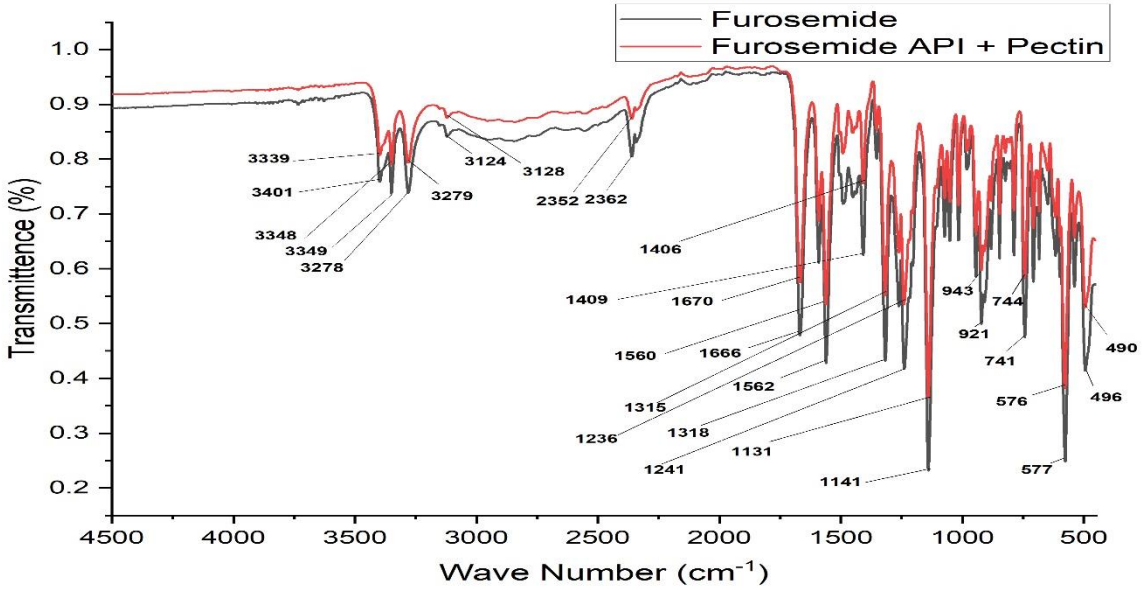

(c)

Figure 11: FTIR spectra of (a) pure furosemide; (b) pure pectin extract; (c) physical blend of furosemide and pectin extract powders.

5.1.8.2. Differential Scanning Calorimetry Study

DSC analyzes the stability of solid formulations, the polymorphic form and purity of medicinal molecules, and interactions between the components. It can also be used to identify the presence of significant chemical interactions among the components of the mixture with the APIs. However, it is not necessarily a guarantee that incompatibility exists when some peak differences are seen in

the physical mixture as it can be substantiated using FTIR analysis (Suvakanta *et al.*, 2014). For instance, the peak alteration at high temperature may not necessarily be due to incompatibilities. There may also be small variations in melting enthalpy or onset, which are conceivable due to physical mixes, do not necessarily indicate incompatibility. Additionally, changes in peak area, peak shape, and transition temperature may occur following binary mixing without necessarily indicating a negative interaction (Ruano *et al.*, 2019).

In the present study, the pure furosemide thermogram showed a main peak and onset at 220.01 ^{o}C and 217 ^{o}C, respectively. In the blend, the peak and onset temperatures showed a slight shift to 226 ^{o}C and 224 ^{o}C, respectively (**Figure 12 c**). It can be seen that there were no significant differences in the onset and peak temperatures between the pure furosemide and physical mixture. These results corroborate the findings of the FTIR investigation. The pectin thermogram's large and asymmetric peaks could be caused by contaminants, multiple endotherms, or the loss of free or bound water from the pectin during the DSC operating temperature range. The results of this study are comparable with the other studies done on pectin powder (Einhorn-Stoll *et al*, 2007; Ruano *et al.*, 2019).

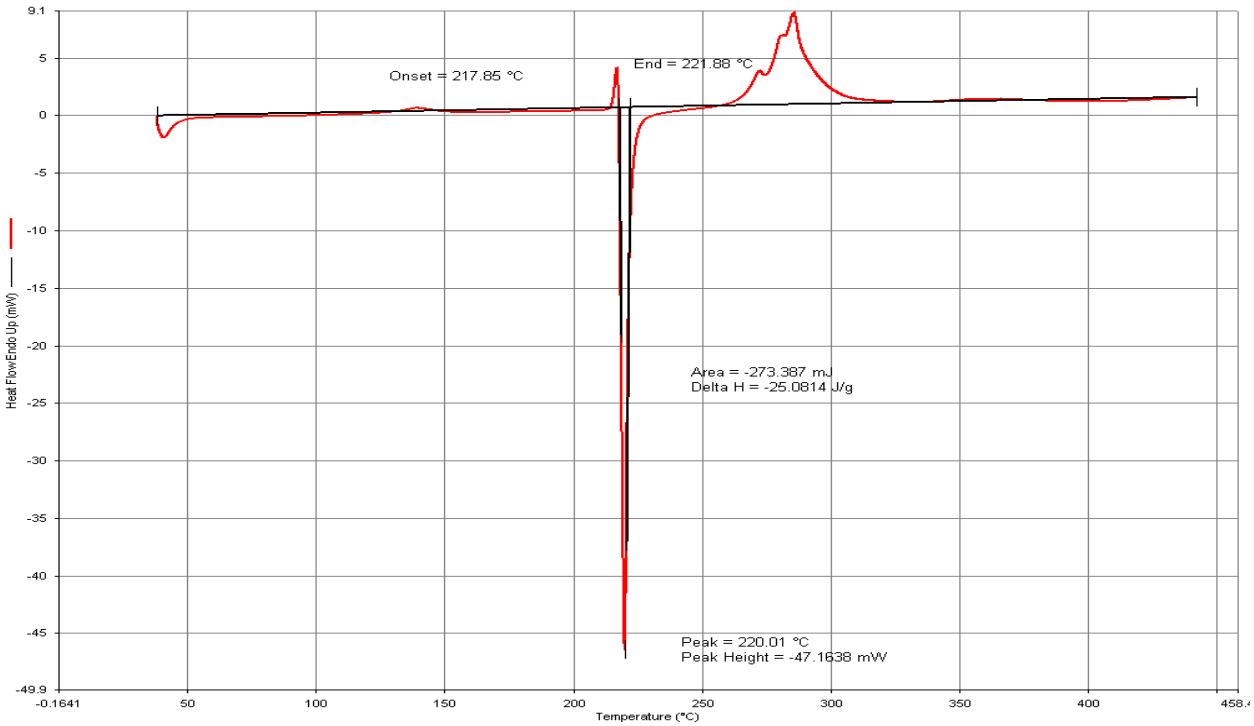

(a)

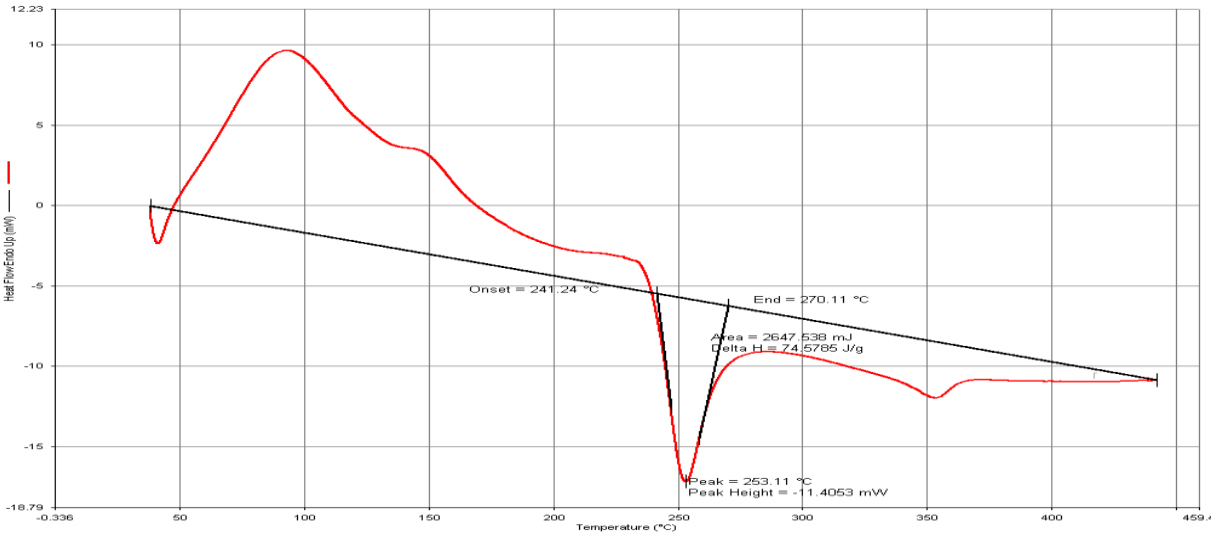

(b)

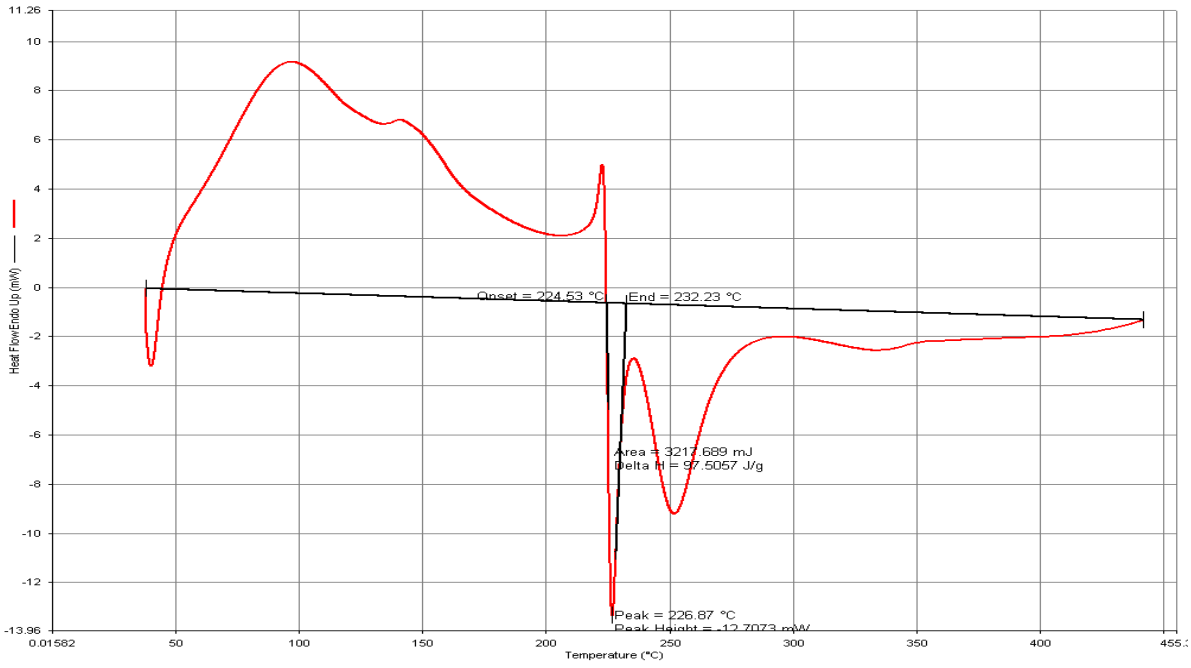

(c)

Figure 12: DSC thermograms of (a) pure furosemide; (b) pure pectin extract; and (c) physical blend of furosemide and pectin.

5.1.9. Evaluation of Furosemide Granules

The granule characteristic greatly determines the formulation process as well as stability of the pharmaceutical formulation. Since granule property largely depends on the particle size, shape, porosity, and distribution, evaluating these parameters gives meaningful image to predict the micromeritic properties (Bansal *et al.*, 2014). Hence, the micromeritic evaluations such as mean

granule size, size distribution, flow and compressibility would give valuable information to obtain proper results and to design possible solutions to improve the granule or powder characteristics (Silva *et al.*, 2013; Kľoc *et al*, 2021). The result of the present study shows that the mean granule size of the sixteen formulations ranges from 487.97 µm to 695.53 µm. Nearly half of the prepared granules were found to be distributed in sieve size 710 µm – 310 µm and less than 15% of the prepared granules was distributed <224 µm sieve size. The results indicated that the formulated granules were in acceptable range for tablet formulation and in line with the other studies (300-1000 µm) (Shekunov *et al.*, 2007). The percentages of granules retained in each sieve size are presented in **Table 11**. It can be seen from the results that the granule size and its distributions are favorable for better tablet formulation. The other study reports on pectin also indicated similar results (Weh *et al.*, 2014). Other investigation on pectin also shows comparable granule characteristics (Siddiqui *et al.*, 2021).

Table 11: Granule size and distribution of furosemide granules in the preliminary study.

Batches	**Sieve pore size in micrometer (% granule retained)**				**Mean Granule size (µm)**
	1000-710 µm	**710-315** µm	**315-224** µm	**224-115** µm	
PF1	28.14	49.03	14.37	8.46	539.62
PF2	24.22	49.13	11.14	15.51	506.26
PF3	27.08	49.41	10.08	13.43	526.96
PF4	51.18	44.49	2.51	1.82	674.40
PF5	21.15	49.05	14.21	15.6	487.97
PF6	44.14	39.82	10.75	5.29	616.37
PF7	24.43	50.15	14.26	11.16	516.82
PF8	28.25	46.38	14.05	11.32	529.77
PF9	25.19	51.38	12.08	11.35	523.96
PF10	50.24	39.77	6.24	3.75	654.39
PF11	48.64	35.76	10.82	4.78	633.65
PF12	54.09	40.29	4.06	1.56	681.64
PF13	50.09	42.18	4.46	3.27	660.12
PF14	57.48	31.17	9.04	2.31	678.15
PF15	50.38	43.51	5.06	1.05	668.55
PF16	59.36	33.12	6.25	1.27	695.53

The micrometric properties of the granules were evaluated as shown **Table 12**. Accordingly, the granules of all formulations exhibit a good flowing property. The finer powder would have higher angle of repose that may result in poor flowing characteristics. The angle of repose should be less than 30^{o} for the powder to achieve good flow property (Srivastava *et al*, 2010). The tapped and bulk densities of the granules range from 0.89 to 0.96 and from 0.74 to 0.82, respectively. The

angle of repose ranges from 24.6º to 27.27º; Hausner ratio from 1.16 to 1.24; compressibility index from 14.81% to 23.68%; and flow rate from 9.42 to 11.85 g/sec. The above results show that the formulated granules improved the flow and compressibility properties of the powders. The results are comparable with study reports on orange peel pectin (Boakye-Gyasi *et al.*, 2021).

Table 12: Micromeritic properties of furosemide granules in the preliminary study.

Formulation Code	Flow rate (g/sec)	Bulk Density(g/ml)	Tapped Density(g/ml)	Compressibility Index (CI, %)	Hausner's ratio	Angle of repose (º)
PF1	11.85±0.46	0.78±0.12	0.93±0.58	19.23±0.69	1.19±0.31	26.50±0.82
PF2	10.90±0.36	0.74±0.38	0.89±0.49	20.27±0.52	1.20±0.54	27.12±0.46
PF3	11.25±0.19	0.77±0.28	0.93±0.72	20.78±0.37	1.21±0.29	25.34±0.38
PF4	12.57±0.57	0.79±0.46	0.94±0.74	18.99±0.41	1.19±0.53	24.96±0.23
PF5	11.91±0.82	0.8±0.51	0.95±0.46	18.99±0.50	1.20±0.38	25.42±0.34
PF6	12.77±0.48	0.76±0.40	0.92±0.63	21.05±0.78	1.21±0.41	26.05±0.62
PF7	10.45±0.39	0.81±0.63	0.93±0.66	14.81±0.68	1.15±0.43	25.18±0.45
PF8	11.28±0.96	0.78±0.19	0.95±0.71	21.79±0.71	1.22±0.60	26.56±0.18
PF9	10.94±0.27	0.76±0.14	0.94±0.38	23.68±0.55	1.24±0.41	26.43±0.23
PF10	9.42± 0.33	0.79±0.27	0.95±0.26	20.25±0.51	1.20±0.66	25.19±0.86
PF11	10.39±0.45	0.82±0.29	0.96±0.30	17.07±0.43	1.17±0.31	27.27±0.56
PF12	11.10±0.21	0.81±0.34	0.94±0.41	16.05±0.76	1.16±0.49	26.70±0.64
PF13	11.32±0.50	0.78±0.71	0.94±0.47	20.51±0.84	1.21±0.53	25.39±0.37
PF14	10.53±0.67	0.81±0.44	0.95±0.55	17.28±0.73	1.17±0.59	25.64±0.51
PF15	9.75 ± 0.79	0.79±0.42	0.94±0.60	18.99±0.92	1.19±0.62	25.49±0.72
PF16	10.06±0.89	0.78±0.43	0.95±0.41	21.79±0.84	1.22±0.68	26.81±0.64

mean ± SD (n=3)

5.2. Evaluation of the Formulated Tablets

The formulated tablets were evaluated for hardness, friability, diameter, thickness, weight and assay tests. In addition, drug release, floating and bioadhesive properties of the tablets were evaluated. Accordingly, the hardness of the prepared tablets ranged from 62.69 N to 75.25 N which is within the acceptable range for good tablet strength (USP43-NF38, 2020). The assay tests for the furosemide floating and bioadhesive tablets ranges from 96.42% to 103.55% which complies with the pharmacopeial specification for the uniform content of different batches and the friability ranges from 0.18% to 0.63% which is within the pharmacopeial specification of less than 1% (USP43-NF38, 2020). The weight of the furosemide floating and bioadhesive matrix tablet ranges from 247.91 mg to 250.6 mg which indicates uniform weight distribution. There was no significant difference in the tablet weight which was less than 5% which is in line with the pharmacopeial specification. Some of the tablet evaluation results are summarized in **Tables 13 and 14**.

Table 13: Common quality attributes of furosemide floating and bioadhesive matrix tablets.

Formulation code	Weight Variation (mg)[a]	Hardness (N)[b]	Thickness (mm)[b]	Friability (%)[a]	Diameter (mm)[b]	Assay (%)[b]
PF1	249.77±1.42	73.68±1.91	4.08±0.06	0.25	10.39± 0.42	103.55 ± 0.60
PF2	250.52±1.51	75.25±1.62	4.13±0.05	0.17	10.03±0.04	100.09 ± 0.94
PF3	249.05±0.80	68.62±0.77	4.19±0.27	0.45	9.79±0.11	100.92 ± 0.80
PF4	250.01±0.49	64.92±1.30	4.23±0.42	0.63	10.05±0.03	99.35 ± 0.46
PF5	250.60±0.66	72.11±1.54	4.07±0.04	0.25	9.79±0.09	102.25 ± 0.88
PF6	250.12±0.21	62.76±0.56	4.08±0.12	0.61	9.69±0.09	97.72 ± 0.29
PF7	250.52±0.52	64.88±0.24	4.06±0.04	0.62	10.06±-0.03	99.49 ± 0.33
PF8	249.88±0.39	69.08±0.84	4.22±0.43	0.49	9.73±0.01	96.42 ± 0.38
PF9	249.95±0.56	65.39±1.13	4.11±0.12	0.58	9.94±-0.01	97.91±0.71
PF10	250.20±0.46	72.36±0.58	4.18±0.20	0.21	9.82±0.02	96.30±0.19
PF11	248.52±0.43	74.66±1.16	4.10±0.11	0.58	10.09±0.07	97.50±0.16
PF12	249.62±0.58	70.98±0.58	3.97±0.22	0.59	9.84±0.09	98.22±0.17
PF13	247.91±0.36	64.18±0.39	4.13±0.09	0.58	9.65±0.02	101.55±0.30
PF14	250.06±0.34	73.61±0.18	4.08±0.04	0.26	9.72±0.01	99.38± 0.22
PF15	248.87±0.56	62.69±0.86	3.83±0.32	0.33	9.40±0.11	96.72± 0.19
PF16	250.05±0.38	64.21±1.08	4.15±0.12	0.18	9.79±0.20	100.81± 0.70

mean ± SD:a:n=20;b:n=5

5.3. Preliminary Studies

Preliminary studies were conducted in order to select the most decisive variables and to identify their effects on different response or dependent variables (Shah *et al.*, 2022). Independent variables such as polymer concentration, polymer ratio, and concentration of floating agent were evaluated for their effect on the response variables such as matrix integrity, floating lag time, floating duration, bioadhesive strength, swelling index, drug release at 1 h, time to 50% drug release, and drug release rate.

Previous studies established that pectin in range between 10-30% w/w was used as sustaining polymer (Sharma *et al*., 2013; Siddam *et al*., 2016; Nagaraju *et al*., 2017; Owusu *et al*., 2021). The other study for the formulation of diclofenac sodium sustained release matrix tablet uses 16-55% of pectin (Rishabha *et al.*, 2010). HPMC used in concentration range between 10% - 80% as drug sustaining matrix agent (Shakya *et al*, 2013), and sodium bicarbonate between 5% to 20% as effervescent agent (Yilma *et al*, 2015). The impact of the independent variables on the response variables are shown in the **Table 14**.

Table 14: Evaluation result of formulation variables on the selected responses during the preliminary studies of furosemide matrix tablets.

Variable	Formulation code	Floating lag time (sec)	Floating duration (h)	Muco-adhesion time (h)	Muco-adhesion strength (gm)	Swelling index (%)	Matrix Integrity	Swelling diameter at 1hr	Swelling diameter at 12 hr	Drug release (%) at 1hr	Release rate on Higuchi model (% / $h^{-1/2}$)
Pectin at different conc (10- 40%)	PF1	8.39 ± 0.15	7.5	NI*	19.37 ± 0.16	NI	NI	NI	NI	38.25	33.33
	PF2	10.35 ±0.14	9.3	10.21	22.68 ± 0.58	177.62±0.43	++	12.52 ± 0.11	13.46 ±0.16	33.02	31.94
	PF3	14.24± 0.16	>12	11.55	29.33 ± 0.08	209.35±0.33	+++	13.38 ± 0.29	14.39±0.36	30.02	29.36
	PF4	19.53±0.18	>12	>12	34.58 ± 0.47	255.65±0.64	+++	14.45 ± 0.36	15.85±0.18	27.75	26.03
HPMC at10%& 40% conc	PF5	6.22±0.20	9.30	10.02	15.67 ± 0.74	176.66±0.58	++	12.50 ± 0.15	13.35±0.18	37.42	34.58
	PF6	4.37±0.16	>12	11.45	22.47 ± 0.31	256.29±0.17	+++	13.43 ± 0.28	15.14±0.18	28.95	28.87
Pectin & HPMC ratio at 10% Conc	PF7	8.04±0.19	11.15	10.5 1	19.21 ± 0.69	195.33±0.29	+	12.62 ± 0.23	13.29±0.22	35.95	35.47
	PF8	7.38±0.23	10.5	NI	17.40 ± 0.31	NI	NI	NI	NI	37.21	34.71
	PF9	7.40 ±0.24	>12	>12	21.5 ± 0.31	185.67±0.64	++	12.54 ± 0.20	13.57±0.20	34.21	30.54
Pectin & HPMC ratio at 40% Conc	PF10	13.41±0.13	11.45	>12	28.50 ± 0.35	261.28±0.46	++	14.49 ± 0.12	15.10±0.21	31.72	28.48
	PF11	11.23±0.25	>12	>12	32.31 ± 0.23	269.31±0.53	+++	14.42 ± 0.15	15.36±1.66	30.80	26.64
	PF12	11.27±0.14	11.35	>12	23.06 ± 0.45	271.33±0.18	+++	12.48 ± 0.23	14.79±0.26	31.80	29.45
Pectin with 40% $NaHCO_3$ at 5 %	PF13	24.49±0.28	>12	>12	37.03 ± 0.57	217.15±0.68	+++	12.58 ± 0.28	14.74±0.08	24.80	24.08
	PF14	14.46±0.20	>12	>12	30.58 ± 0.65	262.43±0.71	+++	14.62 ± 0.34	16.12±0.07	37.54	28.48
HPMC with 40% & 20% $NaHCO_3$	PF15	8.05±0.18	>12	>12	26.30 ± 0.42	231.87±0.64	+++	13.54 ± 0.27	14.45±0.14	25.15	25.77
	PF16	3.55±0.23	>12	>12	20.90 ± 0.95	277.16±0.47	++	14.68 ± 0.39	15.46±0.13	35.81	30.59

Mean ± SD

*NI = Not Intact

5.3.1. Effect of polymer type and concentration

The floating lag time for PF5 & PF1 was found to be 6.22 sec & 8.39 sec, respectively. The floating duration was also 7.5 hr for P10 & 9.3 hr for PF5. Hence, at 10% concentration there is higher floating lag time, and shorter floating duration for pectin than HPMC ($p< 0.05$). In addition, pectin showed good bioadhesive strength than HPMC though it didn't maintain the matrix integrity and rapid release of the drug was observed. Meanwhile, the HPMC matrix maintained its physical integrity for more than 12 hr at the same concentration. This may be due to the lower concentration of polymer that couldn't entrap the drug and the effervescent agent which provides pore for faster release of the drug. This may also be due to the formation of pores around the matrix tablet which provides access to the dissolution medium by the effervescent agent (Yilma *et al*, 2015). The drug release for 1 hr at 10% Pectin and HPMC were 38.25% and 37.42%, respectively. **Figure 13** presents the cumulative drug release pattern of furosemide matrix tablets at different variable groups and concentrations. It is reported in literature that more than 30% drug release in the first hour of dissolution shows the chance for dose dumping (Yilma *et al*, 2015).

At 40% concentration, both Pectin and HPMC based formulations showed higher floating duration, floating lag time, bioadhesive strength and bioadhesion time while there is a decrease in drug release rate. The floating lag time of both HPMC and pectin were less than a minute, while the floating durations were more than 12 hr for both HPMC and pectin ($p > 0.05$). These results are almost comparable with the other reports on floating tablet formulation that exhibits similar pattern of floating duration (Nanjwade, Adichwal and Sutar, 2012). The pectin polymer shows higher bioadhesive strength and bioadhesion time compared to the HPMC at this concentration level ($p<0.05$). This may be due to increasing the polymer concentration improves the gelling strength and binding effect of pectin (Srivastava *et al*, 2010). Other reports also indicate that increasing the polymer concentration increases the adhesion strength and prolongs the adhesion time (Jyotirmoy, 2010; Laurén *et al.*, 2018; Nigusse, Gebre-Mariam and Belete, 2021). In most cases, mucoadhesion develops as a result of interactions between medication and carrier molecules and various mucus membranes in two stages: the contact stage and the consolidation stage. However, the process underlying mucoadhesion is incredibly intricate and still not entirely understood. The process of mucoadhesion, which enables drug molecules to interact across the interface, involves a variety of chemical interactions, including ionic bonds, covalent bonds, hydrogen bonds, van der Waals forces, and hydrophobic interactions (Patil *et al*, 2016). The bioadhesion time also shows similar pattern though majority of the

formulations resulted in bioadhesion time of greater than 12 hr. Other reports also indicate that increasing the polymer concentration increases the adhesion strength and prolongs adhesion time (Laurén *et al*., 2018; Nigusse *et al*., 2021).

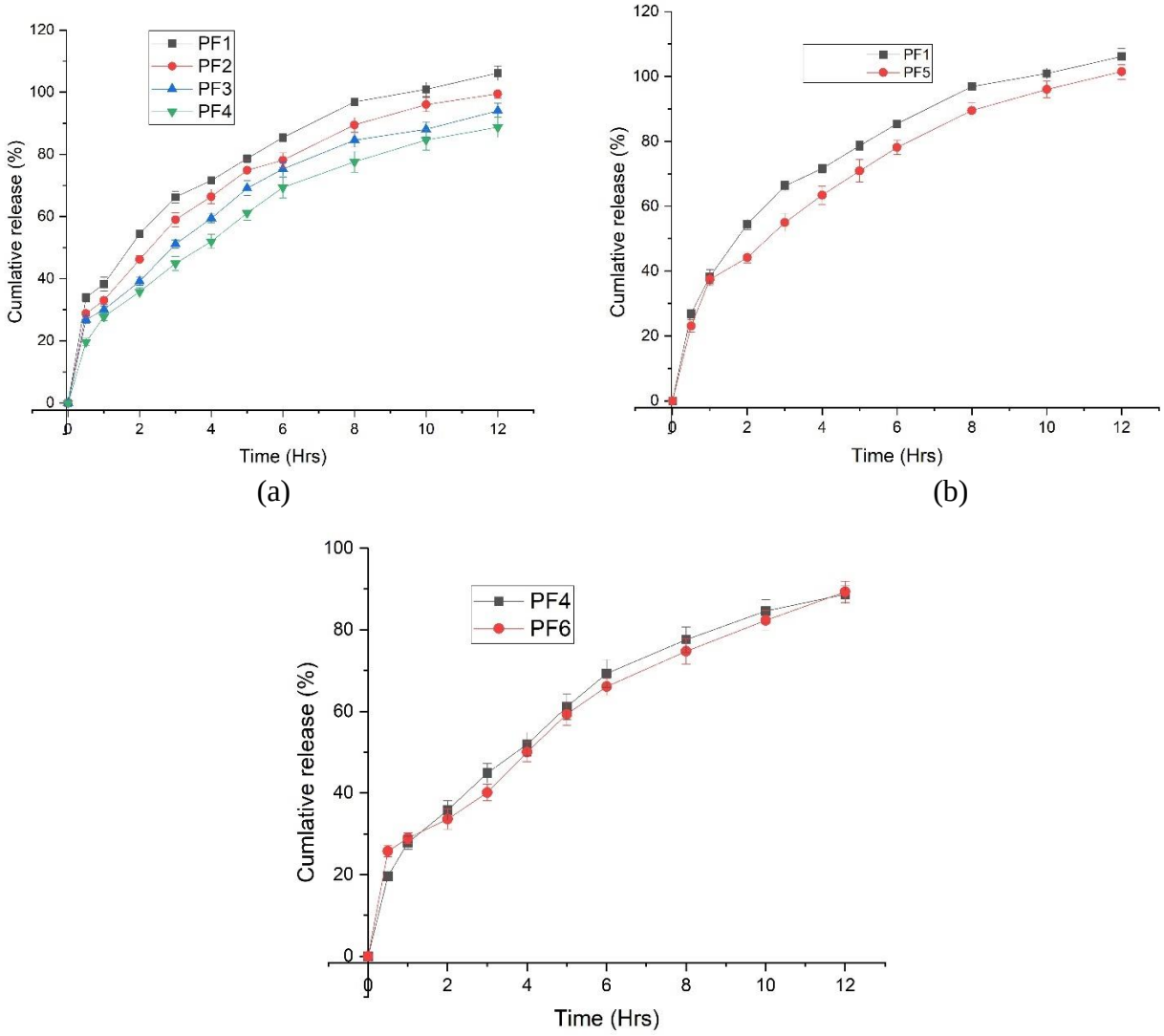

Figure 13: Cumulative release from furosemide matrix tablets (a) 10%, 20%, 30%, 40% pectin; (b) 10% Pectin and 10% HPMC; (c) Cumulative release from furosemide matrix tablets with 40%Pectin and 40%HPMC concentrations.

As depicted in **Figure 14** the swelling index for both polymers at 40% concentration showed statistically insignificant difference ($p > 0.05$) but it increases with increasing polymer concentration. Both polymers maintained their matrix integrity for a period of 12 hr, and the cumulative release during the 1 hr was not statistically significant ($p > 0.05$). Pectin polymer showed slower release rate than HPMC at similar concentration level ($p < 0.05$). The cumulative drug release decreased with

increasing polymer concentration of pectin ($p < 0.05$). In this study, the release study showed that the drug release decreases with increasing polymer concentration. This is due to the formation of strong gel layer at higher polymer concentrations which surrounds the drug particle and delays the drug release by preventing the erosion and diffusion of the polymer (Rani *et al.*, 2021). Furthermore, a higher polymer concentration results in a thicker gel layer with a longer diffusion path which slows down drug diffusion and, as a result, lowers the rate of drug release from the gel (Weh *et al.*, 2014; Ravindrakullai and Manjunath, 2015). The study finding on pectin showed that a slow release rate, due of the rapid formation of a high viscosity gel surrounding the tablet results reduced tablet erosion rate and tablet stability which is in line with the study findings (Akhgari *et al*, 2011). The results are comparable with other findings (Yilma *et al*, 2015).

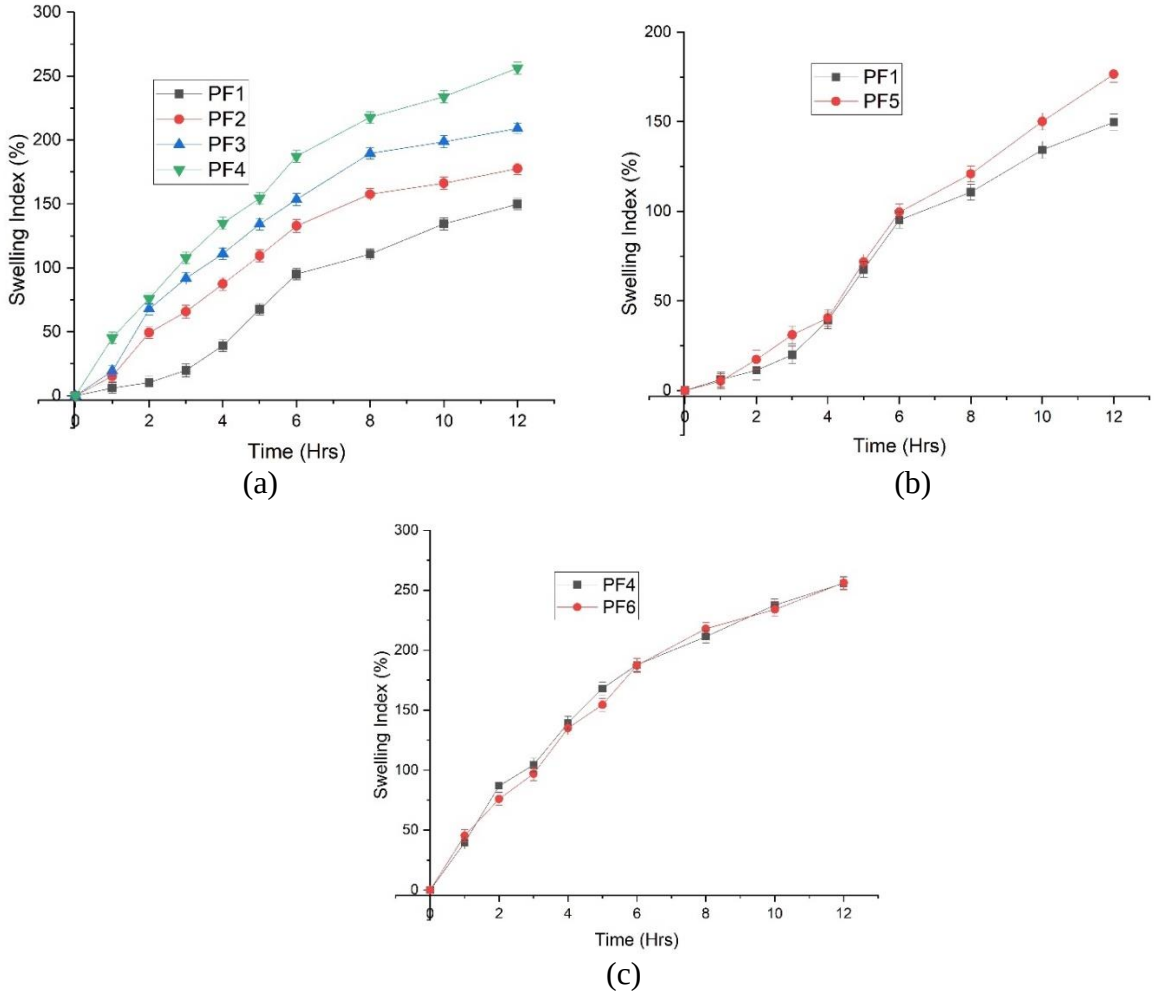

Figure 14: Swelling index of furosemide matrix tablets (a) 10%, 20%, 30%, 40% pectin; (b) 10% Pectin and 10% HPMC; (c) 40% Pectin and 40% HPMC concentrations.

5.3.2. Effect of Pectin to HPMC Ratio

Formulations with higher levels of pectin showed an improved bioadhesion time and bioadhesive strength compared to those containing higher HPMC level though all the formulations showed greater than 12 hr of adhesion time for different ratio combinations ($p < 0.05$). Overall, the formulations containing different proportions of pectin & HPMC showed less bioadhesive strength and time compared to formulations containing pectin only preparations. At 40% concentration PF10, PF11, P12, showed bioadhesion strength of 23.1g, 28.5g, and 32.3g, respectively. This may be due to the higher gelling property of pectin (Bansal *et al.*, 2014). PF11 (261.28%) showed less swelling index than PF12 (271.33 %) ($p < 0.05$). This may be due to the increase in polymer hydration over time which increased the swelling index of the produced tablets with time. It is likely that the gel layer formed matrices with high polymer contents because the concentration of polymer impacts the gel strength of pectin (Sriamornsak *et al.*, 2007). This may also be due to the swelling of high methoxylated pectin is associated to the formation of hydrogen bonds among the hydrophobic groups of polysaccharide chains (Akhgari *et al*, 2011). The drug release behavior of the polymer combinations showed that there is more delayed release with increased pectin proportion in the mixture as shown in **Figure 15**. The matrix integrity of the two formulations was not intact for pectin at 10% concentration, and with pectin and HPMC mixture at 1:3 ratio. The results are in line with other study results (Sriamornsak *et al*, 2007; Rishabha *et al.*, 2010; Siddam *et al.*, 2016).

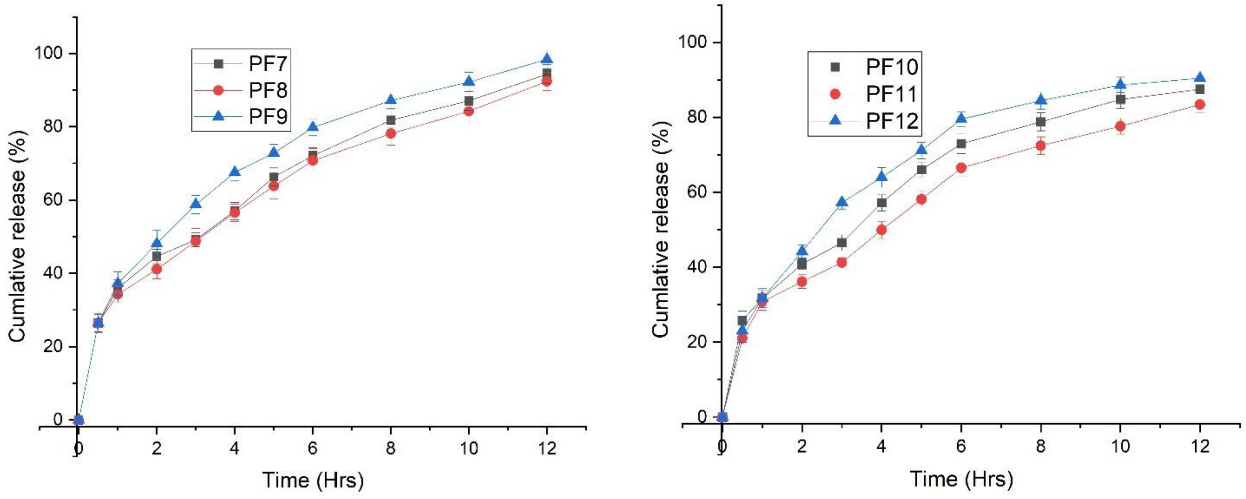

(a) (b)

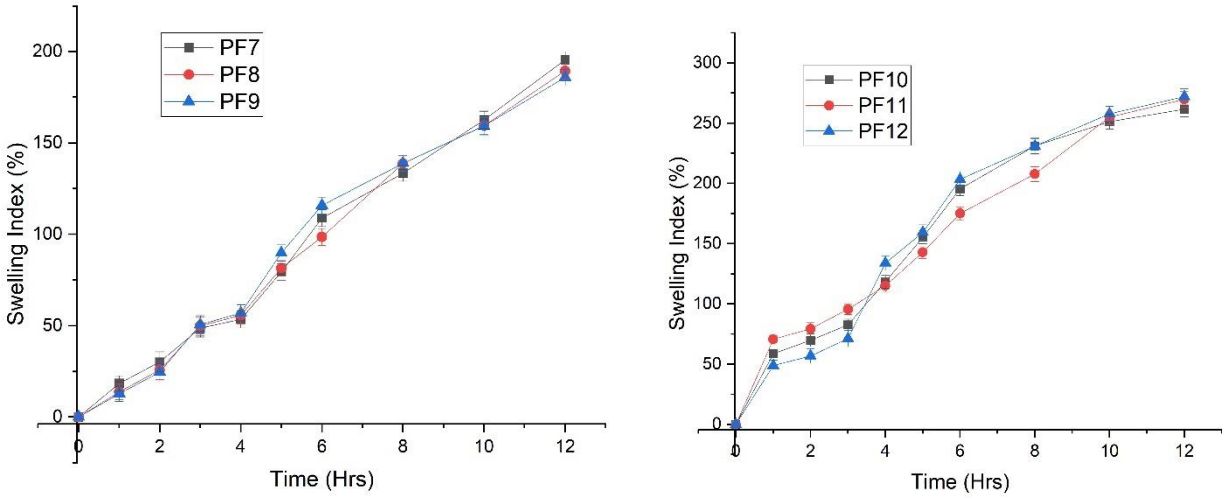

(c) (d)

Figure 15: The cumulative drug release of furosemide matrix tablets at 10 % combination (a) and at 40% combination (b); and their swelling index at 10 % combination © andat 40% combination (d).

5.3.3. Effect of Effervescent Agent

As the concentration of $NaHCO_3$ was increased, the bioadhesive strength decreased. This may be explained by the fact that greater CO_2 bubbles that formed on the tablet surface in formulations that contain more sodium bicarbonate (Arun *et al.*, 2020). The result is similar with the other study reports (Yilma *et al*, 2015). Additionally, the findings suggested that at higher effervescent agent concentrations, the drug release was faster. This might be due to the increased porosity of the tablet, which promotes access to the dissolution medium that could rapidly dissolve the drug (Siddam *et al.*, 2016). The swelling index increases when the concentration of $NaHCO_3$ increases. This is due to the rapid hydration of the polymer via the pores created by the gas forming agent. The effect of the effervescent agent on the swelling index and % cumulative release is depicted in **Figure 16**.

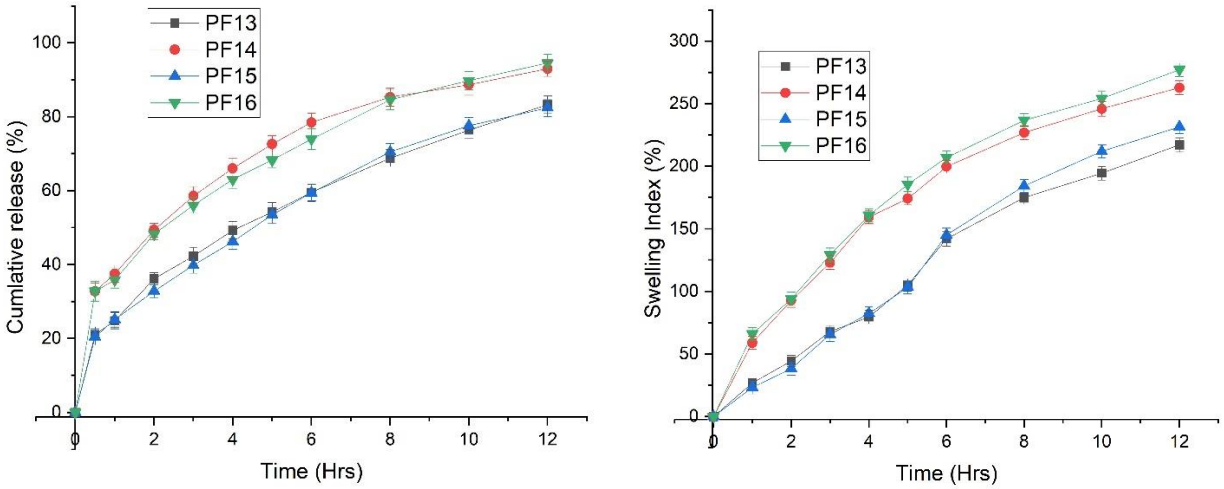

(a) (b)

Figure 16: Cumulative release (a) and swelling index (b) of furosemide matrix tablets at different concentration of $NaHCO_3$.

As the amount of $NaHCO_3$ increased, the floating lag time decreased. This is expected as floating lag time has inverse relationship with $NaHCO_3$. Comparable results are shown in the report from another study using HPMC polymer (Tamizharasi, Rathi and Rathi, 2011). As the concentration of $NaHCO_3$ increased, more carbon dioxide became available which makes the tablet more porous (Rehman *et al.*, 2019). The trapped gas in the gel would provide quick buoyancy, which accounts for the decrease in floating lag time. This implies that the polymer is more responsible for the prolonged floating duration than the effervescent agent (Nigusse *et al*, 2021) as it is presented in **Figure 17**.

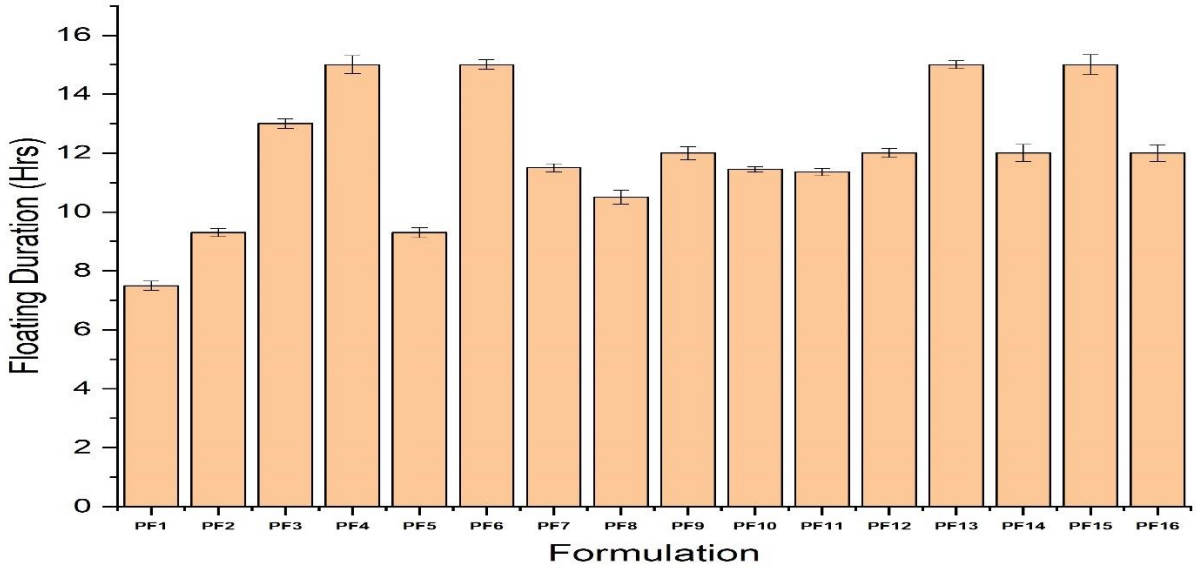

Figure 17: Floating duration of all furosemide matrix tablet formulations for preliminary study.

5.4. Optimization

According to the preliminary evaluation, the most significant variables ($p< 0.05$) was selected for optimization. Since pectin is the polymer of interest, it was considered for optimization. Five response variables were selected for optimization study based on their significance. The response variables such as floating duration (Y1), mucoadhesive strength (Y2), swelling index (Y3), % cumulative drug release at 1 hr (Y4), and drug release rate (Y5) were selected to be optimized as per the CCD.

5.4.1. Density related Evaluation of Granules

The density related physical characteristics were investigated for all batches including the bulk density, tapped density, compressibility index, Hausner ratio, and angle of repose as per CCD-prepared formulations. The granules showed good flow properties for all the formulations. The bulk density ranged from 0.58 to 0.64 g/ml, while their tapped densities varied from 0.66 to 0.80 g/ml. In addition, the Hausner ratios were between 1.12 and 1.22, the compressibility index values ranged from 10.34 to 13.79%, the angle of repose varied from 23.51 to 28.71^{o} and the flow rate ranged from 9.52 to 12.51 gm/sec showing good flow properties. The micromeritic evaluation results of the formulated furosemide granules are presented in **Table 15**.

Table 15: Micromeritic evaluation results of the furosemide granules for optimization study.

Formulation code	Bulk density (g/ml)	Tapped density (g/ml)	Carr's Index (%)	Hausner ratio	Angle of repose (^{0})	Flow rate (g/sec)
F1	0.61 ± 0.30	0.68 ± 0.20	12.2 ± 0.16	1.12 ± 0.02	24.05 ± 0.23	10.21± 0.61
F2	0.64 ± 0.28	0.75 ± 0.15	18.2 ± 0.24	1.18 ± 0.03	25.42 ± 0.21	11.42 ± 0.35
F3	0.58 ± 0.17	0.66 ± 0.18	15.4 ± 0.19	1.15 ± 0.01	27.22 ± 0.12	10.31± 0.22
F4	0.66 ± 0.39	0.80 ± 0.14	22.3 ± 0.25	1.22 ± 0.02	23.51± 0.52	11.49± 0.16
F5	0.60 ± 0.15	0.72 ± 0.11	22.1 ± 0.15	1.20 ± 0.03	26.33 ± 0.61	11.52 ± 0.29
F6	0.63 ± 0.13	0.73 ± 0.17	16.3 ± 0.30	1.16 ± 0.03	24.17 ± 0.33	10.66 ± 0.81
F7	0.65 ± 0.21	0.73 ± 0.16	13.3 ± 0.22	1.13 ± 0.06	25.26 ± 0.11	12.51± 0.21
F8	0.59 ± 0.22	0.66 ± 0.10	13.01 ± 0.10	1.13 ± 0.04	27.44 ± 0.84	10.14 ± 0.96
F9	0.62 ± 0.14	0.74 ± 0.12	22.1 ± 0.28	1.22 ± 0.07	28.18 ± 0.70	11.40 ± 0.34
F10	0.60 ± 0.29	0.70 ± 0.24	17.05 ± 0.23	1.17 ± 0.08	26.47 ± 0.31	9.82 ± 0.27
F11	0.63 ± 0.17	0.73 ± 0.27	17.2 ± 0.27	1.17 ± 0.05	25.32 ± 0.58	10.47 ± 0.60
F12	0.62 ± 0.11	0.71 ± 0.19	16.4 ± 0.21	1.16 ± 0.09	28.71 ± 0.64	11.62 ± 0.58
F13	0.64 ± 0.50	0.73 ± 0.10	15.2 ± 0.11	1.15 ± 0.04	24.18 ± 0.27	11.51 ± 0.44

Mean +SD (n=3)

5.4.2. Tablet Evaluation

The tablets of the 13 formulations were evaluated for tablet quality parameters and the results are summarized in **Table 16 & 17**. The hardness of the tablets ranged from 70.14-85.28N. The average tablet thickness varied from 3.96 mm to 4.09 mm. The friability and content assay of the prepared tablets were within the pharmacopeial specification (USP43-NF38, 2020). All tablets maintained their matrix integrity for 12 hr with the exception of formulation F5. This formulation was not intact due to its low polymer concentration. The floating lag time of the formulated matrix tablets increased with polymer concentration. On the other hand, the floating lag time decreased with increasing effervescent agent concentration. The floating lag time of the formulations was less than 1 min. The floating duration was greater than 12 hr for the majority of the formulation except F5 that may be due to its lower polymer concentration (3.7% polymer). Higher polymer concentration showed prolonged buoyancy duration.

Table 16: Some physicochemical property of the furosemide matrix tablet formulations for optimization study.

Formulation code	Hardness (N)	Thickness (mm)	Friability (%)	Content assay (%)	Weight variation(mg)
F1	76.93 ± 0.53	4.06 ± 0.07	0.33	98.56 ± 0.55	249.6 ± 0.34
F2	74.51 ± 0.12	4.03 ± 0.19	0.29	99.24 ± 0.16	249.8 ± 0.52
F3	78.39 ± 0.02	3.99 ± 0.23	0.17	99.86 ± 0.18	250.4 ± 0.09
F4	75.38 ± 0.43	3.98 ± 0.09	0.36	97.35 ± 0.23	251.8 ± 0.18
F5	81.60 ± 0.22	3.94 ± 0.34	0.42	98.60 ± 0.39	250.4 ± 0.27
F6	78.15 ± 0.34	4.01 ± 0.11	0.51	99.44 ± 0.17	252.6 ± 0.16
F7	70.14 ± 0.08	4.08 ± 0.26	0.48	98.25 ± 0.08	250.9 ± 0.44
F8	78.34 ± 0.45	4.06 ± 0.24	0.57	101.6 ± 0.43	251.1 ± 0.26
F9	77.68 ± 0.18	3.98 ± 0.14	0.35	99.17 ± 0.14	248.7 ± 0.07
F10	79.08 ± 0.76	3.99 ± 0.15	0.40	98.58 ± 0.66	249.5 ± 0.08
F11	82.63 ± 0.54	4.00 ± 0.66	0.56	97.93 ± 0.02	249.2 ± 0.28
F12	83.19 ± 0.06	4.02 ± 0.07	0.59	99.62 ± 0.45	251.8 ± 0.33
F13	85.28 ± 0.37	4.05 ± 0.43	0.25	98.39 ± 0.68	250.9 ± 0.40

Mean ±SD

Table 17: Floating, bio adhesive, swelling and release characteristics of the furosemide matrix tablet formulations as per the Central Composite Design.

Formulation code	Floating lag time (sec)	Floating duration (hrs)	Matrix integrity	Bioadhesive strength (gm)	Mucoadhesion time (hrs)	Average diameter at 1 hr	Average diameter at 12 hr	Swelling index (%)	Drug release at 1 hr	Drug release rate
F1	9.11± 0.25	12.15 ± 0.22	++	26.46±0.41	>12	13.62±0.15	14.24±0.07	230.9± 0.16	29.95± 0.11	30.95±0.31
F2	12.2± 0.11	16.85 ± 0.19	+++	31.52±0.35	>12	13.36±0.13	14.19±0.19	266.5±0.21	23.84±0.14	23.55± 0.25
F3	7.23± 0.08	10.65 ± 0.26	++	23.42±0.20	>12	14.25±0.07	14.88±0.13	249.3±0.31	31.99± 0.34	34.48±0.20
F4	10.31± 0.12	15.31 ± 0.17	+++	29.36±0.11	>12	14.14±0.12	14.82±0.06	280.5±0.27	26.55± 0.20	25.85±0.18
F5	8.35± 0.29	9.25 ± 0.20	+	23.25±0.32	7.5	13.35±0.22	14.38±0.16	225.3±0.15	34.05± 0.15	35.58±0.23
F6	13.64±0.58	16.45 ± 0.16	+++	32±0.18	>12	13.39±0.15	14.71±0.08	279.1±0.18	24.5± 0.18	23.05±0.41
F7	17.59±0.15	15.05 ± 0.13	+++	29.74±0.370	11.05	13.12±0.18	13.08±0.15	245.2±0.29	26.6±0.26	26.64±0.36
F8	10.27±0.16	11.25 ± 0.14	+	25.38±0.41	>12	14.43±0.09	14.91±0.28	271.1±031	31.2± 0.37	32.15±0.12
F9	11.70±0.27	13.01 ±0.15	+++	27.53±0.22	>12	14.37±0.17	14.70±0.33	277.4±0.12	28.01± 0.22	29.39±0.39
F10	10.85±0.43	14.01 ± 0.26	++	27.62±0.15	>12	14.40±0.16	14.68±0.25	273.2±0.41	28.5± 0.38	29.05±0.27
F11	10.75± 0.12	14 ± 0.17	+++	27.73±0.47	>12	14.39±0.24	14.72±0.23	274.6±0.29	29.70± 0.29	29.02± 0.32
F12	10.77± 0.09	14.02±0.22	++	28.27±0.25	>12	14.40±0.30	14.69±0.17	270.8± 0.18	29.06± 0.06	28.66±0.25
F13	10.64±0.19	14 ± 0.34	++	27.58±0.24	>12	14.37±0.19	14.59±0.09	271.7±0.26	29.25± 0.13	28.05±0.40
Mean ± SD +++: ?? ; ++:?? ; +: ??;										

5.4.3. Drug release kinetics

A better understanding of the mechanism of drug release using kinetic studies is important to develop a pharmaceutical modified release dosage form as deeper understanding of drug release mechanisms is crucial. Different mathematical models, including zero-order, first-order, Higuchi, Hixson-Crowell, and Korsmeyer-Peppas were used to kinetically evaluate the *in vitro* drug release data from the matrix tablets of the various formulations. These models are helpful for comprehending and predicting drug release in matrix systems (Paarakh *et al.*, 2019). **Table 18** shows the results of fitting to these mathematical models. As for each of the models under consideration, the R^2 value (correlation coefficient) was used to identify the best fitting model. Accordingly, the Higuchi model was found to be the best fit model (r^2 = 0.981 - 0.994). The Korsmeyer-Peppas model fitting showed that the n-value ranged from 0.433 to 0.572 which indicates that the release mechanism was a combination of both diffusion and erosion where the drug release process is under the control of the polymer matrix.

Table 18: Kinetic data from regression fitting of dissolution profiles of furosemide matrix tablets

Formulation	Zero order		First Order		Higuchi		Hixon-Crowell		Korsmeyer-Pappas		
	K_0	R^2	K_1	R^2	K_H	R^2	K_{HC}	R^2	K	R^2	n
F1	6.21	0.950	-0.096	0.922	26.97	0.992	-0.210	0.969	1.454	0.991	0.484
F2	6.70	0.963	-0.090	0.947	28.92	0.993	-0.211	0.986	1.356	0.992	0.572
F3	6.35	0.928	-0.113	0.927	27.75	0.981	-0.234	0.980	1.488	0.980	0.433
F4	6.71	0.962	-0.107	0.932	29.00	0.994	-0.232	0.986	1.414	0.993	0.528
F5	6.47	0.924	-0.161	0.803	28.33	0.987	-0.274	0.956	1.501	0.980	0.468
F6	6.70	0.960	-0.096	0.926	28.93	0.991	-0.217	0.979	1.372	0.991	0.560
F7	6.73	0.962	-0.110	0.927	29.08	0.994	-0.236	0.986	1.418	0.993	0.526
F8	6.44	0.923	-0.115	0.925	28.24	0.981	-0.237	0.980	1.473	0.981	0.486
F9	6.28	0.949	-0.094	0.927	27.30	0.993	-0.210	0.978	1.436	0.990	0.502
F10	6.26	0.950	-0.095	0.926	27.20	0.993	-0.211	0.977	1.441	0.992	0.496
F11	6.22	0.951	-0.096	0.923	27.03	0.993	-0.211	0.976	1.450	0.993	0.488
F12	6.24	0.951	-0.095	0.923	27.13	0.992	-0.211	0.976	1.445	0.990	0.493
F13	6.25	0.950	-0.096	0.923	27.15	0.992	-0.212	0.971	1.447	0.993	0.492

5.4.4. Selection of Response Variables

According to the preliminary evaluation, five response variables were selected for optimization study based on their significance. The response variables such as floating duration (Y1), mucoadhesive strength (Y2), swelling index (Y3), % cumulative drug release at 1 hr (Y4), and drug release rate (Y5) were selected to be optimized as per the CCD.

5.4.5. Mathematical Model Selection

RSM was employed to analyze the interaction between the independent variables (Pectin concentration and $NaHCO_3$ concentration) and response variables (Y1, Y2, Y3, Y4, and Y5). The Design of Expert software was employed to generate different polynomial models. The models were selected based on evaluation of different statistical parameters: multiple correlation coefficient (R^2), adjusted multiple correlation coefficient (adjusted R^2), coefficient of variation (CV), and predicted residual sum of square (PRESS). The results are depicted in **Table 19**.

Table 19: Fit summary statistics for response variables as per Central Composite Design.

Response	Source	SD	R-Squared	Adjusted R-Squared	Predicted R-squared	PRESS	Suggestion
Floating duration(Y_1)	**Linear**	**0.57**	**0.9447**	**0.9336**	**0.9003**	**5.97**	**Suggested**
	2FI	0.60	0.9447	0.9262	0.8609	8.33	
	Quadratic	0.66	0.9489	0.9124	0.7478	15.11	
	Cubic	0.67	0.9617	0.9080	0.2014	71.97	Aliased
Mucoadhesive strength(Y_2),	**Linear**	**0.31**	**0.9887**	**0.9864**	**0.9796**	**1.74**	**Suggested**
	2FI	0.29	0.9909	0.9879	0.9777	1.91	
	Quadratic	0.32	0.9914	0.9852	0.9624	3.21	
	Cubic	0.27	0.9955	0.9892	0.9791	1.79	Aliased
Swelling index(Y_3),	Linear	10.17	0.7526	0.7031	0.6050	1652.04	
	2FI	10.70	0.7538	0.6717	0.4881	2140.67	
	Quadratic	**2.54**	**0.9892**	**0.9814**	**0.9588**	**172.26**	**Suggested**
	Cubic	2.54	0.9923	0.9815	0.9091	380.19	Aliased
% cumulative drug release at 1 hr (Y_4)	**Linear**	**0.72**	**0.9477**	**0.9372**	**0.9048**	**9.47**	**Suggested**
	2FI	0.75	0.9488	0.9317	0.8395	15.96	
	Quadratic	0.81	0.9533	0.9199	0.7661	23.25	
	Cubic	0.86	0.9621	0.9090	0.3216	131.39	Aliased
Drug release rate (Y_5).	**Linear**	**0.55**	**0.9814**	**0.9777**	**0.9658**	**5.74**	**suggested**
	2FI	0.55	0.9837	0.9783	0.9581	7.02	
	Quadratic	0.61	0.9845	0.9732	0.9235	12.84	
	Cubic	0.60	0.9892	0.9740	0.6900	52.01	Aliased

A model is considered to be a good fit when the R^2 value is near to 1, the difference between adjusted R^2 and predicted R^2 less than 0.2 and lower PRESS values. Accordingly, linear model was

selected for floating duration, drug release at 1 hr, bioadhesieve strength and drug release rate, whereas quadratic model was selected for swelling index. The R^2 values greater than 0.90 indicate that there is a strong correlation among the predicted and experimental values of different responses (Singh *et al*, 2006). The difference between adjusted R^2 and predicted R^2 less than 0.2 indicates the presence of good agreement between the values and the model. The PRESS value is an important parameter used to assess the model prediction ability which is helpful information to confirm how well a model fits the data, and the selected model should have lower PRESS value in comparison to alternative models being considered (Nigusse *et al*, 2021).

5.4.6. Model Adequacy Checking

ANOVA was used to confirm the model reliability to evaluate the data and determine how the linear, lack of fit and interaction effects are significant between the independent variables and response variables (Sundarraj *et al*, 2018). As shown in **Table 19**, X_1 for Y_1; X_1 and X_2 for Y_2; X_1, X_2, X_1^2 and X_2^2 for Y_3; X_1 for Y_4; and X_1 for Y_5 were found to be significant model terms as their p-values were less than 0.05. The lack of fit (LOF) is a special diagnostic test for a model's adequacy that compares the pure error and describes the percentage variation of data around the fitted model (Yilma *et al*, 2015). It should be insignificant for a model to be successfully used for prediction (Sundarraj *et al*, 2018). **Table 20** shows that all of the response variables had p-values of LOF greater than 0.05, which ascertains the models' reliability.

All of the proposed models can be utilized to explore the design space, according to **Table 21**, which contains enough accuracy (signal to noise ratio) values higher than 4 for all of the models. All of the models' % CV were less than 10%, demonstrating the models' ability to be replicated and the precision of the experimental data (Xie *et al*, 2016). Both the ANOVA analysis and different diagnostic plots determined the suitability of the model, were within their range, and demonstrated its predictability (Bakhaidar *et al.*, 2022).

The model term results are summarized in **Table 22**. Mathematical correlations between the dependent and independent variables were derived in order to identify the levels of elements that produce the optimized results (Equations 4.26 – 4.30).

Table 20: Summary of the ANOVA results of different response variables as per Central Composite Design.

Response	Source	Sum of squares	df	Mean square	F value	p- Value	Remark
Floating duration (Y1)	Model	56.59	2	28.29	85.38	< 0.0001	Significant
	A-X_1	47.74	1	47.74	144.06	< 0.0001	
	B-X_2	8.85	1	8.85	26.7	0.0004	
	Residual	3.31	10	0.3314			
	Lack of fit	2.11	6	0.3523	1.17	0.4585	Not significant
	Pure error	1.20	4	0.3000			
	Cor total	59.90	12				
Mucoadhesive strength (Y2)	Model	84.44	2	42.22	436.05	< 0.0001	Significant
	A-X_1	68.30	1	68.30	705.33	< 0.0001	
	B-X_2	16.15	1	16.15	166.77	< 0.0001	
	Residual	0.9683	10	0.0968			
	Lack of fit	0.6033	6	0.1006	1.10	0.4845	Not significant
	Pure error	0.3649	4	0.0912			
	Cor total	85.41	12				
Swelling index (Y3)	Model	4132.07	4	1033.02	164.85	< 0.0001	Significant
	A-X_1	2552.00	1	2552.00	407.25	< 0.0001	
	B-X_2	595.61	1	595.61	95.05	< 0.0001	
	A^2	733.55	1	733.55	117.06	< 0.0001	
	B^2	370.08	1	370.08	59.06	< 0.0001	
	Residual	50.13	8	6.27			
	Lack of fit	23.13	4	5.78	0.8567	0.5578	Not significant
	Pure error	27.00	4	6.75			
	Cor total	4182.20	12				
Drug release at 1 hr (Y4)	Model	94.22	2	47.11	90.52	< 0.0001	Significant
	A-X_1	78.41	1	78.41	150.67	< 0.0001	
	B-X_2	15.81	1	15.81	30.37	0.0003	
	Residual	5.20	10	0.5204			
	Lack of fit	3.44	6	0.5738	1.30	0.4165	Not significant
	Pure error	1.76	4	0.4403			
	Cor total	99.42	12				
Drug release rate (Y5)	Model	164.63	2	82.31	264.41	<0.0001	Significant
	A-X_1	141.43	1	141.43	454.31	<0.0001	
	B-X_2	23.20	1	23.20	74.51	<0.0001	
	Residual	3.11	10	0.3113			
	Lack of fit	2.08	6	0.3475	1.35	0.4020	Not significant
	Pure error	1.03	4	0.2570			
	Cor total	167.74	12				

Table 21: Numerical test results of model adequacy as per Central Composite Design

Response	Sources	R-squared	Adjusted R-squared	Predicted R- squared	Adequate precision	% CV
Floating duration	Linear	0.9447	0.9336	0.9003	25.27	4.28
Mucoadhesive strength	Linear	0.9887	0.9864	0.9796	58.1	1.12
Swelling index	Quadratic	0.9880	0.9820	0.9658	35.24	0.95
Drug release at 1 hr	Linear	0.9477	0.9372	0.9048	26.18	2.51
Drug release rate	Linear	0.9814	0.9777	0.9658	44.36	1.93

Table 22: Estimated model term regression coefficient for the responses.

Response	Intercept	X_1	X_2	X_1X_2	X_1^2	X_2^2
Y_1	13.46	2.44	- 1.05			
P value		< 0.0001	0.0004			
Y_2	27.68	2.92	-1.42			
P value		< 0.0001	< 0.0001			
Y_3	273.55	17.86	8.63	-	-10.27	-7.29
P value		< 0.0001	< 0.0001		< 0.0001	< 0.0001
Y_4	28.71	-3.13	1.41			
P value		< 0.0001	0.0003			
Y_5	28.95	-4.20	1.70			
P value		< 0.0001	< 0.0001			

The model term coefficients reported in **Table 22** were used to construct the final equations in terms of coded factors (Equations 4.26 – 4.30).

$$Y_1 = +13.46+2.44*X_1 – 1.05*X_2$$ ---------- Equation 4.26

$$Y_2 = +27.68+2.92*X_1 – 1.42*X_2$$ ---------- Equation 4.27

$$Y_3 = +273.55+17.86*X_1+8.63*X_2 — 10.27 *X_1^2+7.29*X_2^2$$ ---------- Equation 4.28

$$Y_4 =+28.71 – 3.13*X_1+1.41*X_2$$ ---------- Equation 4.29

$$Y_5 =+28.95 – 4.20*X_1+1.70*X_2$$ ---------- Equation 4.30

The importance of each coefficient was examined using the p-values as a tool, which was important to comprehend the pattern of the reciprocal interactions between the optimized factors. The significance of the associated coefficients increases with decreasing p-value (Sastry *et al*, 1997). When one of the factors is modified by one unit while the other factor remains constant, the response variables' result changes by the magnitude of the coefficients and its sign, in linear models. The physical significance of the generated model coefficients on response variables was assessed. The coefficients' magnitude and sign are significant to illustrate the relationship between the variables. The sign of the factor variable on the related response variable shows its direction,

whilst the magnitude indicates its strength. A positive sign denotes a positive impact, whereas a negative sign denotes a negative impact on the responses (Chelladurai *et al.*, 2020). The floating duration is affected positively by X_1 (Pectin concentration) and negatively by X_2 variable ($NaHCO_3$ concentration**)**. The bioadhesive strength (Y_2) is affected positively by X_1 and negatively by X_2. The swelling index Y_3 is positively affected by X_1 and X_2. The quadratic equation X_2^2 results in positive impact on the swelling index whereas X_1^2 shows negative result. The Y_4 (Drug release at 1 hr) is negatively affected by the X_1 and positively affected by the X_2. The Y_5 (Drug release rate) shows that X_1 results in negative impact whereas X_2 in positive effects.

5.4.7. Residual Plots

Externally studentized residuals are more sensitive to the detection of outliers compared to internally studentized residuals. As a result, over the duration of the diagnosis procedure, the Design of Expert software was altered at externally studentized residuals (Bakhaidar *et al.*, 2022). The residual graphs' visual examination can also yield insightful data regarding the model's applicability. Hence, if the mathematical model is well fitted, the residuals graph will behave in a way towards a normal distribution of those points. It is not possible to draw exact conclusions about the behavior of the data in the investigated experimental area if the model produces greater residuals. Also, the residual graph will display a behavior that indicates the type of term that must be added to the model if the model requires any additional terms (Bezerra *et al.*, 2008).

Figure 18 (a, e, i, m, q) presents the different normal residual plots of the response variables. As the normal plots of the residuals are demonstrated to be closer to the straight line, they are considered to be normally distributed data (Hasan *et al*, 2009). The box-cox plot determines the power law of transformation attempts to normalize the dependent variables. If the 95% confidence interval centers around lambda 1, the distribution of the dependent variables is said to be normal (Naveen *et al*., 2020). Hence, as shown in the figure, all the responses have lamda value of one which suggests it is not recommended to consider transformation. The Cook's distance displays any adjustments that the quadratic model might make in the absence of data points. A Cook's distance of less than 1 is preferable because it suggests the absence of any missed data points that would affect the regression coefficient prediction (Rashid, Anwar and Arif, 2009). The results of all responses are in line with the above requirements.

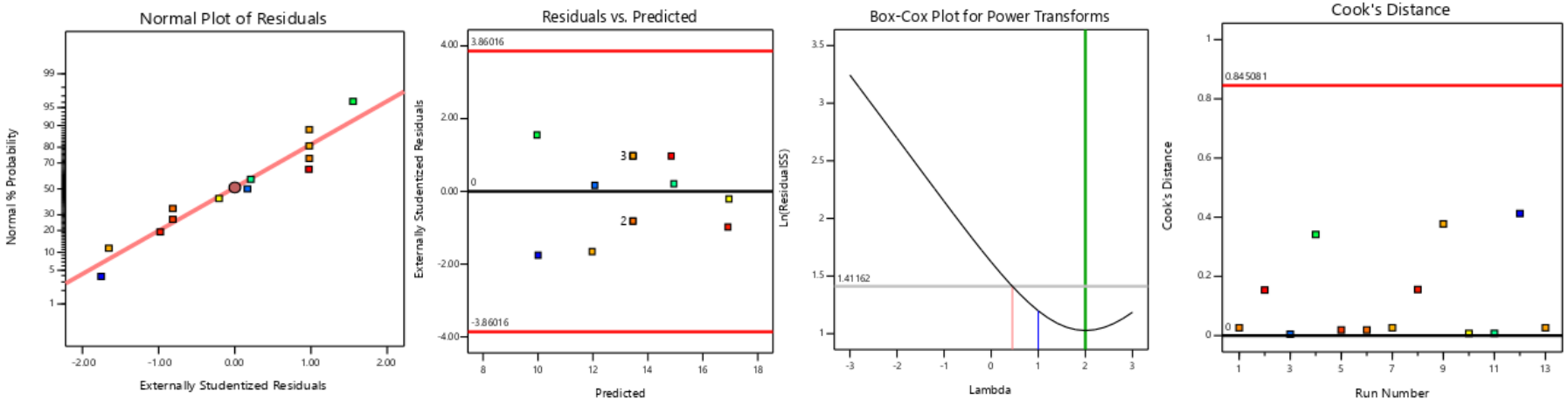
Normal Plot of Residuals
Normal % Probability
Externally Studentized Residuals
Residuals vs. Predicted
Externally Studentized Residuals
Predicted
3.86016
-3.86016
Box-Cox Plot for Power Transforms
Ln(ResidualSS)
Lambda
1.41162
Cook's Distance
Cook's Distance
Run Number
0.845081

(a) **(b)** **(c)** **(d)**

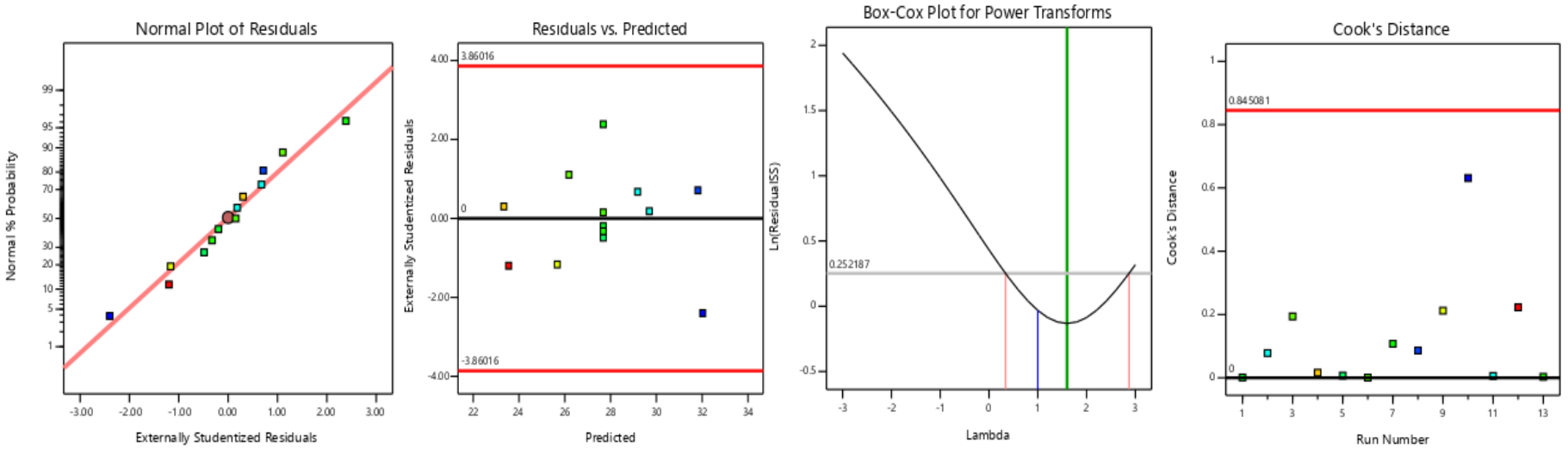
Normal Plot of Residuals
Normal % Probability
Externally Studentized Residuals
Residuals vs. Predicted
Externally Studentized Residuals
Predicted
3.86016
-3.86016
Box-Cox Plot for Power Transforms
Ln(ResidualSS)
Lambda
0.252187
Cook's Distance
Cook's Distance
Run Number
0.845081

(e) **(f)** **(g)** **(h)**

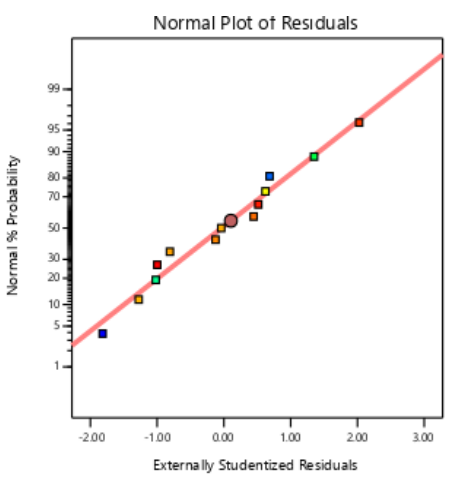
Normal Plot of Residuals
Normal % Probability
Externally Studentized Residuals

(i)

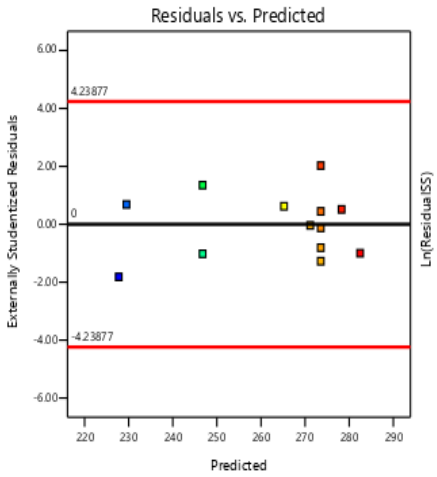
Residuals vs. Predicted
Externally Studentized Residuals
4.23877
-4.23877
Predicted

(j)

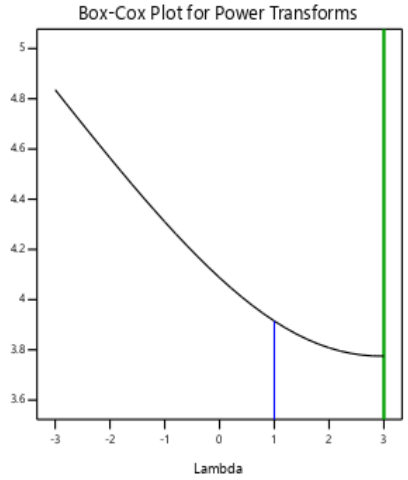
Box-Cox Plot for Power Transforms
Ln(ResidualSS)
Lambda

(k)

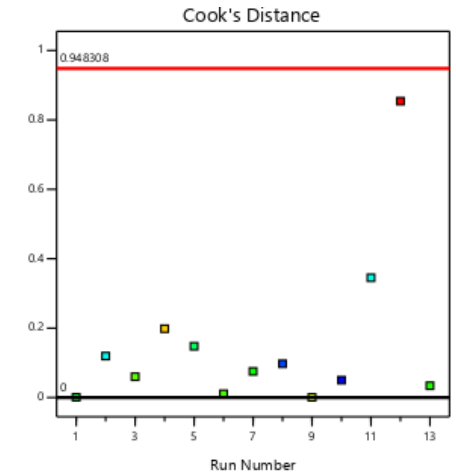
Cook's Distance
0.948308
Cook's Distance
Run Number

(l)

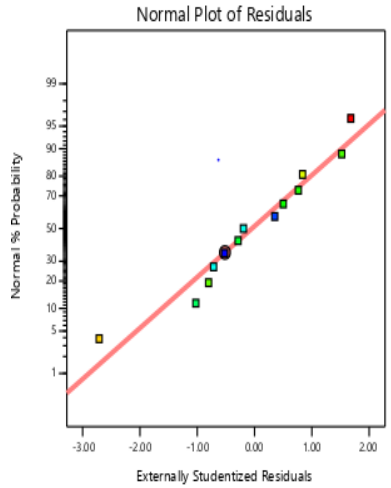
Normal Plot of Residuals
Normal % Probability
Externally Studentized Residuals

(m)

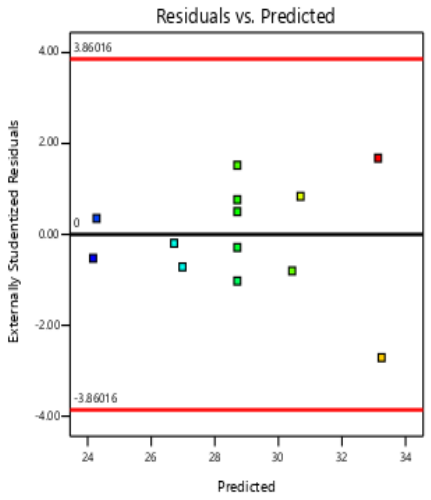
Residuals vs. Predicted
Externally Studentized Residuals
3.86016
-3.86016
Predicted

(n)

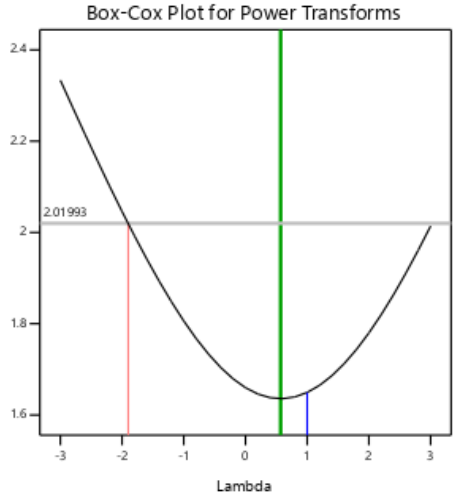
Box-Cox Plot for Power Transforms
Ln(ResidualSS)
2.01993
Lambda

(o)

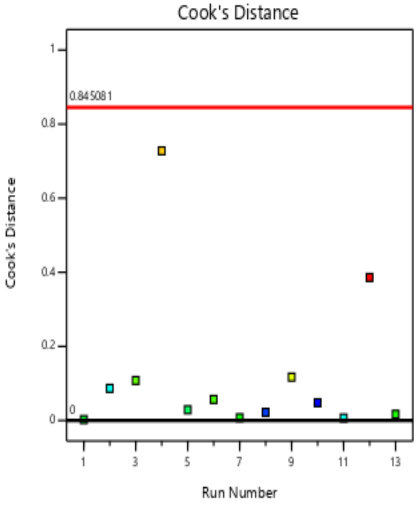
Cook's Distance
0.845081
Cook's Distance
Run Number

(p)

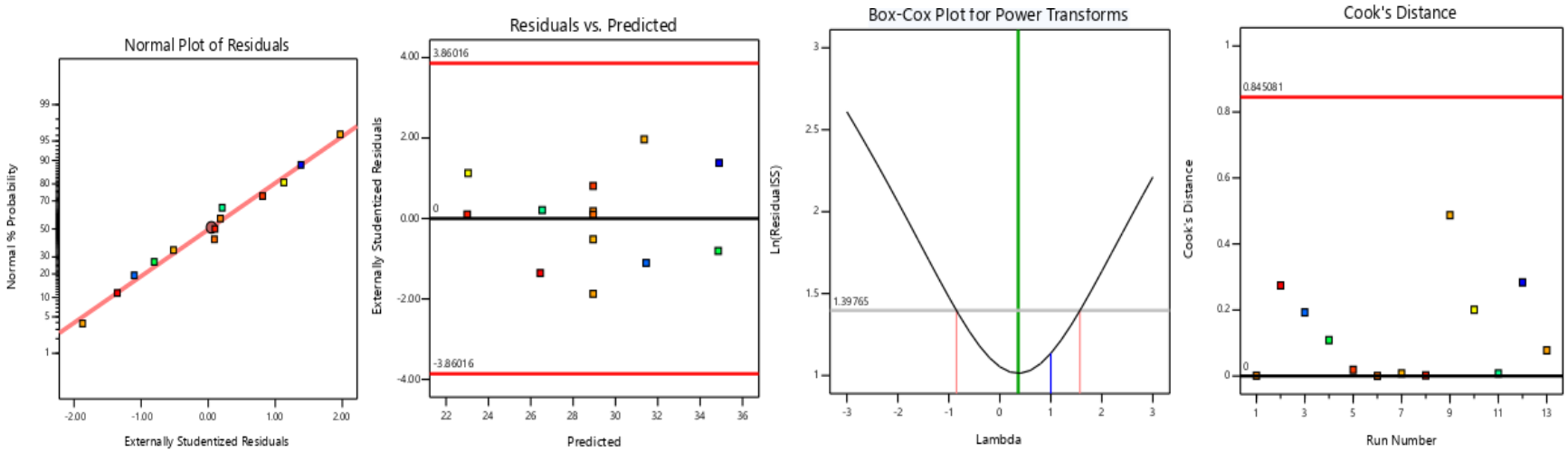

(q) **(r)** **(s)** **(t)**

Figure 18: Normal, residual, box-cox, and Cook's distance plots for response variables (Y1, Y2, Y3, Y4, and Y5)

(a) – Normal plot for Y_1

(b) – Residual Vs predicted plot for Y_1

(c) – Box-cox plot for Y_1

(d) – Cook´s distance plot for Y_1

(e) – Normal plot for Y_2

(f) – Residual Vs predicted plot for Y_2

(g) – Box-cox plot for Y_2

(h) – Cook´s distance plot for Y_2

(i) – Normal plot for Y_3

(j) – Residual Vs predicted plot for Y_3

(k) – Box-cox plot for Y_3

(l) – Cook´s distance plot for Y_3

(m)– Normal plot for Y_4

(n) – Residual Vs predicted plot for Y_4

(o) – Box-cox plot for Y_4

(p) – Cook´s distance plot for Y_4

(q) – Normal plot for Y_5

(r) – Residual Vs predicted plot for Y_5

(s) – Box-cox plot for Y_5

(t) – Cook´s distance plot for Y_5

5.4.8. Predicted Vs actual plots

The predicted vs. actual plot is a plot used to determine how well the prediction matches the actual findings obtained during the experiment and the perfect straight line produced by the software (Rashid *et al*, 2009). The good agreement between the actual and projected data and the ideal line in the plots presented by **Figure 19** demonstrated good predictability for all responses.

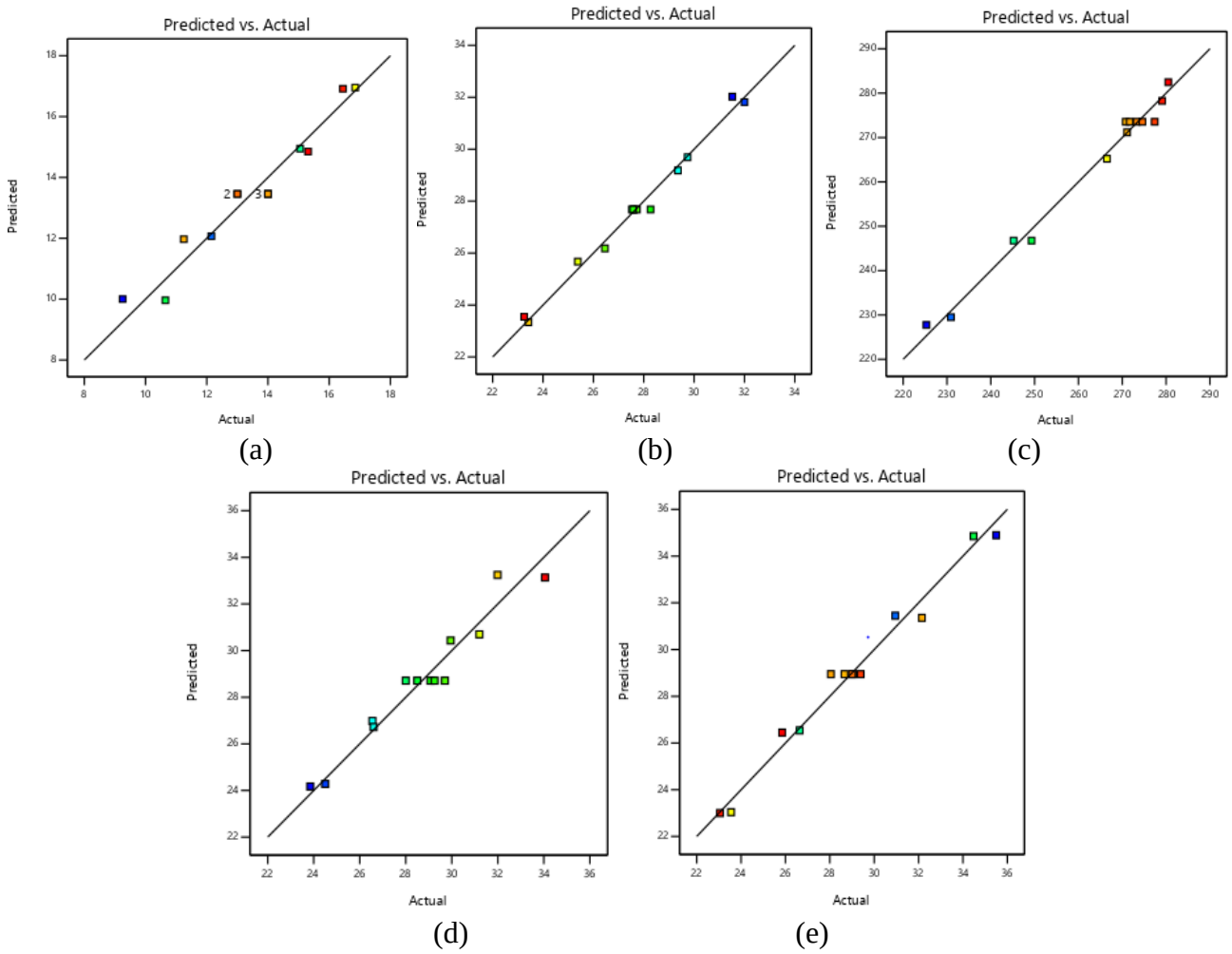

Figure 19: Predicted vs actual normal probability plots of floating duration (a); bioadhesive strength (b); swelling index (c); drug release at 1hr (d); and drug release rate (e).

5.4.9. Contour and response surface plots

The graphical representations of the fitted regression models are expressed by the 2D contour plots and the 3D response surface plots. These graphs, which are based on the model equations, show how the independent variables interact with one another and help determine the optimized values

for the variables within the ranges under consideration (Chopra *et al*, 2007; Suhendra *et al.*, 2017). The coefficients of the 2D circular contour plot and 3D response surface shows mutual interactions between the variables (Sundarraj *et al*, 2018). Contour plots and response surface plots for the obtained responses (Y_1, Y_2, Y_3, Y_4, & Y_5) were drawn based on the model polynomial function to assess the change of the response surface (**Figure 20**). As it can be seen from **Figures 20, a and b**, the contour and 3D plots indicated that the impact of X_1 (pectin concentration) and X_2 ($NaHCO_3$ concentration) on the response Y_1 (floating duration) of the formulation was in line with the ANOVA test results obtained. The two factors have linear relationship with Y_1. This means that, increment of X_1 concentration increases the floating duration significantly due to the polymer effect and its effect is more pronounced than X_2 ($NaHCO_3$) that have also slightly positive impact on the floating duration. Like that of the ANOVA prediction, X_1 showed more significant effect ($p < 0.001$) than X_2 ($p = 0.3023$) on Y_1. This result suggests that the polymer has more impact on the floating duration than the effervescent agent. This result is in line with other reports on pectin (Siddam *et al.*, 2016). On the other hand, as X_1 (Pectin concentration) increased, the Y_2 (bioadhesive strength) also increased. Whereas, an increase in X_2($NaHCO_3$) decreases the bio adhesive potential confirming its negative impact to the response as depicted in **Figure 20, c and d**. These implications are similar with the ANOVA result that the p values for both independent variables were < 0.001.

The swelling index (Y_3) has shown non-linear relationship with the responses and affected positively by both X_1(pectin concentration) and X_2 (NaHCO3 concentration). Even though, the increase in both X_1 and X_2 concentration increases the swelling index of the matrix tablet the effect is more pronounced for pectin concentration as depicted in **Figure 20, d and e**. This result is similar with the equation and ANOVA findings. As it can be observed from the **Figure 20, e and f,** the drug release at 1hr decreases with increasing the X_1 (pectin concentration) and increases with the rise in X_2($NaHCO_3$) concentration. In terms of their impact, the pectin concentration showed more pronounced effect than $NaHCO_3$ counterparts which was in line with the mathematical models. On the other hand, the **Figure 20, g and h** showed linear relationship of X_1 and X_2 on the drug release rate (Y_5). The serious of parallel straight lines in the 2D plot and non-twisted 3D response surface indicates the absence of interaction effect from both independent variables. The factors influence the drug release rate separately. According to the **Figure 20, i and j** the drug

release rate (Y_5) decreases with increasing X_1 concentration and increases with the increasing in X_2 concentration. The influence of X_1 is more exaggerated than X_2 which is similar with the mathematical models coefficient (-4.20 and 1.70 for X_1 and X_2 respectively)

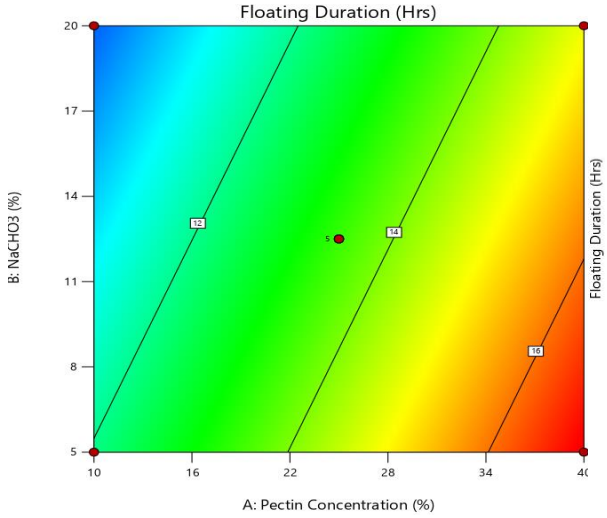

(a)

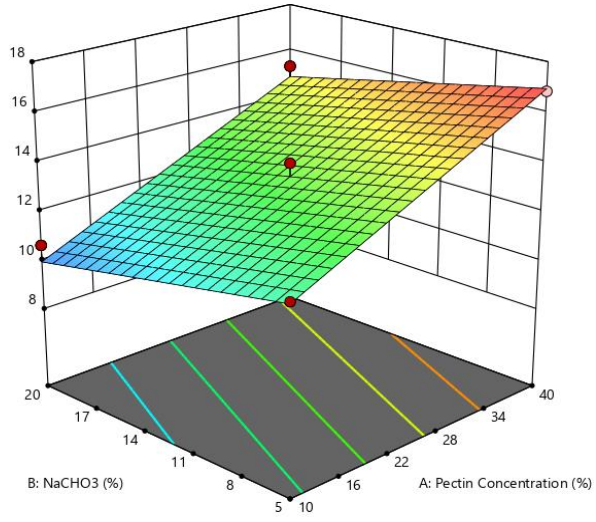

(b)

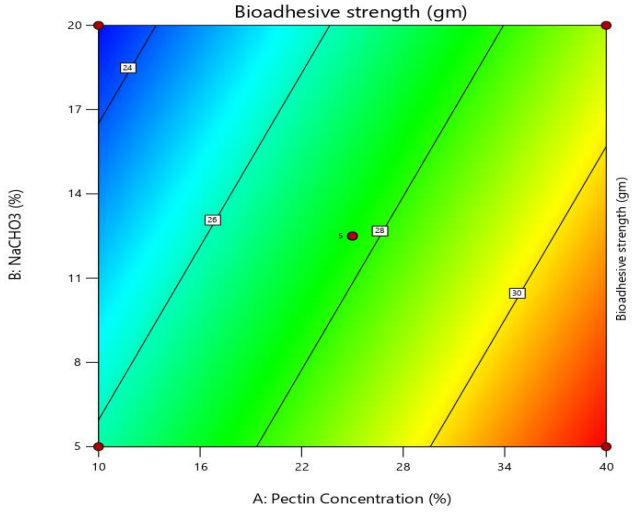

(c)

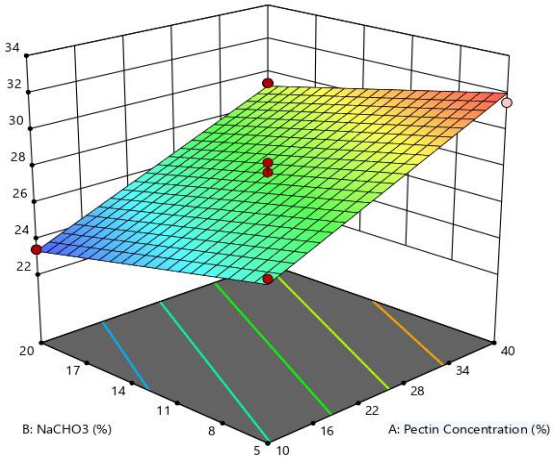

(d)

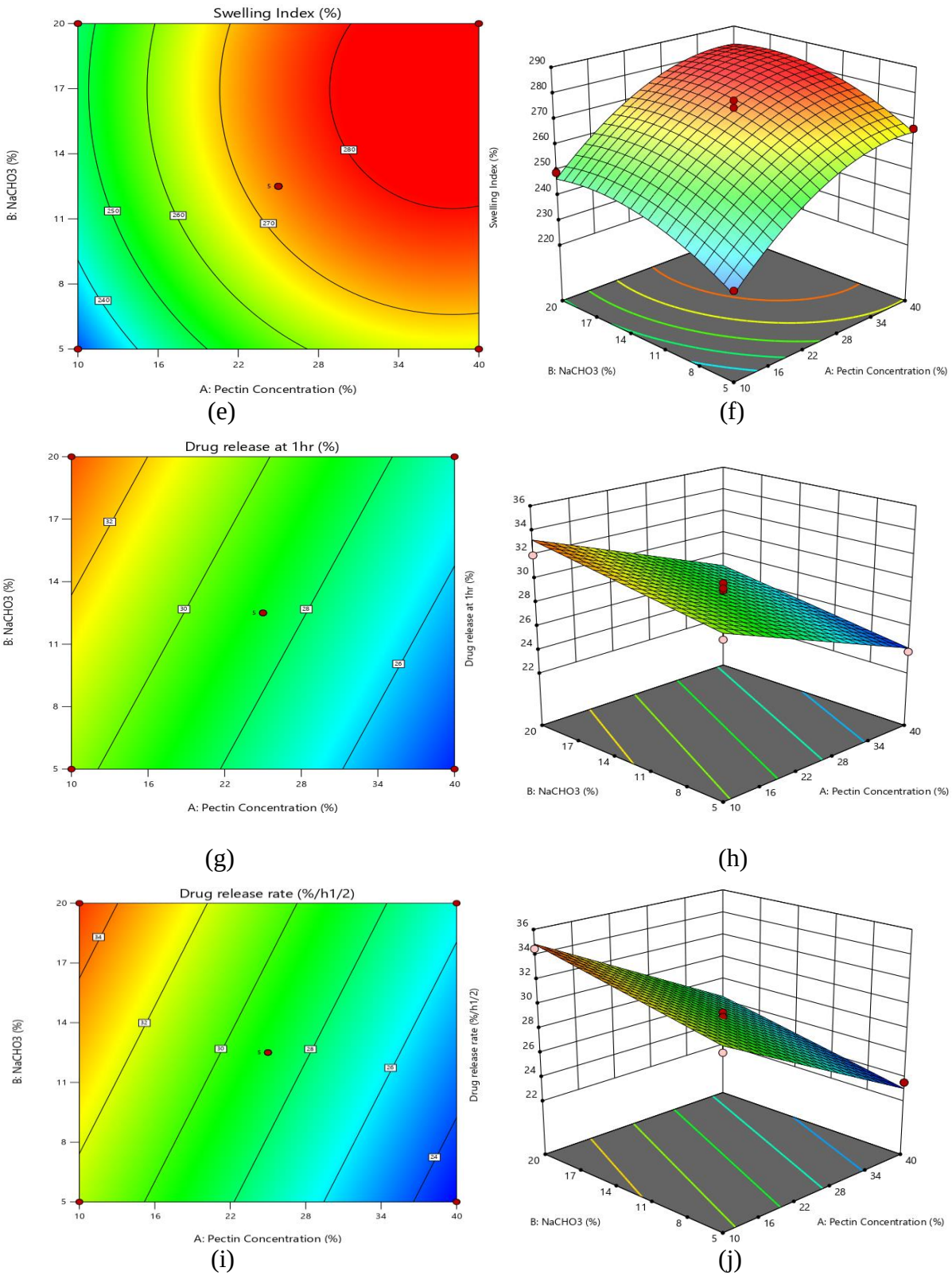

Figure 20: Contour plot and 3D diagram of the variable relationships

Y1 (a and b), Y2 (c and d), Y3 (e and f), Y4 (g and h) and Y5 (i and j).

5.5. Simultaneous Optimization of Response Variables

The formulation was simultaneously optimized for the responses after generating the model polynomial equations showing the relationship between the dependent and independent variables. The criteria established for variables and actions during optimization using both numerical and graphical methods are shown in **Table 23**. Design-Expert 10.0.7.0 software was used, which permits compromise among alternative responses and searches for a combination of factor levels that jointly optimize a collection of responses by satisfying the requirements for each response in the set, was used to find the final optimal experimental settings.

Table 23: The criteria established for variables and actions during optimization.

Factor Constraints				
Factor	**Low**		**High**	
Pectin concentration	10		40	
$NaHCO_3$ concentration	5		20	
Response Constraints				
Response	**Goal**	**Lowe limit**	**Upper limit**	**Importance**
Floating duration (hrs)	Maximize	9.25	16.85	3
Bioadhesive strength (gm)	Maximize	23.25	32	3
Swelling index (%)	In range	225.3	280.5	3
% Drug release at 1hr	Minimize	23.5	34.05	3
Drug release rate (%/ $hr^{-1/2}$)	Target (28)	24.12	35.5	3

5.5.1. Optimized Factors

One of the most popular approaches for the optimization of multiple responses is the desirability function technique. The satisfaction of the combined goals for all responses is estimated by the overall desirability function. Desirability function has a value between 0 and 1, with values closer to 1 indicating more response goal satisfaction (Suhendra *et al.*, 2017). The estimated ideal values in relation to the objectives are displayed in Table 21 above. There was a total of 5 results in this investigation, and the software had chosen the one with an overall desirability of 0.718.

5.5.1.1. Numerical Optimization

The numerically optimized factor settings are displayed using a ramps graph in accordance with their optimal responses. The criteria that are set for each factor for independent variables X_1 and X_2 are by red dots while the response variables are represented by blue dots in **Figure 21**.

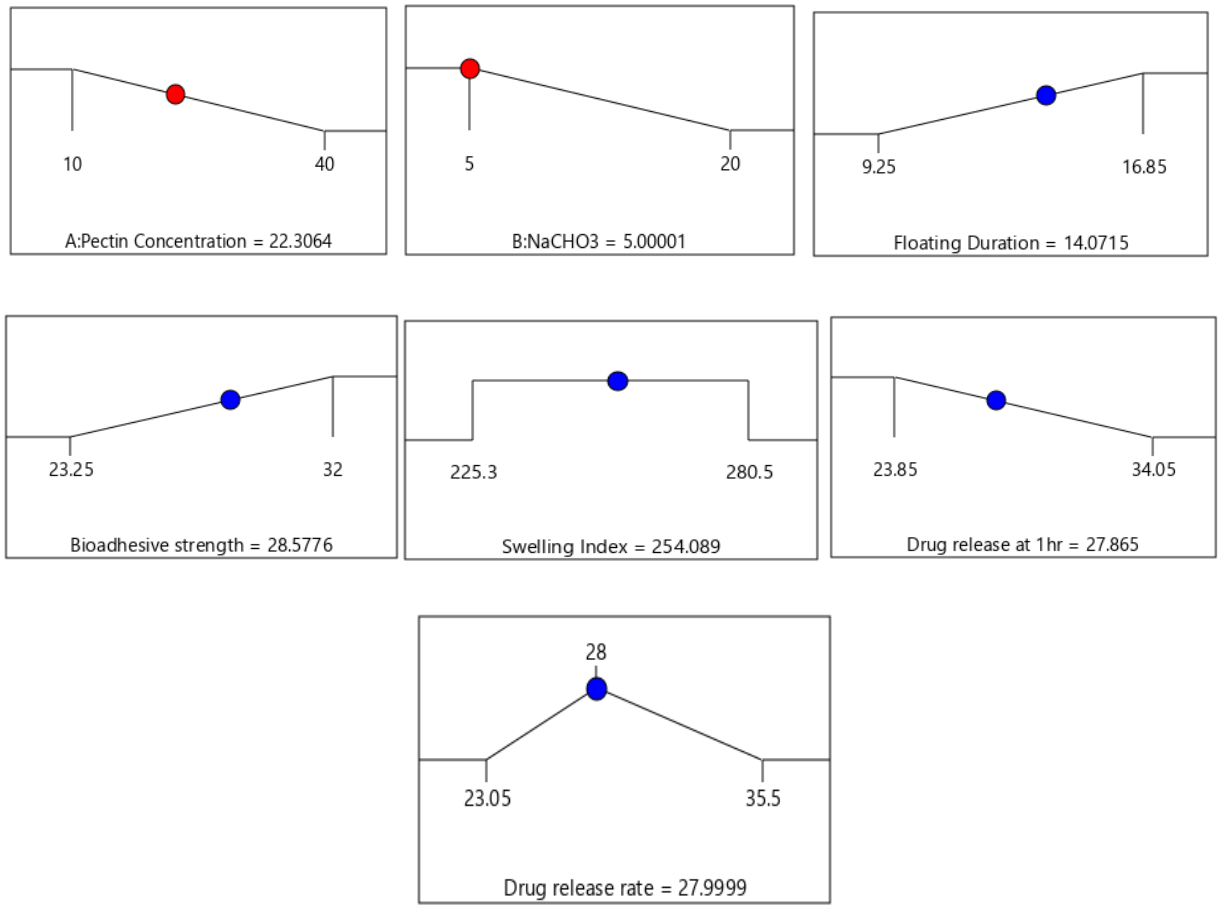

Figure 21: The numerical optimization plots for the predicted values and its corresponding limits.

5.5.1.2. Desirability Plots

Desirability is a relative quantity with a range of 0 and 1. The function shows for maximum possibility of the predicted values, the values closer to one, is what the Design of Expert software seeks to achieve for obtaining best possible combination of the variables. Finding the best maximum combination begins at several design space locations and gets narrower as it gets closer to one. The overall desirability function's 3D plot is displayed in **Figure 22**.

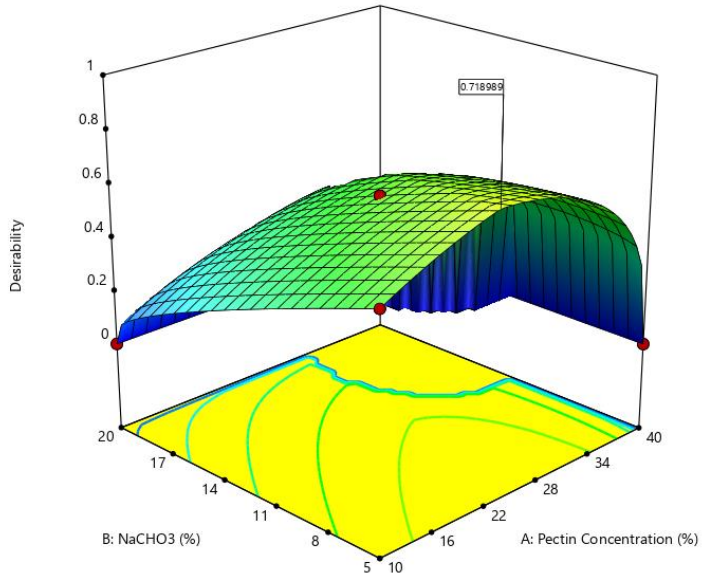

Figure 22: Desirability plots of optimized formulations

5.5.1.3. Graphical Optimization

The region of optimized formulations was also ratified using overlay plot. As indicated in **Figure 23**, the yellow area showed the possibility of the imposed criteria. Based on the results presented, the white flag indicates point results recommendation by the software. The recommendation is 22.03% for X_1 (Pectin concentration) and 5% for X_2 ($NaHCO_3$ concentration) in order to achieve optimum levels of the responses Y_1 (14.07 hr), Y_2 (28.57 gm), Y_3 (254.98%,), Y_4 (27.86%), and Y_5 (28% / $h^{-1/2}$) .

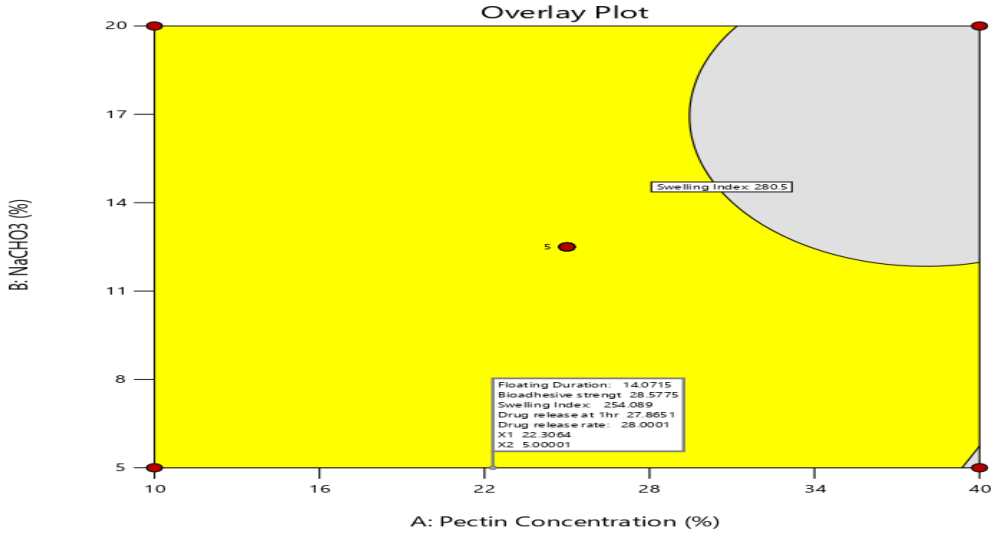

Figure 23: Over lay plot for optimized formulation

5.6. Validation of the optimized formulation

5.6.1. Evaluation of the granule of the optimized formulation

The granule properties and the tablet characterization tests were done for the optimized formulation. The micromeritic evaluation results are presented below in **Table 24**. The angle of repose was 27.33± 0.42^{o}. The results showed the optimized granule has good flow properties as all the values were within the acceptable range of the pharmacopeial specification. The tablet evaluation also indicated that the tablets exhibit excellent hardness and lower friability property as the values lies within the acceptable range for the tablet quality parameters. The thickness, hardness and friability results of optimized tablets were 3.99 ± 0.12 mm, 85.4 ± 0.36 N, 0.19 ± 0.08%, respectively.

Table 24: Experimental results of optimized furosemide granule and tablet formulation.

Parameters	**Values (Mean ± SD)**
Granule property	
Tapped density (g/ml)	0.56 ± 0.04
Bulk density (g/ml)	0.50 ± 0.09
Carrs Index (%)	10.7 ± 0.05
Hausners ratio	1.14 ± 0.08
Angle of repose(^{o})	27.33± 0.42
Tablet Characteristics	
Thickness (mm)	3.99 ± 0.12
Hardness (N)	85.4 ± 0.36
Friability (%)	0.19 ± 0.08

5.6.2. *In Vitro* Drug Release and Release Kinetics of Optimized Formulation

The % cumulative release profile of three optimized batches was evaluated through the *in vitro* dissolution study at 0.5, 1, 2, 3, 4, 5, 6, 8, 10, and 12 hrs. The release characteristics of the optimized formulations at 1 hr were 27.33% and at 12 hr were 95.47% as shown in **Figure 24**. This result indicated that the release profile of the drug is in line with the software recommendation.

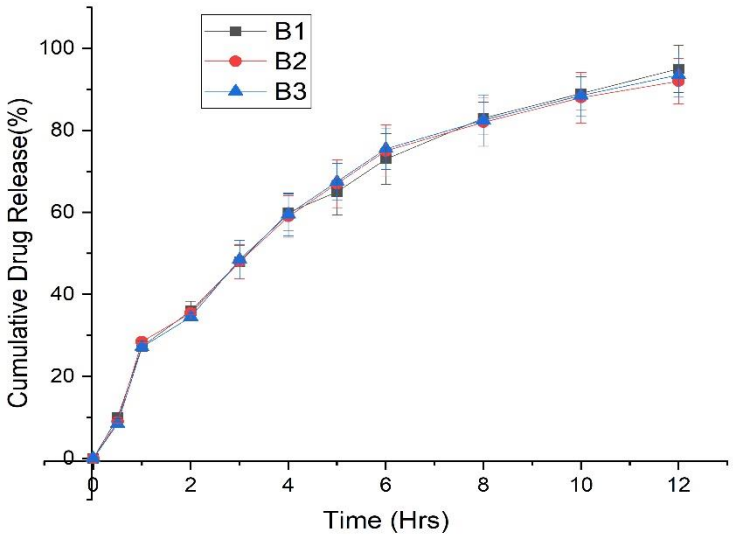

Figure 24: *In-vitro* dissolution profiles of three different batches of the optimized furosemide matrix tablet formulation.

The drug release kinetics was evaluated using different models. As presented in **Table 25**, Higuchi model was the best fit model for the drug release from the optimized formulation with $R^2 = 0.981$. Regarding to the mechanism of release, the drug involves both diffusion and erosion system as the n value is 0.586.

Table 25: Drug release kinetics study of optimized furosemide matrix tablet formulation

Optimized values	Model	Parameters	Values
X_1 (22.3%)	Zero order	K_0	1.17
X_2 (5%)		R^2	0.956
	First order	K_1	9.54
		R^2	0.981
	Higuchi model	K_H	0.32
		R^2	0.985
	Hixon-crowell	K_{HC}	1.17
		R^2	0.94
	Korsmeyer- Pappas	K	0.13
		R^2	0.924
		n	0.586

5.6.3. Validation of the Experiment

The validation test was done using three batches of the optimized formulation to confirm agreement between the software prediction and the actual experimental values. The difference between predicted and actual values was calculated using the % relative error (RE) formula. The result showed that the relative error for all the formulation ranges from 0.22% to 3.20% as shown

in **Table 26**. As all the values were below 5% (the acceptable level of marginal error), the overall result confirms the agreement of predicted and actual values. Hence, the optimization technique was effective in preparing optimized furosemide floating and bioadhesive matrix tablets.

Table 26: Model validation using three check points

Batches	Optimized formulation compositions	Response variables	Predicted values	Experimental values	% RE
1	A= 22.306%	Y_1	14.07 hr	14.05 hr	0.14
	B= 5%	Y_2	28.57gm	29.32 gm	-2.62
		Y_3	254.98%	263.12 %	-3.19
		Y_4	27.86%	27.33 %	1.90
		Y_5	28 % / $h^{-1/2}$	27.45 % / $h^{-1/2}$	1.96
2	A= 22.49%	Y_1	14.10 hr	14.35 hr	-1.77
	B= 5%	Y_1	28.61gm	29.56 gm	-3.40
		Y_3	255.36%	254.49 %	0.39
		Y_4	27.82%	28.53 %	-2.55
		Y_5	27.94% / $h^{-1/2}$	28.38 % / $h^{-1/2}$	-1.57
3	A= 22.60%	Y_1	14.12hr	14.75 hr	-4.46
	B= 5%	Y_2	28.63gm	29.24gm	-2.13
		Y_3	254.51%	265.25%	-4.21
		Y_4	27.80%	27.17%	2.26
		Y_5	27.91% / $h^{-1/2}$	27.48% / $h^{-1/2}$	3.63

5.6.4. Evaluation of the optimized tablet (mean ± SD).

Figure 24 illustrates the release pattern of the optimized formulation. Accordingly, similar cumulative drug release pattern was exhibited among all batches as compared to the predicted values seen from the software. As it can be seen from the **Table 26** all batches have shown to a comparable result for the outcome variables and in acceptable marginal error. The tablet evaluation results are also in acceptable limit of the pharmacopeial specification.

5. CONCLUSION

Pectin was isolated from *Citrus aurantifolia* waste peel and used as a polymer in the preparation of floating and bioadhesive matrix tablets in this study. The wet granulation method was used and the prepared tablets met the pharmacopeial physicochemical and tablets quality specifications. The DSC and FTIR analysis also showed that there were no significant interactions between furosemide and citrus pectin.

Based on the preliminary investigation, pectin concentration and $NaHCO_3$ were found to be the determinant independent variables that affect the response variables (floating duration, bioadhesive strength, swelling index, drug release at 1hr and drug release rate). As a result, the effect of pectin and $NaHCO_3$ was further studied and successfully optimized using the CCD. Based on the results, the increase in pectin concentration showed positive impact on the floating duration, bioadhesive strength, swelling index and negatively affects the drug release at 1 hr and the drug release rate. The rise in $NaHCO_3$ concentration increase the swelling index, the drug release at 1hr, drug release rate and also decreases bioadhesive strength and floating duration.

The result indicates that 22.309 % of pectin concentration and 5% of $NaHCO_3$ were found to be the optimized level of independent variables to obtain better response. Under this condition, the response of dependent variables was floating duration (> 12 hr), bioadhesive strength (29.32 g), swelling index (263.12%), drug release at 1hr (27.33%) and the drug release rate (27.45 $\% / h^{-1/2}$). The kinetic study revealed that the drug release best fits to Higuchi model with combined diffusion and erosion release mechanism. The developed mathematical models were proven to be valid and statistically significant for predicting the response parameters values at particular levels of formulation variables.

In conclusion, the results of this study suggest that waste-derived citrus pectin can be used as an alternative pharmaceutical excipient in the formulation and manufacture of floating and bioadhesive matrix tablets.

6. RECOMMENDATIONS

The promising findings of this study lead to the following suggestions for further work:

- Investigating the accelerated and long-term stability studies of the formulations.
- Conducting *in vivo* buoyancy and bio adhesive study to correlate with the *in vitro* performance and release profile study of the matrix tablets.

REFERENCES

Abrantes, G., Duarte, D. and Reis, C.P. (2019) 'An Overview of Pharmaceutical Excipients : Safe or Not Safe ', 105(2016). Available at: https://doi.org/10.1016/j.xphs.2016.03.019.

Akhgari, A., Rezaee, S. and Kuchak, A. (2011) 'Evaluation Of The Swelling , Erosion And Drug Release From Polysaccharide Matrix Tablets Based On Pectin And Inulin', 6(1), pp. 51–58.

Alicja Mortensen, Fernando Aguilar, Riccardo Crebelli, A.D.D. (2017) 'EFSA Journal - 2017 - - Re-evaluation of pectin E 440i and amidated pectin E 440ii as food additives.pdf'.

Altaf, U., Immanuel, G. and Iftikhar, F (2018) 'Extraction And Characterization Of Pectin Derived From Papaya (Carica papaya Linn .) Peel Extraction And Characterization Of Pectin Derived From Papaya', 3(October), pp. 1–6. Available at: https://doi.org/10.2348/ijset07150970.

Arias, D., Rodríguez J., Lopez, B., Mendez, P. (2021) 'Evaluation of the physicochemical properties of pectin extracted from Musa paradisiaca banana peels at different pH conditions in the formation of nanoparticles', *Heliyon*, 7(1). Available at: https://doi.org/10.1016/j.heliyon.2021.e06059.

Arollado, E.C., Ponsaran, K.M.G. and Loquias, M.M. (2018) 'Isolation and characterization of pectin from the ripe fruit peels of jackfruit (Artocarpus heterophyllus Lam.)', *Acta Medica Philippina*, 52(5), pp. 453–457. Available at: https://doi.org/10.47895/amp.v52i5.322.

Arun, J.K, Pattanayak ,D., Ramesh Adepu, R., Hossain,C.M., Shrivastava1,B., Ramya Sri Sura, R.S. (2020) 'Formulation and evaluation of floating and mucoadhesive tablets containing glipizide', *International Journal of Research in Pharmaceutical Sciences*, 11(1), pp. 899–907. Available at: https://doi.org/10.26452/ijrps.v11i1.1912.

Azad, A.K.M. (2014) 'Isolation and Characterization of Pectin Extracted from Lemon Pomace during Ripening', *Journal of Food and Nutrition Sciences*, 2(2), p. 30. Available at: https://doi.org/10.11648/j.jfns.20140202.12.

Bakhaidar, R.B., Naveen, N.R., Basim, P., Samar S. Murshid, S.S., Kurakula, M., Alamoudi, A.J., Bukhar, D.M.,Jali, A.M., Majrashi, M.A., Alshehri,S., Alissa, M., Rayan A. Ahmed,R.A. (2022) 'Response Surface Methodology (RSM) Powered Formulation Development, Optimization and Evaluation of Thiolated Based Mucoadhesive Nanocrystals for Local Delivery of Simvastatin', *Polymers*, 14(23), pp. 1–17. Available at: https://doi.org/10.3390/polym14235184.

Bansal, J. (2014) 'Evaluation of Banana Peel Pectin as Excipient in Solid Oral Dosage Form', *Global Journal of Pharmacology*, 8(2), pp. 275–278. Available at: https://doi.org/10.5829/idosi.gjp.2014.8.2.83288.

Barbosa Ribeiro, A.C. (2021) 'Cashew apple pectin as a carrier matrix for mangiferin: Physicochemical characterization, in vitro release and biological evaluation in human neutrophils', *International Journal of Biological Macromolecules*, 171, pp. 275–287. Available at: https://doi.org/10.1016/j.ijbiomac.2021.01.001.

Başarır, N.S., Mesut, B. and Özsoy, Y. (2021) 'A Review On Current Perspective Of Gastroretentive Drug Delivery Systems Prioritising Floating Dosage Forms Güncel Bakış Açısı ile Yüzen Dozaj Formlarına Öncelik Vererek Gastroretentif İlaç Salım Sistemlerinin Derlemesi'. Available at: https://doi.org/10.26650/JARHS2021-807525.

Belkheiri, A., Forouhar, A., Ursu, V.A., Pascal Dubessay, P., Pierre,G., Cedric Delattre, C., Gholamreza Djelveh, G., Abdelkafi,S., Hamdami,N., Michaud, P (2021) 'applied sciences Extraction , Characterization , and Applications of Pectins from', *Applied Sciences Journal*, 11(14), pp. 1–25.

Beyech Hundie, K. and Abdissa, D. (2021) 'Extraction and Characterization of Pectin from Lemon Waste for Commercial Applications', *Journal of the Turkish Chemical Society Section A: Chemistry*, 8(4), pp. 1111–1120. Available at: https://doi.org/10.18596/jotcsa.901973.

Bezerra, M.A. (2008) 'Response surface methodology (RSM) as a tool for optimization in analytical chemistry', *Talanta*, 76(5), pp. 965–977. Available at: https://doi.org/10.1016/j.talanta.2008.05.019.

Mariam El Boakye-Gyasi, E.M., Owusu,W.A.F., Entsie, P., Agbenorhevi, K.J, Banful, K.B.B., Bayor, T.M. (2021) 'Pectin from Okra (Abelmoschus esculentus L.) Has Potential as a Drug Release Modifier in Matrix Tablets', *Scientific World Journal*, 2021. Available at: https://doi.org/10.1155/2021/6672277.

Chaiwarit,T., Masavang, S., Mahe, J., Sommano,S., Ruksiriwanich,W., Brachais, C.H., Chambin, O., Jantrawut, P (2020a) 'Mango (cv. Nam Dokmai) peel as a source of pectin and its potential use as a film-forming polymer', *Food Hydrocolloids*, 102(December 2019). Available at: https://doi.org/10.1016/j.foodhyd.2019.105611.

Chelladurai, S.J.S. (2020) 'Optimization of process parameters using response surface methodology: A review', *Materials Today: Proceedings*, 37(Part 2), pp. 1301–1304. Available at: https://doi.org/10.1016/j.matpr.2020.06.466.

Chomto, P. and Nunthanid, J. (2017) 'Physicochemical and powder characteristics of various citrus pectins and their application for oral pharmaceutical tablets', *Carbohydrate Polymers*, 174, pp. 25–31. Available at: https://doi.org/10.1016/j.carbpol.2017.06.049.

Chopra, S., Patil, G. V. and Motwani, S.K. (2007) 'Release modulating hydrophilic matrix systems of losartan potassium: Optimization of formulation using statistical experimental design', *European Journal of Pharmaceutics and Biopharmaceutics*, 66(1), pp. 73–82. Available at: https://doi.org/10.1016/j.ejpb.2006.09.001.

Choudhary, P.D. and Pawar, H.A. (2014) 'Recently Investigated Natural Gums and Mucilages as Pharmaceutical Excipients : An Overview', 2014(ii).

Cserjési, P., Bélafi-Bakó, K., Csanádi, Z., Beszédes, S., Hodúr, C. (2011) 'Simultaneous recovery of pectin and colorants from solid agro-wastes formed in processing of colorful berries', *Progress in Agricultural Engineering Sciences*, 7(1), pp. 65–80. Available at: https://doi.org/10.1556/Progress.7.2011.5.

Daisy Chella Kumari, S. (2012) 'Formulation and evaluation of floating tablets of Ondansetron Hydrochloride', *International Journal of Drug Development and Research*, 4(4), pp. 265–274.

Dhanal, S.S., Tamboli, F.A., More, H.N., Kamble, S.J Savani R., Shere, S. (2022) 'Use of natural polymers as excipients in the pharmaceutical industry Use of natural polymers as excipients in the pharmaceutical industry', (August).

Einhorn-Stoll, U., Kunzek, H. and Dongowski, G. (2007) 'Thermal analysis of chemically and mechanically modified pectins', *Food Hydrocolloids*, 21(7), pp. 1101–1112. Available at: https://doi.org/10.1016/j.foodhyd.2006.08.004.

FAO (2020) 'Citrus'. Available at: https://www.fao.org/markets-and-trade/commodities/citrus/en/.

Farooq, U., Malviya, R. and Sharma, P.K. (2014) 'Extraction and characterization of artocarpus integer gum as pharmaceutical excipient.', *Polimery w medycynie*, 44(2), pp. 69–74.

Fatohy, H.A. and Abdul-rasool, A.A. (2013) 'Effect of Different Diluent and Binder Types on the Preparation of Bisoprolol Fumarate as Tablet Dosage Form', 22(1), pp. 32–39.

El Fihry, N. (2022) 'Physicochemical and functional characterization of pectin extracted from Moroccan citrus peels', *Lwt*, 162(April), p. 113508. Available at: https://doi.org/10.1016/j.lwt.2022.113508.

Da Gama, B.M.V. (2015) 'Extraction and characterization of pectin from citric waste', *Chemical Engineering Transactions*, 44(3), pp. 259–264. Available at: https://doi.org/10.3303/CET1544044.

Gandhi, K.J., Deshmane, S. V. and Biyani, K.R. (2012) 'Polymers in pharmaceutical drug delivery system: A review', *International Journal of Pharmaceutical Sciences Review and Research*, 14(2), pp. 57–66.

Granero, G.E., Longhi,M.R., Mora, M.J., Junginger, H.E., Midha, K.K., Shah, V.P., Stavchansky, S., J.B. Dressman, J.B., Barends, D.M. (2010) 'Biowaiver Monographs for Immediate Release Solid Oral Dosage Forms : Furosemide', 99(6), pp. 2544–2556. Available at: https://doi.org/10.1002/jps.

Haggag, E.G. (1998) 'Volatile Oils and Pectins from Citrus aurantifolia (Lime) and Citrus limonia (Lemon)', *Asian Journal of Chemistry*, 10(4), pp. 828–833.

Haile, T.G., Sibhat, G.G. and Molla, F. (2020) 'Physicochemical Characterization of Grewia ferruginea Hochst. ex A. Rich Mucilage for Potential Use as a Pharmaceutical Excipient', *BioMed Research International*, 2020. Available at: https://doi.org/10.1155/2020/4094350.

Hasan, S.H., Srivastava, P. and Talat, M. (2009) 'Biosorption of Pb(II) from water using biomass of Aeromonas hydrophila: Central composite design for optimization of process variables', *Journal of Hazardous Materials*, 168(2–3), pp. 1155–1162. Available at: https://doi.org/10.1016/j.jhazmat.2009.02.142.

Hashim, A.Z. (2018) 'Extraction and Characterization of Pectin from Dragon Fruit (Hylocerens polyrhizus) Peel Using Different Concentration of Ammonium Oxalate', *Basrah Journal of Agricultural Sciences*, 31(1), pp. 12–19. Available at: https://doi.org/10.37077/25200860.2018.70.

Haywood, A. and Coast, G. (2011) 'Pharmaceutical excipients – where do we begin ?', pp. 4–6.

Horowitz, M. (2000) 'Pectin', *Radiology*, 234(1), pp. 541–559. Available at: https://www.ncbi.nlm.nih.gov/pmc/articles/PMC3624763/pdf/nihms412728.pdf.

Khodaiyan, S.S.H.F., Kazemi, M., Najari, Z. (2019) 'Optimization and characterization of pectin extracted from sour orange peel by ultrasound assisted method', *International Journal of Biological Macromolecules*, 125, pp. 621–629. Available at: https://doi.org/10.1016/j.ijbiomac.2018.12.096.

Ibrahim, M, Naguib, Y.W., Sarhan, H.A., Abdelkader, H., (2019) 'Gastro-retentive oral drug delivery systems: a promising approach for narrow absorption window drugs', *Journal of advanced Biomedical and Pharmaceutical Sciences*, 0(0), pp. 0–0. Available at: https://doi.org/10.21608/jabps.2019.11357.1042.

Ismail, N.S.M. (2012) 'Extraction and characterization of pectin from dragon fruit (Hylocereus polyrhizus) using various extraction conditions', *Sains Malaysiana*, 41(1), pp. 41–45.

Jain, S., Arora, P. and Popli, H. (2020) 'A comprehensive review on Citrus aurantifolia essential oil: its phytochemistry and pharmacological aspects', *Brazilian Journal of Natural Sciences*, 3(2), p. 354. Available at: https://doi.org/10.31415/bjns.v3i2.101.

Jyotirmoy, D. (2010) 'Formulation and Evaluation of Metformin HCl Floating Tablet using Pectin as a Natural Polymer', *International Research Journal of Pharmaceutical Sciences*, 1(1), p. 5.

Kancherla, N., Dhakshinamoothi, A., Chitrac, K., Komarama, R.B, (2019) 'Preliminary Analysis of Phytoconstituents and Evaluation of Anthelminthic Property of Cayratia auriculata (In Vitro).', *Maedica*, 14(4), pp. 350–356. Available at: https://doi.org/10.26574/maedica.2019.14.4.350.

Kanmani, P., Dhivya, E., Aravind, J., Kumaresan, K. (2014) 'Extraction and Analysis of Pectin from Citrus Peels : Augmenting the Yield from Citrus limon Using Statistical Experimental Design', 5(3), pp. 303–312. Available at: https://doi.org/10.5829/idosi.ijee.2014.05.03.10.

Kar, M., Chourasiya, Y., Maheshwari, R., Tekade, R.K. (2018) *Current developments in excipient science:*

Implication of quantitative selection of each excipient in product development, *Basic Fundamentals of Drug Delivery*. Elsevier Inc. Available at: https://doi.org/10.1016/B978-0-12-817909-3.00002-9.

Kebebe, D., Belete, A. and Gebre-Mariam, T. (2012) 'Evaluation of Two Olibanum Resins as Rate Controlling Matrix Forming Excipients in Oral Sustained Release Tablets', *Ethiopian Pharmaceutical Journal*, 28(2). Available at: https://doi.org/10.4314/epj.v28i2.4.

Kedir, W.M., Deresa, E.M. and Diriba, T.F. (2022) 'Pharmaceutical and drug delivery applications of pectin and its modified nanocomposites', *Heliyon*, 8(9), p. e10654. Available at: https://doi.org/10.1016/j.heliyon.2022.e10654.

Khamsucharit, P., Laohaphatanalert, K., Gavinlertvatana, P., Sriroth, K., Sangseethong, K. (2018) 'Characterization of pectin extracted from banana peels of different varieties', *Food Science and Biotechnology*, 27(3), pp. 623–629. Available at: https://doi.org/10.1007/s10068-017-0302-0.

Khan, Bibi, Z. (2015) 'Optimization of Process Conditions for Pectin Extraction from Citrus Peel', *science,technology and development*, 34 (1), pp. 9–15. Available at: https://www.researchgate.net/journal/Science-Technology-and-Development-0254-6418.

Khan, R. (2013) 'Gastroretentive drug delivery system - A review', *International Journal of Pharma and Bio Sciences*, 4(2), pp. 24–35. Available at: https://doi.org/10.21276/apjhs.2014.1.2.9.

Khule, N.R., Mahale, N.B., Shelar, D.S., Rokade, M.M., ChaudhariKhule, S.R. (2012) 'Extraction of pectin from citrus fruit peel and use as natural binder in paracetamol tablet', 4(2), pp. 558–564.

Khuri, A.I. and Mukhopadhyay, S. (2010) 'Response surface methodology', *Wiley Interdisciplinary Reviews: Computational Statistics*, 2(2), pp. 128–149. Available at: https://doi.org/10.1002/wics.73.

Kľoc, D., Wolaschka, T. and Ruttkay, F. (2021) 'Formulation and Evaluation of Tablets Compressed from Granules Prepared by Thermoplastic Granulation', *European Pharmaceutical Journal*, 68(1), pp. 72–75. Available at: https://doi.org/10.2478/afpuc-2021-0003.

Kurita, O., Fujiwara, T. and Yamazaki, E. (2008) 'Characterization of the pectin extracted from citrus peel in the presence of citric acid', *Carbohydrate Polymers*, 74(3), pp. 725–730. Available at: https://doi.org/10.1016/j.carbpol.2008.04.033.

Laurén, P. (2018) 'Pectin and Mucin Enhance the Bioadhesion of Drug Loaded Nanofibrillated Cellulose Films', *Pharmaceutical Research*, 35(7). Available at: https://doi.org/10.1007/s11095-018-2428-z.

Lee, K.Y. and Choo, W.S. (2020) 'Extraction Optimization and Physicochemical Properties of Pectin from Watermelon (Citrullus lanatus) Rind: Comparison of Hydrochloric and Citric acid Extraction', *Journal of Nutraceuticals and Food Science*, 5(1), pp. 1–8. Available at: https://doi.org/10.36648/nutraceuticals.5.1.1.

Lopes, C.M. (2016) 'Overview on gastroretentive drug delivery systems for improving drug bioavailability', *International Journal of Pharmaceutics*, 510(1), pp. 144–158. Available at: https://doi.org/10.1016/j.ijpharm.2016.05.016.

Mada, T., Duraisamy, R. and Guesh, F. (2022) 'Optimization and characterization of pectin extracted from banana and papaya mixed peels using response surface methodology', (October 2021), pp. 1222–1238. Available at: https://doi.org/10.1002/fsn3.2754.

Malviya, R. (2011) 'Extraction Characterization and Evaluation of Selected Mucilage as Pharmaceutical Excipient', *Polimery w Medycynie* [Preprint].

Mandal, U.K., Chatterjee, B. and Senjoti, F.G. (2016) 'Gastro-retentive drug delivery systems and their in vivo success : A recent update', *Asian Journal of Pharmaceutical Sciences*, 11(5), pp. 575–584. Available at: https://doi.org/10.1016/j.ajps.2016.04.007.

Manner, H.I., Buker, R.S., Smith, V.E, Ward, D., EleManner, C.R.. (2006) 'Citrus (citrus) and Fortunella (kumquat)', *Distribution* [Preprint], (April).

Freitas, C.M.P., Coimbra,J.S.R., Souza, V.G.L., Sousa, R.C.S. (2021) 'Structure and Applications of Pectin in Food, Biomedical, and Pharmaceutical Industry: A Review'.

Mashinchian, O. (2014) 'Impacts of quantum dots in molecular detection and bioimaging of cancer', *BioImpacts*, 4(3), pp. 149–166. Available at: https://doi.org/10.15171/bi.2014.008.

Miao, M.X., Qi S.Z., Yi, X.W., Quan, K.F., Gu..Y. (2005) 'Study on the characteristics of pectin-ketoprofen for colon targeting in rats', *International Journal of Pharmaceutics*, 298(1), pp. 91–97. Available at: https://doi.org/10.1016/j.ijpharm.2005.04.012.

Mohamed, H. (2016) 'Extraction and Characterization of Pectin from Grapefruit Peels', *MOJ Food Processing & Technology*, 2(1), pp. 31–38. Available at: https://doi.org/10.15406/mojfpt.2016.02.00029.

Durán-Aranguren, D.D., Ramírez, C.J.A., Díaz, L.C.V., Valderrama, M.A., Sierra, R. (2016) 'Production of Pectin from Citrus Residues: Process Alternatives and Insights on Its Integration under the Biorefinery Concept, *Intech*, pp. 225–240. Available at: https://www.intechopen.com/books/advanced-biometric-technologies/liveness-detection-in-biometrics.

Murthy, S.N. (2016) 'In vitro Physico-chemical, Phytochemical and Fluroscence Assessment of Mucuna sps', *IOSR Journal of Biotechnology and Biochemistry (IOSR-JBB*, 2(1), pp. 2455–264. Available at: www.iosrjournals.orgwww.iosrjournals.org1%7CPage.

Nafei, A.T. (2014) 'Formulation of Furosemide as a Gastroretentive Floating In-Situ Gelling System for an Oral Controlled Release Dosage Form Anas Tarik Nafei', *MSC. Thesis*, pp. 1–139.

Nagaraju, B. (2017) 'Formulation and evaluation of floating bioadhesive Doxofylline tablets', *International Journal of Drug Delivery*, 8(4), pp. 134–141. Available at: https://doi.org/10.5138/09750215.1871.

Nanjwade, B.K., Adichwal, S.A. and Sutar, K.P. (2012) 'Development and evaluation of glipizide floating tablet', *Journal of Drug Delivery Science and Technology*, 22(4), pp. 327–333. Available at: https://doi.org/10.1016/S1773-2247(12)50055-9.

Narang, N. and Jiraungkoorskul, W. (2016) 'Anticancer activity of key lime, Citrus aurantifolia', *Pharmacognosy Reviews*, 10(20), pp. 118–122. Available at: https://doi.org/10.4103/0973-7847.194043.

Nayak, A.K., Malakar, J. and Sen, K.K. (2010) 'Gastroretentive drug delivery technologies: current approaches and future potential.', *Journal of Pharmaceutical Education and Research*, 1(2), pp. 1–12.

Nigusse, B., Gebre-Mariam, T. and Belete, A. (2021) 'Design, development and optimization of sustained release floating, bioadhesive and swellable matrix tablet of ranitidine hydrochloride', *PLoS ONE*, 16(6 June), pp. 1–16. Available at: https://doi.org/10.1371/journal.pone.0253391.

Ogaji, I.J., Nep, E.I. and Audu-Peter, J.D. (2012) 'Advances in Natural Polymers as Pharmaceutical Excipients', *Pharmaceutica Analytica Acta*, 03(01), pp. 1–16. Available at: https://doi.org/10.4172/2153-2435.1000146.

Omale Ayeni, G and Omale, A, J.A. (2017) 'Extraction, Physicochemical and Characterization of Pectin from Sweet Orange (Citrus sinensis), Lime (Citruss aurantifolia) and Lemon (Citrus limon).', *International Journal of Current Research*, 9(9), pp. 56992–56995.

Frederick William Akuffo Owusu , W.A.F., Boakye-Gyasi, M.E, Agbenorhevi, J.K., Bayor, M.T., Owusu, K.W. (2021) 'Potential and Comparative Tablet Disintegrant Properties of Pectin Obtained from Five Okra Genotypes in Ghana', *Scientifica*, 2021. Available at: https://doi.org/10.1155/2021/2902335.

Owusu , W.A.F., Boakye-Gyasi, M.E., Entsie, P., Bayor, M.T., Owusu, K.O. (2021) 'Utilization of Pectin from Okra as Binding Agent in Immediate Release Tablets', *BioMed Research International*, 2021. Available at: https://doi.org/10.1155/2021/6002286.

Paarakh, M.P. (2019) 'Release Kinetics – Concepts and Applications', *International Journal of Pharmacy Research & Technology*, 8(1), pp. 12–20. Available at: https://doi.org/10.31838/ijprt/08.01.02.

Pasandide, B., Khodaiyan,F., Mousavi, Z.E., Hosseini, S.S. (2017) 'Optimization of aqueous pectin extraction from Citrus medica peel', *Carbohydrate Polymers*, 178, pp. 27–33. Available at: https://doi.org/10.1016/j.carbpol.2017.08.098.

Pasupathi A., M.. A. (2020) 'Review Article An Updated Review on Gastroretentive Drug Delivery System: An Approach to Enhance Gastric Retention * 1', *International Journal of Pharmaceutical Sciences Review and Research*, 61(14), pp. 78–83.

Patil, H., Tiwari, R. V. and Repka, M.A. (2016) 'Recent advancements in mucoadhesive floating drug delivery systems: A mini-review', *Journal of Drug Delivery Science and Technology*, 31, pp. 65–71. Available at: https://doi.org/10.1016/j.jddst.2015.12.002.

Pérez, J., Gómez, K. and Vega, L. (2022) 'Optimization and Preliminary Physicochemical Characterization of Pectin Extraction from Watermelon Rind (Citrullus lanatus) with Citric Acid', *International Journal of Food Science*, 2022. Available at: https://doi.org/10.1155/2022/3068829.

Porwal, A., Dwivedi, H. and Pathak, K. (2017) 'Decades of research in drug targeting using gastroretentive drug delivery systems for antihypertensive therapy', *Brazilian Journal of Pharmaceutical Sciences*, 53(3), pp. 1–15. Available at: https://doi.org/10.1590/s2175-97902017000300173.

Prajapati, S.T., Mehta,A.P., Modhia, I.P., Patel, C.N. (2012) ' Formulation and optimisation of raft-forming chewable tablets containing H 2 antagonist ', *International Journal of Pharmaceutical Investigation*, 2(4), p. 176. Available at: https://doi.org/10.4103/2230-973x.106988.

Prinderre, P., Sauzet, C. and Fuxen, C. (2011) 'Advances in gastro retentive drug-delivery systems', pp. 1189–1203.

Raghavendra Naveen, N., Kurakula, M. and Gowthami, B. (2020) 'Process optimization by response surface methodology for preparation and evaluation of methotrexate loaded chitosan nanoparticles', *Materials Today: Proceedings*, 33(xxxx), pp. 2716–2724. Available at: https://doi.org/10.1016/j.matpr.2020.01.491.

Raj, S. (2012) 'A Review on Pectin: Chemistry due to General Properties of Pectin and its Pharmaceutical Uses', 1(12), pp. 10–13. Available at: https://doi.org/10.4172/scientificreports.550.

Rani, K.C. (2021) 'Preparation and evaluation of gelatin and pectin-based Moringa oleifera chewable-gummy tablets', *IOP Conference Series: Earth and Environmental Science*, 913(1). Available at: https://doi.org/10.1088/1755-1315/913/1/012082.

Rashid, U., Anwar, F. and Arif, M. (2009) 'Optimization of base catalytic methanolysis of sunflower (helianthus annuus) seed oil for biodiesel production by using response surface methodology', *Industrial and Engineering Chemistry Research*, 48(4), pp. 1719–1726. Available at: https://doi.org/10.1021/ie801136h.

Ravindrakullai, M. and Manjunath, K. (2015) 'Formulation and In Vitro Evaluation of Hydrodynamically Balanced Matrix Tablets of Famotidine Using Pectin as Controlled Release Polymer', (June 2013).

Rehman,A., Ahmad,T., Aadilb,R.M., Spottic,M.J., Bakryd, A.M., Khana,I.M., Zhaoa, Li., Riaza,T., Tong, Q. (2019) 'Pectin polymers as wall materials for the nano-encapsulation of bioactive compounds', *Trends in Food Science and Technology*, 90(June), pp. 35–46. Available at:

https://doi.org/10.1016/j.tifs.2019.05.015.

Rishabha, M., Pranati, S., Mayank, B., Kumar, S.P., (2010) 'Formulation and optimization of sustained release matrix tablets of Diclofenac sodium using pectin as release modifier', *International Journal of Drug Development and Research*, 2(2), pp. 330–335.

Rosland Abel, S.E. (2020) 'Characterisation of physicochemical properties of gum arabic powder at various particle sizes', *Food Research*, 4, pp. 107–115. Available at: https://doi.org/10.26656/fr.2017.4(S1).S32.

Roy, M.S., Alam, M., Saeid, A., Das,B.C., Mia, M.B., Rahman, M.A., Eun, J.B., Ahmed, M. (2018) 'Extraction and characterization of pectin from pomelo peel and its impact on nutritional properties of carrot jam during storage', *Journal of Food Processing and Preservation*, 42(1), pp. 1–9. Available at: https://doi.org/10.1111/jfpp.13411.

Ruano,P., Delgado, L.L., Picco, S.,Villegas, L., Tonelli, F., Mario Eduardo Aguilera Merlo, M.E.A., Rigau, R., Diaz, D., Masuelli, M. (2019) 'Extraction and Characterization of Pectins From Peels of Criolla Oranges (Citrus sinensis): Experimental Reviews', pp. 1–44.

Saha, T., Masum, Z.U., Mondal, K.S., Hossain, M.S., Jobaer, M.A., Shahin, R.S., Fahad, T. (2018) 'Application of natural polymers as pharmaceutical excipients', *Global Journal of Life Sciences and Biological Research*, 04(01). Available at: https://doi.org/10.35248/gjlsbr.2018.4.1.

Salbu, L. (2011) 'Compressibility and compactibility of pectin powders -A study of their potential as direct compression excipients in tablets', (May), pp. 27–28.

Saluja, V. and Sekhon, B.S. (2013) 'The regulation of pharmaceutical excipients .', 4(September), pp. 95–106.

Sandarani, M. (2017) 'A Review: Different Extraction Techniques of Pectin', *Journal of Pharmacognosy & Natural Products*, 03(03), pp. 1–5. Available at: https://doi.org/10.4172/2472-0992.1000143.

Sastry, S. V., Reddy, I.K. and Khan, M.A. (1997) 'Atenolol gastrointestinal therapeutic system: Optimization of formulation variables using response surface methodology', *Journal of Controlled Release*, 45(2), pp. 121–130. Available at: https://doi.org/10.1016/S0168-3659(96)01553-2.

Sathish, S.(2016) 'Extraction of pectin from used citrus Limon and optimization of process parameters using response surface methodology', *Research Journal of Pharmacy and Technology*, 9(12), pp. 1451–1456. Available at: https://doi.org/10.5958/0974-360X.2016.00453.4.

Shah, N., Sharma, O.P., Mehta, T., Amin. A. (2022) 'Design And Optimization Studies Of Tablet In Tablet Formulation Of Diclofenac And Misoprostol : Application Of Response Surface Methodology and'.

Shaha, R.K., Punichelvana, Y.N.A.P. and Afandi, A. (2013) 'Optimized Extraction Condition and Characterization of Pectin from Kaffir Lime (Citrus hystrix)', *Research Journal of Agriculture and Forestry Sciences*, 1(2), pp. 1–11.

Shakya, R., Thapa, P. and Saha, R.N. (2013) 'In vitro and in vivo evaluation of gastroretentive floating drug delivery system of ofloxacin', *Asian Journal of Pharmaceutical Sciences*, 8(3), pp. 191–198. Available at: https://doi.org/10.1016/j.ajps.2013.07.025.

Sharma, S., Nanda, A. and Singh, L. (2013) 'Formulation and optimization of gastric bioadhesive tablets of diltiazem hydrochloride using central composite design', *Tropical Journal of Pharmaceutical Research*, 12(6), pp. 861–867. Available at: https://doi.org/10.4314/tjpr.v12i6.1.

Shekunov, B.Y., Chattopadhyay, P., Tong, H.H. and Chow, A.H. (2007) 'Particle size analysis in pharmaceutics: Principles, methods and applications', *Pharmaceutical Research*, 24(2), pp. 203–227. Available at: https://doi.org/10.1007/s11095-006-9146-7.

Shinde, S., Tadwee, I. and Shahi, S. (2021) 'Gastro retentive Drug Delivery System : A Review', 1, pp. 1–13.

Siddam, H., Kotla, N.G., Maddiboyina, B., Singh, S., Sunnapu , O., Kumar, A. (2016) 'Formulation and evaluation of atenolol floating bioadhesive system using optimized polymer blends', *International Journal of Pharmaceutical Investigation*, 6(2), p. 116. Available at: https://doi.org/10.4103/2230-973x.177832.

Siddiqui, N.H., Baber, R.B., Sultan, R.F., Azhar, I., Ahmed, W., Mahmood, Z.A. (2021) 'Studies on Fruit Pectin in the Development of Tablet Formulations of Ibuprofen', *RADS Journal of Pharmacy and Pharmaceutical Sciences*, 8(4). Available at: https://doi.org/10.37962/jpps.v8i4.397.

Silva, A.F.T. (2013) 'Particle sizing measurements in pharmaceutical applications: Comparison of in-process methods versus off-line methods', *European Journal of Pharmaceutics and Biopharmaceutics*, 85(3 PART B), pp. 1006–1018. Available at: https://doi.org/10.1016/j.ejpb.2013.03.032.

Singh, B., Chakkal, S.K. and Ahuja, N. (2006) 'Formulation and optimization of controlled release mucoadhesive tablets of atenolol using response surface methodology', *AAPS PharmSciTech*, 7(1), pp. 1–10. Available at: https://doi.org/10.1208/pt070103.

Singh, H., Pahwa, S., Dhamija, K., Arora, V. (2020) 'Formulation and Evaluation of Floating Tablets of Cimetidine', (January 2018). Available at: https://doi.org/10.20902/IJCTR.2018.110944.

Singh, R., Malviya, R. and Sharma, P.K. (2011) 'Extraction and characterization of tamarind seed polysaccharide as a pharmaceutical excipient', *Pharmacognosy Journal*, 3(20), pp. 17–19. Available at: https://doi.org/10.5530/pj.2011.20.4.

Singhal, S. and Swami Hulle, N.R. (2022) 'Citrus pectins: Structural properties, extraction methods, modifications and applications in food systems – A review', *Applied Food Research*, 2(2), p. 100215. Available at: https://doi.org/10.1016/j.afres.2022.100215.

Solanki, H.K. (2010) 'Recent advances in granulation technology', *International Journal of Pharmaceutical Sciences Review and Research*, 5(3), pp. 48–54.

Gupta, R., Sharma, P.K., Arora, A., Malviya, R (2012) 'Gastroretentive drug delivery systems: A review', *Research Journal of Pharmaceutical, Biological and Chemical Sciences*, 3(3), pp. 965–980.

Sriamornsak, P., Thirawong, N., Weerapol., Nunthanid, J., Sungthongjeen,S. (2007) 'Swelling and erosion of pectin matrix tablets and their impact on drug release behavior', *European Journal of Pharmaceutics and Biopharmaceutics*, 67(1), pp. 211–219. Available at: https://doi.org/10.1016/j.ejpb.2006.12.014.

Sriamornsak, P. (2011) 'Application of pectin in oral drug delivery', *Expert Opinion on Drug Delivery*, 8(8), pp. 1009–1023. Available at: https://doi.org/10.1517/17425247.2011.584867.

Sriamornsak, P., Sungthongjeen, S. and Puttipipatkhachorn, S. (2007) 'Use of pectin as a carrier for intragastric floating drug delivery: Carbonate salt contained beads', *Carbohydrate Polymers*, 67(3), pp. 436–445. Available at: https://doi.org/10.1016/j.carbpol.2006.06.013.

Srivastava, P. and Malviya, R. (2011a) 'Extraction, Characterization and Evaluation of Orange Peel Waste Derived Pectin as a Pharmaceutical Excipient', *The Natural Products Journal*, 1(1), pp. 65–70. Available at: https://doi.org/10.2174/2210316311101010065.

Srivastava, P. and Malviya, R. (2011b) 'Sources of pectin, extraction and its applications in pharmaceutical industry - an overview', *Indian Journal of Natural Products and Resources*, 2(1), pp. 10–18.

Srivastava, P., Malviya, R. and Kulkarni, G.T. (2010) 'FORMULATION AND EVALUATION OF PARACETAMOL TABLETS TO ASSESS BINDING PROPERTY OF ORANGE PEEL PECTIN', 3(1), pp. 30–34.

Suhendra, D. (2017) 'Optimization of the enzymatic synthesis of biodiesel from Terminalia cattapa L. Kernel oil using response surface methodology', *Journal of Oleo Science*, 66(3), pp. 209–215. Available at: https://doi.org/10.5650/jos.ess16167.

Sundarraj, A.A. and Ranganathan, T.V. (2017) 'A Review -Pectin from Agro and Industrial Waste', *International Journal of Applied Environmental Sciences ISSN*, 12(10), pp. 973–6077. Available at: http://www.ripublication.com.

Sundarraj, A.A., Thottiam Vasudevan, R. and Sriramulu, G. (2018) 'Optimized extraction and characterization of pectin from jackfruit (Artocarpus integer) wastes using response surface methodology', *International Journal of Biological Macromolecules*, 106, pp. 698–703. Available at: https://doi.org/10.1016/j.ijbiomac.2017.08.065.

Enejoh, O.S., Ogunyemi, O.I., Bala, M.S., Oruene,I..S., Suleiman, M.M., Ambali, S.F (2015) 'Ethnomedical Importance of Citrus Aurantifolia (Christm) Swingle', *The Pharma Innovation Journal*, 4(8), pp. 1–6.

Suvakanta, D. (2014) 'Optimization and characterization of purified polysaccharide from Musa sapientum L. as a pharmaceutical excipient', *Food Chemistry*, 149(1), pp. 76–83. Available at: https://doi.org/10.1016/j.foodchem.2013.10.068.

Tamizharasi, S., Rathi, V. and Rathi, J.C. (2011) 'Floating drug delivery system', *Systematic Reviews in Pharmacy*, 2(1), pp. 19–29. Available at: https://doi.org/10.4103/0975-8453.83435.

Tanwar, D., Chandra Rathi, J. and Sharma, R. (2021) 'Formulation Development and Evaluation of Floating Tablet of Levofloxacin', *Certified Journal │ Tanwar et al. World Journal of Pharmaceutical Research*, 10(2), pp. 820–829. Available at: https://doi.org/10.13040/IJPSR.0975-8232.12(2).820-29.

Teklehaymanot, T., Giday, M., Medhin, G. and Mekonnen, Y. (2007) 'Knowledge and use of medicinal plants by people around Debre Libanos monastery in Ethiopia', *Journal of Ethnopharmacology*, 111(2), pp. 271–283. Available at: https://doi.org/10.1016/j.jep.2006.11.019.

Thu Dao, T.A., Webb, H.K. and Malherbe, F. (2021) 'Optimization of pectin extraction from fruit peels by response surface method: Conventional versus microwave-assisted heating', *Food Hydrocolloids*, 113, p. 106475. Available at: https://doi.org/10.1016/j.foodhyd.2020.106475.

Tibbits, C.W., Macdougall, A.J. and Ring, S.G. (1998) 'Calcium binding and swelling behaviour of a high methoxyl pectin gel', 310, pp. 101–107.

Tripathi, J. (2019) 'Current state and future perspectives on gastroretentive drug delivery systems', *Pharmaceutics*, 11(4). Available at: https://doi.org/10.3390/pharmaceutics11040193.

Twinomuhwezi, H., Godswill, A.C. and Kahunde, D. (2020) 'Extraction and Characterization of Pectin from Orange (Citrus sinensis), Lemon (Citrus limon) and Tangerine (Citrus tangerina)', *American Journal of Physical Sciences*, 1(1(2)), pp. 17–30.

Tyagi, S. (2016) 'Extraction, Characterization and Evaluation of Pectin from Orange Peels as Pharmaceutical Excipient', *Global Journal of Pharmacology*, 10(2), pp. 41–44. Available at: https://doi.org/10.5829/idosi.gjp.2016.10.02.92160.

USP<1217> (2021) 'States Pharmacopeia and National Formulary (USP 43-NF 38)', *United States Pharmacopeial Convention*, (c), pp. 868–870.

USP (2011) 'USP Powder Flow', *'Physical Characteristics of Food Powders,' in Physical Properties of Foods (M. Peleg and E. B. Bagley, eds.), Westport, CT: AVI, Inc.*, 30(60)(6), pp. 293–323. Available at: https://demonstrations.wolfram.com/VolumeAndMassOfASpoonfulOfPowder/.

USP43-NF38 (2020) 'United State Pharmacopeia 2020', *United states pharmacopeial convention*

[Preprint], (c).

Value, S.J.R.I., Ravindrakullai, M. and Manjunath, K. (2015) 'Evaluation of Pectin derived from Orange peel as a Pharmaceutical Excipient Available online http://www.ijddr.in Covered in Official Product of Elsevier , The Netherlands Evaluation of Pectin derived from Orange peel as a Pharmaceutical Excipient Full Len', (June 2013).

Vipul Kumar, Vijay Sharma and Lalit Singh (2018) 'Pectin from fruit peels and its uses as pharmaceutical and food grade', *European Journal of Biomedical and Pharmaceutical Sciences*, 5(5 185-199).

Wang, X., Chen, Q., Lü, X (2016) 'AC SC', *Food Hydrocolloids* [Preprint]. Available at: https://doi.org/10.1016/j.foodhyd.2016.06.019.

Wathoni, N., Shan, C.Y., Shan,W.Y., Rostinawati, T., Raden Bayu Indradi, R.B., Pratiwi, R., Muchtaridi, M (2019) 'Characterization and antioxidant activity of pectin from Indonesian mangosteen (Garcinia mangostana L.) rind', *Heliyon*, 5(8), p. e02299. Available at: https://doi.org/10.1016/j.heliyon.2019.e02299.

Weh., F.H., Razavi, M., Erh, C.H., Noordin, M.I., Shaik Nyamathulla., Karimian, H., Khajuria, D.K (2014) 'Formulation and in Vitro evaluation of hydrodynamically balanced matrix tablets of famotidine using pectin as controlled release polymer', *Latin American Journal of Pharmacy*, 33(3), pp. 420–431.

Willats, W.G.T., Knox, J.P. and Mikkelsen, J.D. (2006) 'Pectin: New insights into an old polymer are starting to gel', *Trends in Food Science and Technology*, 17(3), pp. 97–104. Available at: https://doi.org/10.1016/j.tifs.2005.10.008.

Wilson, R.L. and Stevenson, C.E. (2019) *Anatomy and Physiology of the Stomach*. Eighth Edi, *Shackelford's Surgery of the Alimentary Tract, 2 Volume Set*. Eighth Edi. Elsevier Inc. Available at: https://doi.org/10.1016/b978-0-323-40232-3.00056-x.

Wong, T.W., Colombo, G. and Sonvico, F. (2021) 'Pectin Matrix as Oral Drug Delivery Vehicle for Colon Cancer Treatment', 12(1). Available at: https://doi.org/10.1208/s12249-010-9564-z.

Wu, G.A., Terol, J., Ibanez,V., López-García, A., Pérez-román, E., Borredá., Domingo, C., francisco r. Tadeo, T.R., Carbonell-caballero, J., Alonso, R., Curk, F., Du, D., Ollitrault, P., Roose, M.L., Dopazo, J., Gmitter Jr, F.G., Rokhsar, D.S., Talon, M. (2018) 'Genomics of the origin and evolution of Citrus', *Nature*, 554(7692), pp. 311–316. Available at: https://doi.org/10.1038/nature25447.

Xie, Y., Chen, L. and Liu, R. (2016) 'Oxidation of AOX and organic compounds in pharmaceutical wastewater in RSM-optimized-Fenton system', *Chemosphere*, 155, pp. 217–224. Available at: https://doi.org/10.1016/j.chemosphere.2016.04.057.

Yang, Z. (2010) 'Crystallization behavior of poly(ε-caprolactone)/layered double hydroxide nanocomposites', *Journal of Applied Polymer Science*, 116(5), pp. 2658–2667. Available at: https://doi.org/10.1002/app.

Yilma, Z., A. Belete and Gebre-Mariam, T. (2015) 'Formulation and Optimization of Sustained Release Floating Matrix Tablets of Salbutamol Sulphate Using Xanthan Gum and Hydroxypropyl Methylcellulose Polymer Blend', *International Journal of Pharmaceutical Sciences and Research*, 6(5), pp. 1877–1892. Available at: https://doi.org/10.13040/IJPSR.0975-8232.6(5).1877-92.

Yin, S. (2017) 'Pectin as a rheology modifier : Origin , structure , commercial production and rheology', 161, pp. 118–139.

Yusif, R.M., Abu Hashim,I.I.,Mohamed, A.E, Badria F.A. (2015) 'Gastroretentive Matrix Tablets of Boswellia Oleogum Resin : Preparation , Optimization , In Vitro Evaluation , and Cytoprotective Effect on Indomethacin-Induced Gastric Ulcer in Rabbits', (11). Available at: https://doi.org/10.1208/s12249-015-

0351-8.